ISSN: 1816-8957

No. 13, April 2012

Scientific Drilling

Reports on Deep Earth Sampling and Monitoring

Published by the Integrated Ocean Drilling Program with the International Continental Scientific Drilling Program

Editorial Preface

Dear Reader:

A year has passed since the disaster of the Great Eastern Japan Earthquake struck on 11 March 2011, causing major devastation including a nuclear power plant accident that has challenged nuclear energy policies in Japan and worldwide. The magnitude of the earthquake, the displacement of the seafloor, and the associated tsunami took not only the people of Japan but also the scientific world by surprise. With less public attention, 2011 also saw a large increase in the anthropogenic emission of CO_2, a trend which, if it continues, may pose long-term global threats to societies.

Can scientific drilling help alleviate such geohazards and climate change? No, just as taking out fire insurance does not prevent fires. But scientific drilling can help predict cycles and frequency of events, potential magnitudes, and general locations of major geohazards. For example, this spring the IODP drilling vessel *Chikyu* will attempt to sample the rupture zone that on 11 March 2011 moved the ocean floor an unprecedented 30–50 meters off the coast of Japan. What conditions along the fault zone make such a displacement possible?

To avoid being taken by surprise by events caused by severe and rapid climate change is also what scientific drilling aims at. Both IODP and ICDP draw on the unique repository of past climate and environmental records preserved in marine and lake sediments, and they maintain a scientific community trained over multiple decades in reading the fine print within such sediment cores. The reading so far is not encouraging. The rate of anthropogenic forcing of atmospheric CO_2 content and associated acidification of the oceans seems unprecedented in the last 50–60 million years of geological history. This suggests we are setting back the climate clock of Earth to a fundamentally different environment from the one that we have adapted to over many millennia.

The question is not about survival of humankind. It is about how quickly and profoundly such changes may take place, and therefore, if and how society can acclimatize to potentially drastic changes in precipitation patterns and climate zones, rising sea level, and ocean acidification—environmental conditions key to food production and infrastructure. Feedback mechanisms within Earth systems are highly complex and may result in tipping points, an "environmental earthquake" if you wish. We cannot afford not to use history as a guide for how rapidly and dramatically the global environment can change. Similarly, we need to study the records of past geohazards and the mechanisms by which they occur.

For the past three decades, planning for scientific drilling has pointed out global environmental change as a key research topic, and has with increasing prominence included geohazards over the last decade. In a time of program renewal (IODP in 2012–2013, ICDP in 2013–2014), many within the scientific community are concerned that such scientific foresight and preparedness to address key societal issues might not be broadly recognized. As a reader of *Scientific Drilling*, you can make a difference by explaining to the public and to funding agencies the high societal importance of scientific drilling—now and in the future.

Hans Christian Larsen
Editor-in-Chief

Ulrich Harms
Editor

Jamus Collier
Managing Editor

Front cover: Instruments deployed on the CORK installed in Hole U1362B on the eastern flank of the Juan de Fuca Ridge (Exp. 327), during Expedition AT18-07 (with the R/V *Atlantis* and the ROV *Jason*) in Summer 2011.
Left inset: A scientist analyzing clean samples in the core splitting room. (Exp.335)

Scientific Drilling

ISSN 1816-8957 (printed version)
1816-3459 (electronic version)

Scientific Drilling is a semiannual journal published by the Integrated Ocean Drilling Program (IODP) with the International Continental Scientific Drilling Program (ICDP). The editors welcome contributions on any aspect of scientific drilling, including borehole instruments, observatories, and monitoring experiments. The journal is produced and distributed by the Integrated Ocean Drilling Program Management International (IODP-MI) for the IODP under the sponsorship of the U.S. National Science Foundation, the Ministry of Education, Culture, Sports, Science and Technology of Japan, and other participating countries. The journal's content is partly based upon research supported under Contract OCE-0432224 from the National Science Foundation.

Electronic versions of this publication and information for authors can be found at http://www.iodp.org/scientific-drilling/ and http://www.icdp-online.org/scientific-drilling/. Printed copies can be requested from the publication office.

IODP is an international marine research drilling program dedicated to advancing scientific understanding of the Earth by monitoring and sampling subseafloor environments. Through multiple drilling platforms, IODP addresses its four principal challenges: Climate and Ocean Change, Biosphere Frontiers, Earth Connections, and Earth in Motion.

ICDP is a multi-national program designed to promote and coordinate continental drilling projects with a variety of scientific targets at drilling sites of global significance.

Publication Office
IODP-MI, Tokyo University of Marine Science and Technology,
Office of Liaison and Cooperative Research 3rd Floor,
2-1-6, Etchujima, Koto-ku, Tokyo
135-8533, JAPAN
Tel: +81-3-6701-3180
Fax: +81-3-6701-3189
e-mail: journal@iodp.org
url: www.iodp.org/scientific-drilling/

Copy Editing
Glen Hill, Obihiro, Japan

Layout, Production and Printing
Mika Saido (IODP-MI), and
Obun Printing, Co. Inc., Tokyo, Japan

IODP-MI
Tokyo, Japan
www.iodp.org
Program Contact: Miyuki Otomo
motomo@iodp.org

ICDP
GFZ German Research Center For Geosciences
www.icdp-online.org
Program Contact: Ulrich Harms
ulrich.harms@gfz-potsdam.de

All figures and photographs courtesy of the IODP or ICDP, unless otherwise specified.

Contents

Science Reports

Progress Reports

Technical Developments

Workshop Reports

News and Views

Schedules

IODP Expedition 327 and *Atlantis* Expedition AT 18-07: Observatories and Experiments on the Eastern Flank of the Juan de Fuca Ridge

by Andrew T. Fisher, Takeshi Tsuji, Katerina Petronotis, C. Geoff Wheat, Keir Becker, Jordan F. Clark, James Cowen, Katrina Edwards, Hans Jannasch, and the IODP Expedition 327 and *Atlantis* Expedition AT18-07 Shipboard Parties

doi:10.2204/iodp.sd.13.01.2011

Abstract

Integrated Ocean Drilling Program (IODP) Expedition 327 (summer 2010) was designed to resolve the nature of fluid-rock interactions in young, upper volcanic crust on the eastern flank of the Juan de Fuca Ridge. Expedition 327 drilled, cased and cored two new basement holes, conducted hydrogeologic experiments, and installed subseafloor borehole observatories (*Circulation Obviation Retrofit Kits*, CORKs). These CORKs were intended to allow borehole conditions to recover to a more natural state after the dissipation of disturbances caused by drilling, casing, and other operations; provide a long-term monitoring and sampling presence for determining fluid pressure, temperature, composition, and microbiology; and facilitate the completion of active experiments to resolve crustal hydrogeologic conditions and processes. Expedition 327 was followed (summer 2011) by R/V *Atlantis* Expedition AT18-07, with the remotely-operated vehicle (ROV) *Jason*, to service these CORKs, collect subseafloor pressure data, recover and deploy autonomous fluid and microbial samplers, collect large volumes of borehole fluids, and initiate a cross-hole hydrogeologic experiment using an electromagnetic flow meter. In addition, *Atlantis* Expedition AT18-07 refurbished an old CORK that could not be replaced during IODP Expedition 327, completing a critical part of the three-dimensional observation network that is currently being used to monitor a large-scale, directional formation response to long-term fluid flow from the crust.

Introduction and Goals

Fluid flow within volcanic ocean crust influences the thermal and chemical evolution of oceanic lithosphere and lithospheric fluids; subseafloor microbial ecosystems; diagenetic, seismic, and magmatic activity along plate-boundary faults; and the creation of ore deposits on and below the seafloor (Coggon et al., 2010; Huber et al., 2006; Parsons and Sclater, 1977). The global hydrothermal fluid mass flux through the upper oceanic crust rivals the global riverine fluid flux to the ocean, passing the volume of the oceans through the crust once every 10^5–10^6 y (Johnson and Pruis, 2003; Mottl, 2003; Wheat et al., 2003). Most of this flow occurs at relatively low temperatures, far from volcanically active seafloor-spreading centers where new ocean floor is created. This "ridge flank" circulation can be influenced by off-axis volcanic or tectonic activity but is driven mainly by the flow of lithospheric heat from below the crust.

Despite the importance of fluid-rock interactions in the crust, little is known about the magnitude and distribution of critical hydrologic properties; the rates and spatial extent of ridge-flank fluid circulation; the extent to which crustal compartments are well connected or isolated (laterally and with depth); or the links between ridge-flank circulation, crustal alteration, and geomicrobial processes. IODP Expedition 327 (Fisher, et al., 2011b) was part of a long-term experimental program that has included multiple survey, drilling, submersible, and ROV expeditions; observatory and laboratory testing, sampling, and monitoring; and modeling of coupled fluid-thermal-chemical-microbial processes. Expedition 327 built from the technical and scientific achievements and lessons learned during Ocean Drilling Program (ODP) Leg 168 (Davis et al., 1997), which focused on hydrothermal processes within uppermost basement rocks and sediments along an age transect, and IODP Expedition 301 (Fisher et al., 2005a), which penetrated deeper into the crust at the eastern end of the Leg 168 transect (Fig. 1). During both expeditions, CORKs were installed in basement holes to allow borehole conditions to recover to a more natural state after the dissipation of disturbances caused by drilling, casing, and other operations; to provide a long-term monitoring and sampling presence for determining fluid pressure, temperature, composition, and microbiology; and to facilitate the completion of active experiments to resolve crustal hydrogeologic conditions and processes (Fisher et al., 2005b, 2011c; Orcutt et al., 2010b; Wheat et al., in review). During subsequent ROV and submersible expeditions, borehole pressure and thermal data were collected, fluid and microbial samples were recovered, batteries, data loggers, and sampling systems were replaced, and long-term, cross-hole experiments were initiated.

We present operational results from IODP Expedition 327, which sailed on the D/V *JOIDES Resolution*, and R/V *Atlantis* and ROV *Jason* expedition AT18-07 (completed in 2011), focusing on the installation and use of CORKs. Data and samples gathered during the second expedition show that newly-installed CORKs are working as intended, and the ambitious monitoring and cross-hole experimental goals that motivated these experiments are being achieved.

Experimental Setting and Selected Earlier Work

Many studies have summarized geology, geophysics, basement-fluid composition, and hydrogeology within young seafloor on the eastern flank of the Juan de Fuca Ridge (Fig. 1; Davis et al., 1992; Elderfield et al., 1999; Hutnak et al., 2006; Wheat et al., 2000). Topographic relief associated with the Juan de Fuca Ridge axis and abyssal hill bathymetry on the ridge flank has helped trap turbidites flowing west from the continental margin (Underwood et al., 2005), resulting in the rapid burial of young oceanic basement rocks. Sediment cover is regionally thicker and more continuous towards the continental margin, but there are basement outcrops north and south of the Expedition 327 work area, up to 100 km east of the spreading center.

During ODP Leg 168, a transect of eight sites was drilled across 0.9–3.6 Ma seafloor; sediment, rock, and fluid samples were collected; thermal, geochemical, and hydrogeologic conditions in basement were determined; and CORKs were installed in the uppermost crust (Davis et al., 1997). Two of the Leg 168 observatories were placed in 3.5–3.6 Ma seafloor in Holes 1026B and 1027C, near the eastern end of the drilling transect (Fig. 1). IODP Expedition 301 returned to this area and drilled deeper into basement; sampled additional sediment, basalt, and microbiological materials; replaced the borehole observatory in Hole 1026B; and established two additional CORK observatories at Site U1301 (Fisher et al., 2005a).

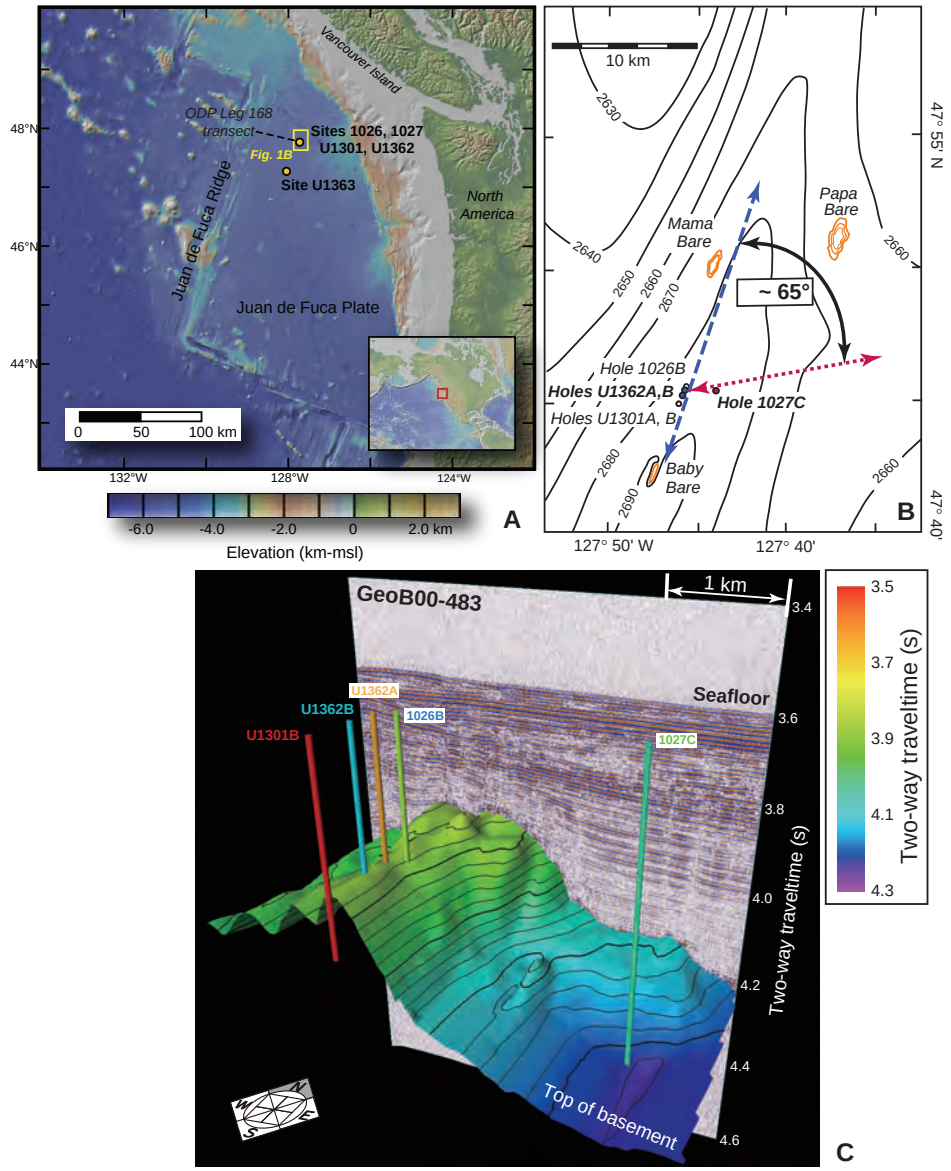

Figure 1. [A] Regional map of field area, eastern flank of the Juan de Fuca Ridge, with inset showing global location. Locations of the ODP Leg 168 transect and sites of IODP Expeditions 301 and 327 and Expedition AT18-07 are shown. [B] Seafloor bathymetric contour map of area around IODP Expedition 301 and 327 sites showing locations of CORK observatories (circles) in Holes 1026B, 1027C, U1301A, U1301B, U1362A, and U1362B, and nearby basement outcrops (gold bathymetric contours) where hydrothermal discharge has been observed (Davis et al., 1992; Wheat et al., 2004b). The blue dashed arrow shows the general structural trend of basement rocks, running sub-parallel to the active spreading center 100 km to the west. The red dotted arrow shows the heading between Holes U1362B and 1027C, which is oriented about 65° clockwise from the primary structural trend in basement. Depth contours in meters. [C] Three-dimensional perspective views of basement relief around CORK sites discussed in this paper. Relief is shown as two-way traveltime.

Before Leg 168 there was a largely two-dimensional view of the dominant fluid circulation pathways in this area, with recharge thought to occur close to the ridge where basement was exposed (near the western end of the Leg 168 transect), and flowing toward the east. Some results from Leg 168 were consistent with this view, including seafloor heat flow and basement temperatures that increase and basement fluids that are warmer and more altered with progression from west to east (Davis et al., 1999; Elderfield et al., 1999; Stein and Fisher, 2003). However, Leg 168 results and related surveys showed that ridge-parallel fluid transport is important in this region. For example, although basement fluids are

warmer and older with increasing distance from the ridge along the western end of the drilling transect, fluids are younger with respect to ^{14}C at additional Leg 168 sites to the east, although the eastern fluids are also warmer and more altered (Elderfield et al., 1999; Walker et al., 2007). Bathymetric data from near the western end of the Leg 168 transect show exposed basement north and south of the drill sites, which may allow hydrothermal fluids to recharge and discharge (Hutnak et al., 2006). Heat flow data from this area support this interpretation, as do geochemical and thermal data from the eastern end of the Leg 168 transect (Fisher et al., 2003; Wheat et al., 2000). Numerical models of outcrop-to-outcrop hydrothermal circulation between recharging and discharging seamounts show that rapid flow can be sustained (as a "hydrothermal siphon") and basement temperatures matched to observations if basement permeability along the flow path is about 10^{-11} m^2 (Hutnak et al., 2006).

Hydrologic (packer) experiments conducted in upper basement during Expedition 301 indicate a layered crustal structure with permeability on the order of 10^{-12}–10^{-11} m^2 (Becker and Fisher, 2008). Fisher et al. (2008) conducted additional hydrogeologic analyses using the formation pressure response to the long-term flow of cold bottom seawater into basement at Site U1301 in the thirteen months after drilling, as observed at Site 1027 (2.4 km away). Their data suggest large-scale permeability at the low end of or below values indicated by single-hole packer testing. This result was unexpected because cross-hole tests should be representative of a much larger crustal volume than single-hole tests, yielding higher apparent permeability values. One possible explanation is that basement permeability is azimuthally anisotropic, a hypothesis that is being tested with Expedition 327 CORKs (as described below).

CORKs installed in this area during ODP Leg 168 and IODP Expedition 301 have produced valuable fluid and microbial samples indicating the nature of linked geochemical and microbiological conditions in basement (Cowen et al., 2003; Orcutt et al., 2010a; Smith et al., in review; Wheat et al., 2004a, 2010). Cells collected from the Hole 1026B wellhead included bacteria and archaea whose closest known phylogenetic neighbors comprise nitrate reducers, thermophilic sulfate reducers, and thermophilic fermentative het-erotrophs. Fluid and microbial samples collected at depth in Holes 1026B and Hole U1301A indicate strongly reducing conditions within basement once recovery to a pre-drilling geochemical state was achieved, and with colonization of incubation substrate by the thermophilic anerobe Fermicutes and mesophilic oligotrophs. The highest cell counts within flow-through experiments from Hole U1301A were found on samples of olivine, and culturable organisms from these samples were capable of nitrate reduction and iron oxidation. Expedition 327 CORKs should provide even better samples of endemic microbial communities from the crust, as newer observatories were designed (a) to reduce the extent of contamination (by using inert materials where possible and coating reactive materials with nonreactive coatings) and (b) to simplify and speed the extraction of large quantities of fluid (using larger diameter tubing and custom fittings).

IODP Expedition 327

The primary goals of Expedition 327 were (1) to drill two new basement holes at Site U1362, core and wireline log one of these holes, run and initiate hydrogeologic tests, and install CORK observatories; (2) to recover an existing CORK from Hole 1027C, deepen the hole and install a new CORK; and (3) to recover and replace an instrument string deployed in the CORK in Hole U1301B (Fisher, et al., 2011b). Secondary objectives included sampling and analyzing sediments and pore fluids near an area of suspected hydrothermal recharge to assess patterns and rates of ridge-flank hydrothermal circulation in basement.

Holes U1362A and U1362B were drilled and cased through the upper ~100 m of basement, without coring, in order to avoid unstable layers and to allow greater depth penetration into the crust (Fig. 2a). Hole U1362A was drilled and cored to 528 meters below seafloor (mbsf), 292 meters sub-basement, 200 m south of Hole 1026B (Fig. 1). Core recovery was ~30%, typical for upper crustal rocks, and eight lithologic units were identified. Numerous samples were collected for post-expedition petrologic, alteration, physical properties, and microbiological analyses. A single wireline logging string helped to determine formation prop-erties and to identify suitable intervals for hydrologic testing and CORK installation. Caliper logs revealed an enlarged borehole over most of the open interval, but there were several near-gauge sections generally corresponding to intervals that produced good core recovery and/or drilled slowly. Short-term packer experiments were completed at depth in Hole U1362A to assess permeability adjacent to the borehole, with hourly injection and recovery periods.

Hole U1362B was drilled to 359 mbsf (117 meters sub-basement), 300 m south of Hole U1362A and 500 m north of Hole U1301B (Fig. 1). A 24-h pumping and tracer injection experiment was initiated prior to CORK installation in this hole (Fisher et al., 2011a). Pressure gauges and fast-sampling reverse osmotic pumps were run in a specially designed "stinger" that extended into the open hole just below the base of casing, which was sealed with a casing running tool. During this experiment, seawater was pumped into the formation at ~7 L s^{-1}. Tracers added during pumping included SF_6 gas (injected continuously for ~22 h), CsCl and $ErCl_3$ salts (during a brief period 3 h into the experiment) and CsCl and $HoCl_3$ salts (at 19 h), fluorescent microspheres (at 20 h), and stained bacteria (at 21 h) extracted from sea-surface water. Fresh water was pumped rather than seawater during two, hour-long periods. Evaluation of tracer transport in the

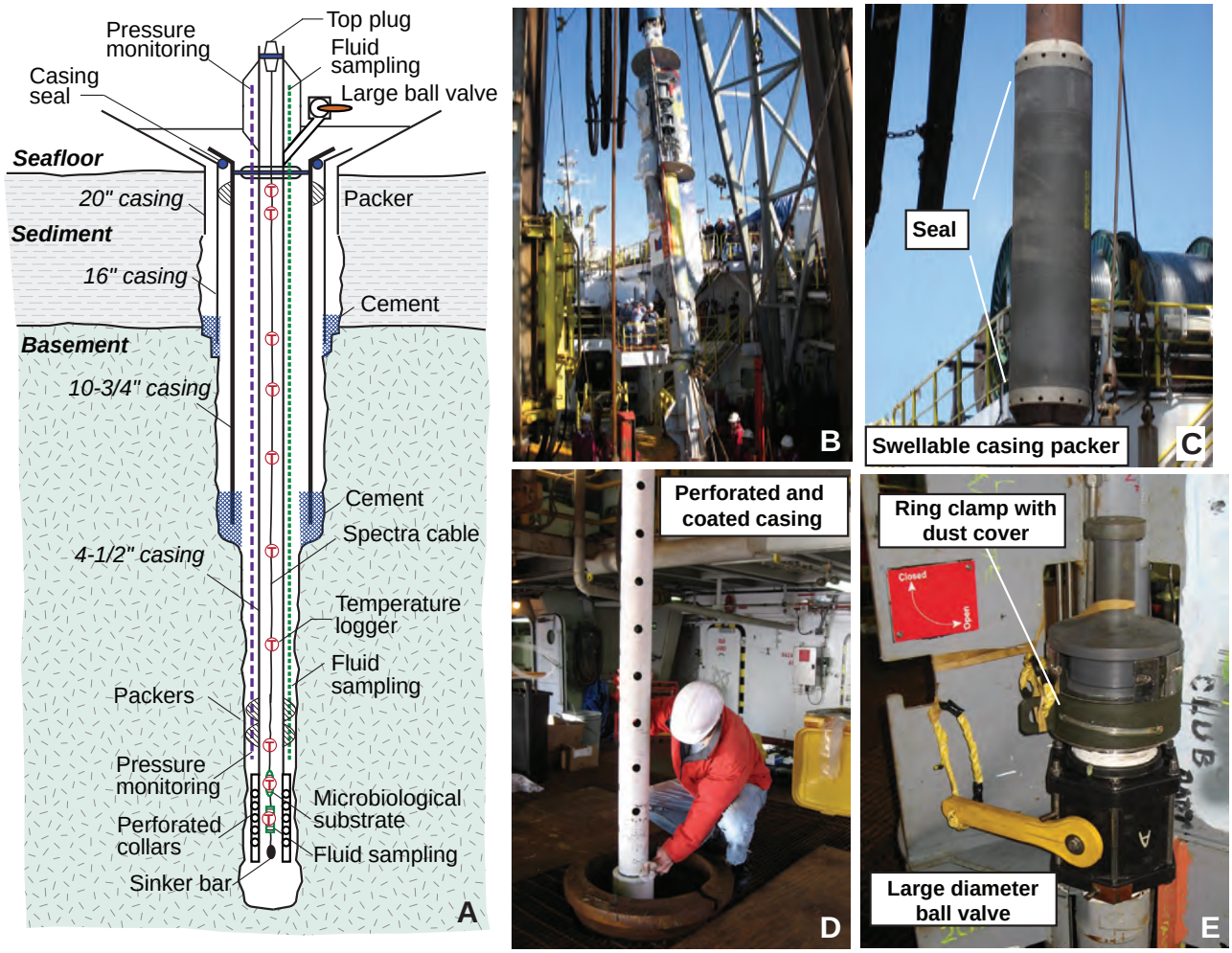

Figure 2. Diagram and photographs showing features of CORK systems deployed during IODP Expedition 327. [A] Schematic of hole completion and design of CORKs deployed in Holes U1362A and U1362B. The upper ~100 m of basement was drilled and cased to improve hole stability. Expedition 327 CORKs are built around two concentric casing strings, with multiple seals at different depths, instruments mounted on the wellhead and downhole, and the ability to monitor and sample from more than one depth interval. They also have perforated and coated drill collars and casing at depth, two kinds of CORK and casing packers (inflatable and swellable), and a ball valve above a lateral pipe that can be used for long-term free-flow experiments. Downhole temperatures are recorded with autonomous sensor and logging instruments incorporated into the fluid and microbiological samplers or hung independently from a cable. [B] CORK wellhead being hoisted on the rig floor during Expedition 327. [C] Swellable packer element, which expands during reaction with fluid in the borehole to seal against casing or the open formation. [D] Perforated and coated casing being cleaned with alcohol prior to deployment. [E] Ball valve in wellhead to be used for free-flow experiment and sampling.

crust will require recovery of borehole samplers from nearby CORKs, as discussed below.

The CORK systems deployed during Expedition 327 to isolate and allow monitoring and sampling of basement fluids and microbes include multiple types of casing and borehole seals (Fig. 2a). The part of the CORK that sits above the seafloor when installed—referred to as the "wellhead"—is constructed from concentric 4½-inch and 10¾-inch casing sections, with parts of the larger casing omitted or cut away between horizontally oriented bulkheads (Fig. 2b). Seafloor sampling and valve manifolds, sensor packages, data loggers, and samplers offset by 120° are arranged within three bays, and separated by vertical gussets. The gussets provide strength to the wellhead, help to guide the ship's camera system and the submersible platform around the bays during CORK installation, and serve as submersible and ROV handholds for stability and leverage. For each of the Expedition 327 CORKs, one bay is dedicated to monitoring and logging pressure data, another is configured for fluid sampling, and a third designed to house a flowmeter and permit microbiological sampling and other experiments.

Expedition 327 CORKs use two kinds of packers to isolate one or more borehole intervals: hydraulic (inflatable) and swellable packers (Fig. 2c). Inflatable packer elements provide an immediate seal, but their long-term reliability is unknown. Swellable elements react with seawater and expand over several months, and should provide a seal that lasts for years. The lower parts of these CORKs (extending down from the base of the lowermost set of packers) are extensively coated with non-reactive materials (Fig. 2d). Perforated and coated casing and drill collars in these CORKs house downhole instruments (fluid samplers, tem-

perature sensors, microbiological growth substrate) that remain in good communication with the surrounding fluids and rocks and are protected from collapse of unstable formation (ensuring future recovery). The Expedition 327 CORKs also have a pipe that comes off the central casing near the wellhead, ending with a ball valve and ring clamp (Fig. 2e). Opening this valve allows overpressured formation fluids to flow from the wellhead without having to remove the top plug. These fluids can be sampled and the rate of flow from the CORK measured, as described below.

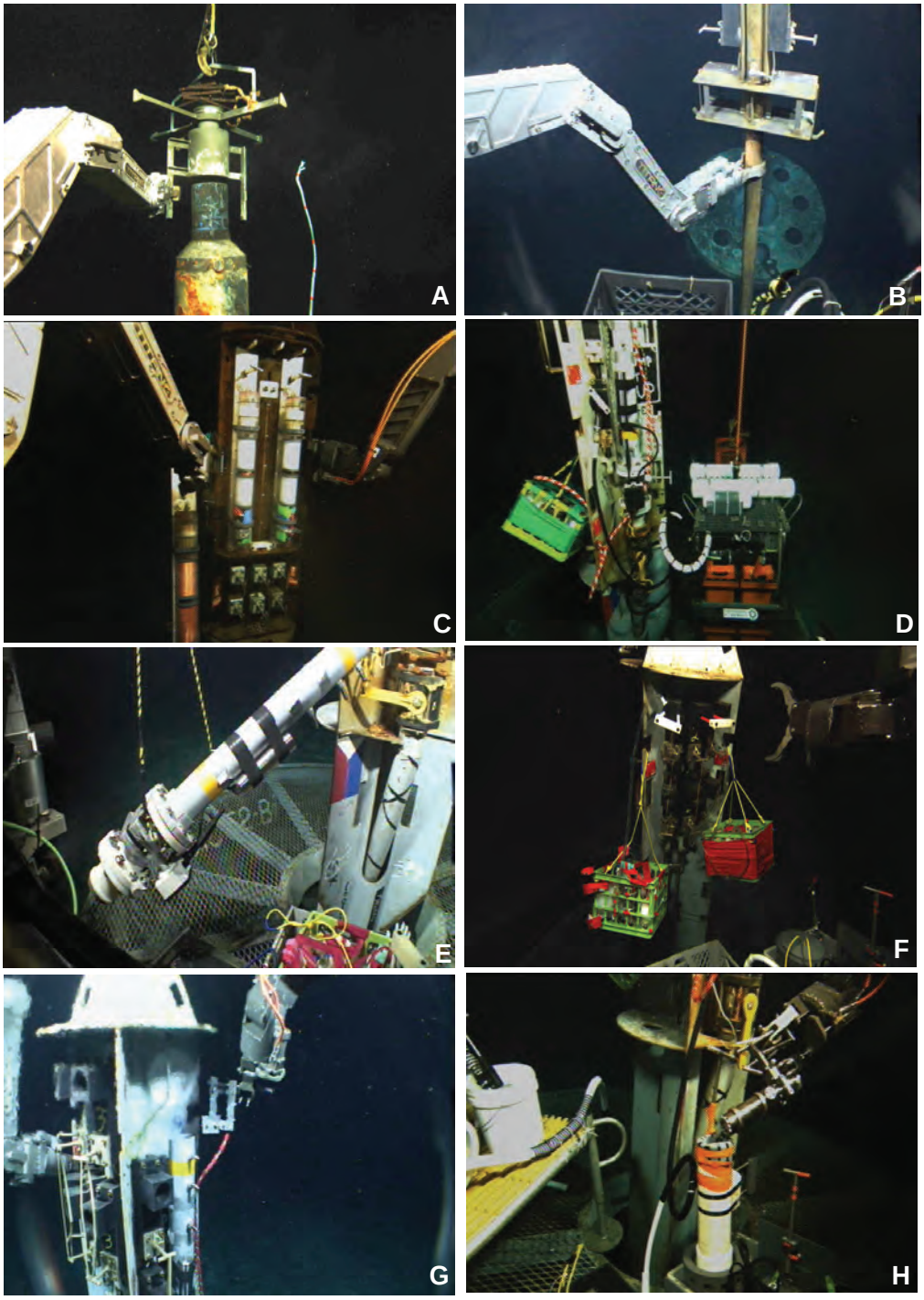

Figure 3. Photographs of CORK servicing activities during Expedition AT18-07. [A] Top Hat Extraction Tool deployed on old CORK wellhead in Hole 1027C. This tool is being used to remove an old electrical connector that was corroded in place, blocking access to the data logger. [B] Manifold insert being carried to CORK in Hole 1027C after removal of old connector and data logger. This tool has valves and fitting for pressure monitoring and a large ball valve and ring clamp (Fig. 2e) that can be used for later instrument deployments. [C] Exchanging OsmoSamplers on CORK in Hole U1301B. Samplers are (left to right): copper (gas tight), geochemistry (Teflon), microbiology. [D] OsmoSamplers in milk crate and GeoMICROBE sled deployed on ROV platform in Hole U1362B. [E] Flowmeter being lifted for deployment on Hole U1362B. [F] Multiple OsmoSampler crates deployed on CORK in Hole U1362A. [G] Fluid sampling inlet being deployed at top of chimney discharging shimmering hydrothermal fluids on Hole U1362B. [H] Gas-tight sampler being used with gas trap to collect fluids from Hole U1362A.

The Hole U1362A CORK was configured to monitor two basement intervals. Pressure in both intervals is monitored through stainless steel tubing connected to mini-screens installed just below inflatable packers at the top of distinct crustal intervals. Stainless steel fluid sampling lines terminate at two depths. A single polytetrafluoroethylene (PTFE) microbiological sampling line ends in a titanium mini-screen. The downhole instrument string includes six OsmoSamplers and microbial growth incubators positioned within coated and perforated casing and collars, and eleven autonomous tem-perature probes.

The Hole U1362B CORK monitors a single basement interval that extends ~75 m below swellable and inflatable packers positioned just inside the base of casing. Pressure is monitored continuously in this basement interval and also in the cased interval above to assess the quality of hydraulic sealing of this observatory. This CORK also contains stainless steel fluid sampling lines and a dedicated PTFE microbiological sampling line. The downhole instrument string comprises six OsmoSamplers, and microbial growth incubators and eight autonomous temperature probes, including two installed in OsmoSamplers suspended inside the perforated and coat-ed casing and collars at depth.

Despite the use of a special unlatching tool and consider-

able force to pull, push, and rotate, Expedition 327 failed to recover the old CORK deployed in Hole 1027C and to install a new, multi-level CORK in the deepened well. But as described in the next section, we were able to retrofit the Hole 1027C CORK with new pressure monitoring equip-ment in summer 2011, allowing this CORK to be used for crustal-scale, multi-directional, hydrogeologic experiments.

R/V *Atlantis* and ROV *Jason* Expedition AT18-07

During *Atlantis* Expedition AT18-07, we planned and accomplished the following goals.

- recovery of wellhead OsmoSampling systems deployed on pre-Expedition 327 CORKs, and deployment of new OsmoSampling systems on the new CORKs (for geochemical sampling and microbial growth experiments)
- downloading of long-term pressure data
- assessment of the condition and retrofitting the old CORK in Hole 1027C for pressure monitoring
- recovery and deployment of a long-term GeoMICROBE sled used for autonomous, large-volume fluid sampling and electrochemistry
- collection of large volumes of fluids from depth below the CORKs using a variety of pumping, sampling, and filtering systems
- deployment of an autonomous flowmeter on one of the Site U1362 CORKs, followed by opening of a ball valve to initiate a long-term, cross-hole flow experiment.

Of the planned operations, our ability to retrofit the CORK in Hole 1027C was the least certain when Expedition AT18-07 began. We did not know if we had damaged the CORK with the vigorous recovery attempt during Expedition 327, and we rushed to design and built a series of tools to upgrade measurement and sampling capabilities in time for the subsequent expedition. The first necessary step was to extract a brass connector that was corroded in place on top of the wellhead (Fig. 3a). This eventually required using a customized harness hanging from below the ROV control vehicle *Medea* to pull out the connector. The old data logger was recovered at the same time, and it subsequently produced a complete pressure record from the previous two years (including the pressure response to nearby drilling during Expedition 327). We were then able to install a manifold insert with valves and fittings (Fig. 3b) and connect a new pressure logger for high-resolution monitoring. We were gratified to see almost immediate pressure equilibration in Hole 1027C following these operations, indicating that the Hole 1027C CORK is sealed and providing reliable information on formation fluid pressure.

Pressure data downloaded from the new CORKs at Site U1362 show that they are functioning as intended. We can see different equilibrium pressures at different depths in Hole 1362A (which isolates distinct crustal intervals) and the setting of the swellable packer element at the base of casing in Hole U1362B (where we have continuous monitoring of the cased interval). OsmoSampler systems were recovered and replaced on older CORKs (Fig. 3c), and new systems were successfully deployed on new CORKs in Holes U1362A and U1362B (Fig. 3d, f). The GeoMICROBE sampling and electrochemical analysis sled was recovered from Hole U1301A (where it had been deployed) and redeployed on the CORK in Hole U1362B (Fig. 3d), where it will filter and collect large volumes of fluid and make electrochemical measurements over the next year. A new electromagnetic flow-meter was deployed above the large-diameter ball valve on the Hole U1362B wellhead (Fig. 3e); opening this valve resulted in a jet of warm (~63°C) hydrothermal fluid from the crust below. The flowmeter is recording fluid discharge hourly, and we will return to recover the tool and download the data in summer 2012. Fluid flow from Hole U1362B is expected to decrease with time over the next year, as the excess pressure in the sealed borehole is reduced. This record of time-varying flow, and the associated pressure responses in nearby observatories, will provide the first direct assessment of azimuthal hydrologic properties in the upper oceanic crust.

The inlets to fluid sampling lines were placed in the top of the "chimney" above the flowmeter after the valve was opened, and discharging fluids are being collected with geochemical and microbiological OsmoSamplers (Fig. 3g). Large volumes of high quality formation fluids were recovered from the new CORKs using pump and manifold systems in 2011 (Fig. 3h), and these CORKs will be visited again for fluid sampling in 2012. Samples recovered in 2011 are being analyzed to learn about formation chemistry and microbiology, and to assess the possible arrival of tracers pumped during the 24-hour injection experiment during IODP Expedition 327. The best tracer samples are likely to come from downhole samplers, which will be recovered over the next several years.

Acknowledgements

We thank the staff of Transocean and the U.S. Implementing Organization for IODP for their dedicated work in preparing for IODP Expedition 327. CORK servicing was skillfully supported by the crew, technicians and officers of the R/V *Atlantis* and ROV *Jason*. These experiments were supported by the U.S. National Science Foundation grants OCE-0727952 and OCE-1031808 (ATF), OCE-0727119 and OCE-1030061 (CGW), OCE-0726887 and OCE-1030350 (KB), OCE-0726563 and OCE-1031352 (JFC),

and MCB-0604014 and OCE-0726838 (JPC). Additional support provided by the Gordon and Betty More Foundation (KJE and CGW). This is contribution #111 from the Center for Dark Energy Biosphere Investigations.

The IODP Expedition 327 Scientists

A. Fisher, T. Tsuji, K. Petronotis, K. Becker, J. Cowen, J.M. Gautier, A. Haddad, J. Kane, S. Keske, M. Harris, S. Hulme, F. Ji, R. Masui, H. Miyamoto, S. Morvan, S. Mrozewski, B. Orcutt, L. Peart, B. Richardson, J. Rutter, B. Thiberge, C.G. Wheat, and D. Winslow

Atlantis Expedition AT18-07 Shipboard Parties

A. Fisher, K. Becker, J. Clark, S. Cooper, J. Cowen, K. Edwards, B. Glazer, S. Hulme, B. Orcutt, C.G. Wheat, A. Ausejo-Robador, R. Brennon, A. Gross, K. Hamner, C.-C. Hseih, S. Jungbluth, J. Kane, H.-T. Lin, G. Ramirez, J. Ringlein, A. Slovacek, and L. Strong

References

Becker, K., and Fisher, A.T., 2008. Borehole tests at multiple depths in 3.5-Ma seafloor resolve distinct hydrologic intervals. *J. Geophys. Res.*, 113:B07105. doi:10.1029/2007JB005446

Coggon, R.M., Teagle, D.A.H., Smith-Duque, C.E., Alt, J.C., and Cooper, M.J., 2010. Reconstructing past seawater Mg/Ca and Sr/Ca from mid-ocean ridge flank calcium carbonate veins. *Science*, 327(5969):1114–1117. doi:10.1126/science.1182252

Cowen, J.P., Giovannoni, S.J., Kenigm, F., Johnson, H.P., Butterfield, D., Rappé, M.S., Hutnak, M., and Lam, P., 2003. Fluids from aging ocean crust that support microbial life. *Science*, 299:120–123. doi:10.1126/science.1075653

Davis, E.E., Chapman, D.S., Mottl, M.J., Bentkowski, W.J., Dadey, K., Forster, C., Harris, R., Nagihara, S., Rohr, K., Wheat, G., and Whiticar, M., 1992. FlankFlux: An experiment to study the nature of hydrothermal circulation in young oceanic crust. *Can. J. Earth Sci.*, 29(5):925–952.

Davis, E.E., Chapman, D.S., Wang, K., Villinger, H., Fisher, A.T., Robinson, S.W., Grigel, J., Pribnow, D., Stein, J., and Becker, K., 1999. Regional heat-flow variations across the sedimented Juan de Fuca Ridge eastern flank: Constraints on lithospheric cooling and lateral hydrothermal heat transport. *J. Geophys. Res.*, 104(B8):17675–17688.

Davis, E.E., Fisher, A.T., and Firth, J., 1997. *Proc. ODP, Init. Repts.* 168, College Station, TX (Ocean Drilling Program).

Elderfield, H., Wheat, C.G., Mottl, M.J., Monnin, C., and Spiro, B., 1999. Fluid and geochemical transport through oceanic crust: A transect across the eastern flank of the Juan de Fuca Ridge. *Earth Planet. Sci. Lett.*, 172:151–165. doi:10.1016/S0012-821X(99)00191-0.

Fisher, A.T., Cowen, J., Wheat, C.G., and Clark, J.F., 2011a. Preparation and injection of fluid tracers during IODP Expedition 327, eastern flank of Juan de Fuca Ridge. *In* Fisher, A.T., Tsuji, T., and Petronotis, K., *Proc. IODP,* 327: Tokyo (Integrated Ocean Drilling Program Management International, Inc.). doi:10.2204/iodp.proc.2327.2108.2011

Fisher, A.T., Davis, E.E., and Becker, K., 2008. Borehole-to-borehole hydrologic response across 2.4 km in the upper oceanic crust: implications for crustal-scale properties. *J. Geophys. Res.*, 113:B07106. doi:10.1029/2007JB005447

Fisher, A.T., Davis, E.E., Hutnak, M., Spiess, V., Zühlsdorff, L., Cherkaoui, A., Christiansen, L., et al., 2003. Hydrothermal recharge and discharge across 50 km guided by seamounts on a young ridge flank. *Nature*, 421:618–621. doi:10.1038/nature01352

Fisher, A.T., Tsuji, T., and Petronotis, K., 2011b. *Proc. IODP,* 327: Tokyo (Integrated Ocean Drilling Program Management International, Inc.). doi:10.2204/iodp.proc.327.2011

Fisher, A.T., Urabe, T., and Klaus, A., 2005a. *Proc. IODP,* 301: Washington, DC (Integrated Ocean Program Management International, Inc.). doi:10.2204/iodp.proc.2301.2005 pp

Fisher, A.T., Wheat, C.G., Becker, K., Cowen, J., Orcutt, B., Hulme, S., Inderbitzen, K., et al., 2011c. Design, deployment, and status of borehole observatory systems used for single-hole and cross-hole experiments, IODP Expedition 327, eastern flank of the Juan de Fuca Ridge. *In* Fisher, A.T., Tsuji, T., and Petronotis, K., *Proc. IODP*, 327: Tokyo(Integrated Ocean Drilling Program Management International, Inc.). doi:10.2204/iodp.proc.327.107.2011

Fisher, A.T., Wheat, C.G., Becker, K., Davis, E.E., Jannasch, H., Schroeder, D., Dixon, R., et al., 2005b. Scientific and technical design and deployment of long-term, subseafloor observatories for hydrogeologic and related experiments, IODP Expedition 301, eastern flank of Juan de Fuca Ridge. *In* Fisher, A.T., Urabe, T., and Klaus, A., *Proc. IODP*, 301: Washington, DC (Integrated Ocean Drilling Program Management International, Inc.). doi:10.2204/iodp.proc.2301.2103.2005

Huber, J.A., Butterfield, D.A., Johnson, H.P., and Baross, J.A., 2006. Microbial life in ridge flank crustal fluids. *Env. Microbiol.*, 88:88–99. doi:10.1111/j.1462-2920.2005.00872.x

Hutnak, M., Fisher, A.T., Zühlsdorff, L., Spiess, V., Stauffer, P., and Gable, C.W., 2006. Hydrothermal recharge and discharge guided by basement outcrops on 0.7-3.6 Ma seafloor east of the Juan de Fuca Ridge: Observations and numerical models. *Geochem. Geophys. Geosys.*, 7:Q07O02. doi:10.1029/2006GC001242

Johnson, H.P., and Pruis, M.J., 2003. Fluxes of fluid and heat from the oceanic crustal reservoir. *Earth Planet. Sci. Lett.*, 216:565–574. doi:10.1016/S0012-821X(03)00545-4

Mottl, M., 2003. Partitioning of energy and mass fluxes between mid-ocean ridge axes and flanks at high and low temperature. *In* Halbach, P., Tunnicliffe, V., and Hein, J. (Eds.), *Energy and Mass Transfer in Submarine Hydrothermal Systems:* Berlin (Dahlem University Press), 271–286.

Orcutt, B.N., Bach, W., Becker, K., Fisher, A.T., Hulme, S., Toner, B.M., Wheat, C.G., and Edwards, K.J., 2010a. Microbial borehole observatories deployed within the oceanic crust: Design considerations and initial results from long-term colonization experiments. [Invited paper presented at American Geophysical Union 2010 Fall Meeting, San Francisco, CA, 12–17 December 2010]. doi:10.1080/

01490450903456772

Orcutt, B.N., Wheat, C.G. and Edwards, K., 2010b. Subseafloor ocean crust microbial observatories: Development of FLOCS (FLow-through Osmo Colonization System) and evaluation of borehole construction materials. *Geomicrobiol. J.*, 27:143–157. doi:10.1080/01490450903456772

Parsons, B., and Sclater, J.G., 1977. An analysis of the variation of ocean floor bathymetry and heat flow with age. *J. Geophys. Res.*, 82:803–829. doi:10.1029/JB082i005p00803

Smith, A., Popa, R., Fisk, M., Nielsen, M., Wheat, C.G., Jannasch, H., Fisher, A.T., Becker, K., Sievert, S., and Flores, G., in review. A novel method for studying *in situ* microbial colonization of igneous minerals and glasses in ocean crust. *Geochem. Geophys. Geosys.*

Stein, J.S., and Fisher, A.T., 2003. Observations and models of lateral hydrothermal circulation on a young ridge flank: Numerical evaluation of thermal and chemical constraints. *Geochem. Geophys. Geosys.*, 4:1026. doi:10.1029/2002GC000415

Underwood, M., Hoke, K.D., Fisher, A.T., Giambalvo, E.G., Davis, E.E., and Zühlsdorff, L., 2005. Provenance, stratigraphic architecture, and hydrogeologic effects of turbidites in northwestern Cascadia Basin, Pacific Ocean. *J. Sediment. Res.*, 75(1):149–164. doi:10.2110/jsr.2005.012

Walker, B.D., McCarthy, M.D., Fisher, A.T., and Guilderson, T.P., 2007. Dissolved inorganic carbon isotopic composition of low-temperature axial and ridge-flank hydrothermal fluids of the Juan de Fuca Ridge. *Mar. Chem.*, 108(1–2):123–136. doi:10.1016/j.marchem.2007.1011.1002

Wheat, C.G., Elderfield, H., Mottl, M.J., and Monnin, C., 2000. Chemical composition of basement fluids within an oceanic ridge flank: Implications for along-strike and across-strike hydrothermal circulation. *J. Geophys. Res.*, 105(B6):13437–13447. doi:10.1029/2000JB900070

Wheat, C.G., Jannasch, H.W., Fisher, A.T., Becker, K., Sharkey, J., and Hulme, S.M., 2010. Subseafloor seawater-basalt-microbe reactions: Continuous sampling of borehole fluids in a ridge flank environment. *Geochem. Geophys. Geosys.*, 11:Q07011. doi:10.1029/2010GC00305

Wheat, C.G., Jannasch, H.W., Kastner, M., Hulme, S., Cowen, J., Edwards, K., Orcutt, B., and Glazer, B., in review. Fluid sampling from oceanic borehole observatories: Design and methods for CORK activities (1990–2010). *In* Fisher, A.T., Tsuji, T., and Petronotis, K., *Proc. IODP,* 327: Washington, DC (Integrated Ocean Drilling Program Management International, Inc.). doi:10.2204/iodp.proc.327.109.2011

Wheat, C.G., Jannasch, H.W., Kastner, M., Plant, J.N., DeCarlo, E., and Lebon, G.T., 2004a. Venting formation fluids from deep-sea boreholes in a ridge flank setting: ODP Sites 1025 and 1026. *Geochem. Geophys. Geosys.*, 5(8):Q08007. doi:08010.01029/02004GC000710.

Wheat, C.G., McManus, J., Mottl, M., and Giambalvo, E.G., 2003. Oceanic phosphorus imbalance: Magnitude of the mid-ocean ridge flank hydrothermal sink. *Geophys. Res. Lett.*, 30:1895. doi:10.1029/2003GL017318

Wheat, C.G., Mottl, M.J., Fisher, A.T., Kadko, D., Davis, E.E., and Baker, E., 2004b. Heat flow through a basaltic outcrop on a sedimented young ridge flank. *Geochem. Geophys. Geosys.*, 5(12):Q12006. doi:10.1029/2004GC000700

Authors

Andrew T. Fisher, Earth and Planetary Sciences Department and Institute for Geophysics and Planetary Physics, University of California at Santa Cruz, 1156 High Street, Santa Cruz, CA 95064, U.S.A., e-mail: afisher@ucsc.edu.

Takeshi Tsuji, Graduate School of Engineering, Kyoto University, C1-1-110 Kyotodaigaku-Katsura, Nishikyo-ku, Kyoto 615-8540, Japan.

Katerina Petronotis, Integrated Ocean Drilling Program, Texas A&M University, 1000 Discovery Drive, College Station, TX 77845-9547, U.S.A.

C. Geoff Wheat, Global Undersea Research Unit, P.O. Box 475, Moss Landing, CA 95039, U.S.A.

Keir Becker, Rosenstiel School of Marine and Atmospheric Science, University of Miami, Division of Marine Geology and Geophysics, 4600 Rickenbacker Causeway, Miami, FL 33149-1098, U.S.A.

Jordan F. Clark, Department of Earth Science and Program of Environmental Studies, University of California Santa Barbara, 1006 Webb Hall, Santa Barbara, CA 93106-9630, U.S.A.

James Cowen, Department of Oceanography, University of Hawaii at Manoa, 1000 Pope Road, Marine Sciences Building, Honolulu, HI 96822, U.S.A.

Katrina Edwards, Center for Earth Sciences, University of Southern California, 3651 Trousdale Parkway, Los Angeles, CA 90089-0740, U.S.A.

Hans Jannasch, Monterey Bay Aquarium Research Institute, 7700 Sandholt Road, Moss Landing, CA, 95039, U.S.A.

and the IODP Expedition 327 and *Atlantis* Expedition AT18-07 Shipboard Parties

Photo Credits

Photographs were provided courtesy of Andrew Fisher (UCSC), the AT18-07 Shipboard Party, and the U.S. National Deep Submergence Facility (WHOI)

IODP Expedition 328: Early Results of Cascadia Subduction Zone ACORK Observatory

by Earl Davis, Martin Heesemann, and the IODP Expedition 328 Scientists and Engineers

doi:10.2204/iodp.sd.13.02.2011

Abstract

Integrated Ocean Drilling Program (IODP) Expedition 328 was devoted to the installation of an "Advanced CORK" (Circulation Obviation Retrofit Kit) in the Cascadia subduction zone accretionary prism to observe the physical state and properties of the formation as they are influenced by long-term and episodic deformation and by gas hydrate accumulation. Pressures are monitored at four levels on the outside of a standard 10¾-inch casing string, two above and two below the base of the gas-hydrate stability zone at 230 mbsf (m below seafloor). The casing was sealed at the bottom, leaving the inside open down to 302 mbsf for installation of a tilt meter, seismometer, and thermistor cable (scheduled for 2013). The initial data, recovered in July 2011, document an initially smooth recovery from the drilling perturbation followed by what may be a sequence of hole-collapse events. Pressure at the deepest screen is roughly 40 kPa above hydrostatic; higher pressures (80 kPa) are observed at the two screens close to the level of hydrate stability. Tidal variations at the deepest screen are in phase with ocean tides, and define a loading efficiency of 0.6, which is reasonable in light of the consolidation state of the for-mation (porosity ~0.5). Tidal signals near the level of gas hydrate stability display large phase lags, probably as a consequence of hydraulic diffusion stimulated by the large contrast in interstitial fluid compressibility at the gas-hydrate boundary. The degree of isolation among the screens, the anticipated good coupling, and the estimated strain-to-pressure conversion efficiency (~5 kPa μstrain^{-1}) indicate that this installation will serve well to host a variety of hydrologic, seismic, and geodynamic experiments.

Introduction

Operations carried out during IODP Expedition 328 were devoted to the installation of a borehole hydrologic observatory near ODP Site 889, the location chosen for one of the first CORK observatories during ODP Leg 146 in 1992 (Westbrook et al., 1994; Davis et al., 1995). In that early attempt, the relatively unstable sediments of the formation intruded rapidly through the perforations and bottom of an open-ended casing liner and prevented proper sealing of the hole. The new installation utilized the ACORK design, developed initially for installations at the Nankai subduction zone during ODP Leg 196 to permit pressure monitoring at multiple formation levels on the outside of a 10¾-inch casing string. The casing is sealed at the bottom, leaving the inside fully isolated from the formation but available for future installations of additional monitoring instruments.

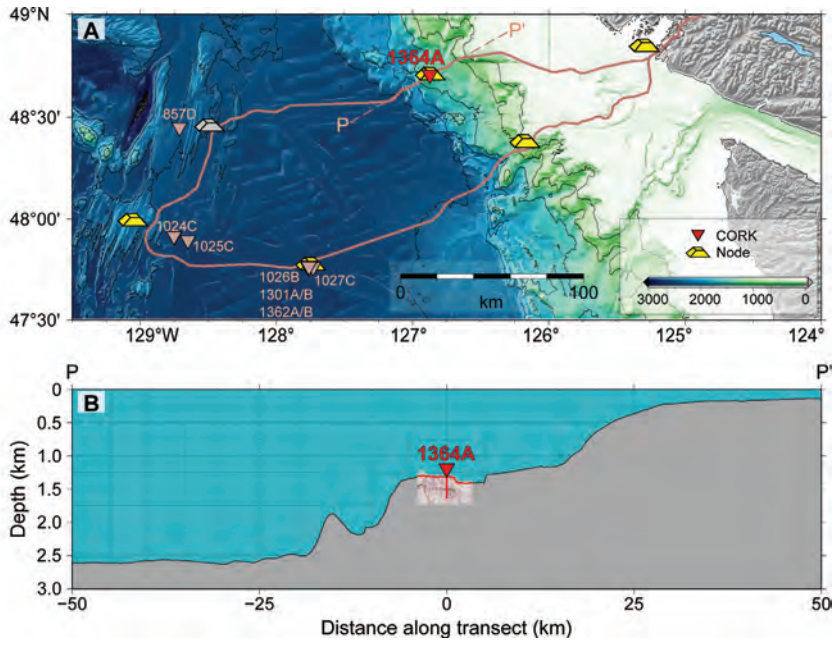

Figure 1. [A] Regional map of East Pacific near Vancouver Island and [B] topographic/bathymetric profile showing context of IODP Hole U1364A roughly 18 km landward of the toe of the accretionary prism, and other "CORKed" boreholes where pressure monitoring is underway. Hole 1026B is currently connected to the NEPTUNE Canada fiber-optic cable (route and nodes shown), and a connection at Hole U1364A is planned for 2013. Location of bathymetric profile P-P' is shown in [A], and location of seismic reflection profile shown in Fig. 2 is indicated on the bathymetric profile as a thumbnail image.

A broad range of objectives will be addressed with monitoring over the decades to come, some the same as those to have been addressed by the original CORK installation in Hole 889C including documenting the average state of pressure and constraining the vertical component of fluid flow from the consolidating sediments in the frontal part of the Cascadia accretionary prism, and investigating the mode of formation of gas hydrates. Other objectives have been added

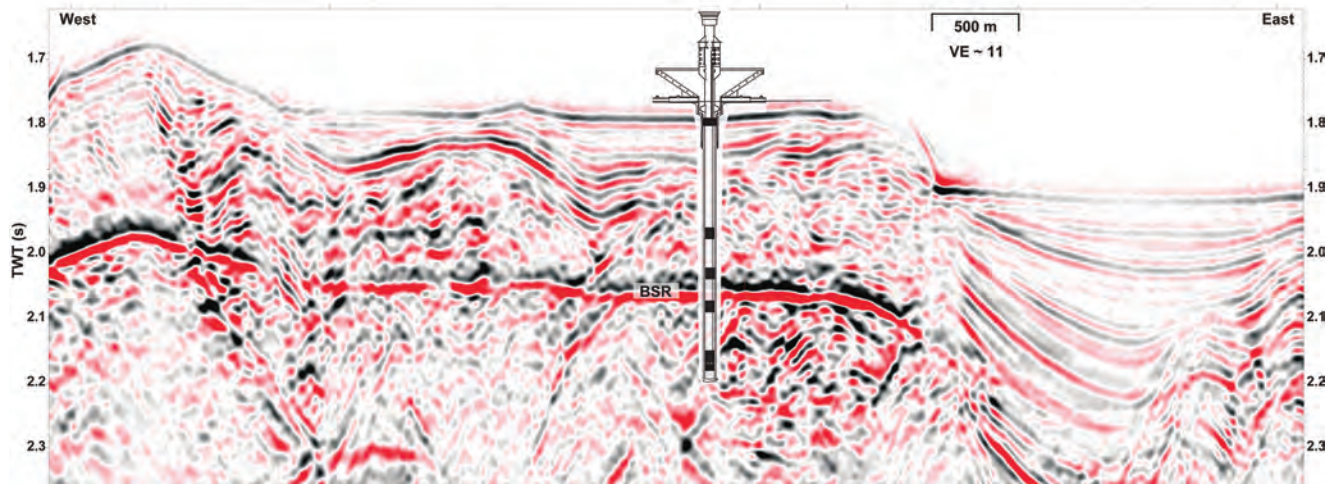

Figure 2. Seismic reflection profile crossing Hole U1364A, showing gently deformed slope basin sediments, strongly deformed accretionary prism sediments, and a bottom-simulating reflector (BSR) marking the boundary between hydrate-bearing sediments above and gas-bearing pore water below. Position of the ACORK with its monitoring screens is indicated. Profile location is shown in Fig. 1b.

subsequently as a result of the multiple discrete monitoring levels provided by the ACORK configuration, advances in measurement resolution and sampling frequency, and knowledge gained from other monitoring experiments. These include determining the influence of gas hydrates and free gas on the mechanical properties of their host lithology, the response of the formation to seismic ground motion, and the magnitude of strain at the site caused by any episodic seismic or aseismic slip in this subduction setting. Instrumentation deployed at the time of drilling includes autonomously recording seafloor and formation pressure and seafloor temperature sensors. Sensors planned for deployment inside the sealed casing at a later date will measure temperature, tilt, and seismic ground motion. In 2013, all instruments will be connected to the NEPTUNE Canada fiber-optic cable for power and real-time communications. This will provide a greater sampling rate, time accuracy, and monitoring lifetime than what is possible with autonomous operations using battery power and local data storage.

Geologic Setting

As shown in Fig. 1, IODP Site U1364 lies 18 km landward of the toe of the Cascadia subduction zone accretionary prism, where much of the thick section of turbidite and hemipelagic sediments deposited on the eastern flank of the Juan de Fuca Ridge are scraped off the underthrusting oceanic crust (Davis and Hyndman, 1989; Hyndman et al., 1990; Westbrook et al., 1994). Convergence of the Juan de Fuca oceanic plate relative to the North American continental plate occurs in a direction roughly normal to the continental margin and at a rate of roughly 42 mm y^{-1} (DeMets et al., 1990). A topographic trench at this subduction zone is absent as a consequence of the extremely high rate of glacial sediment supply from the continent during the Pleistocene. The majority of the supply has been impounded by the elevated igneous crustal topography of the Juan de Fuca Ridge. At the accretionary prism toe (also referred to as the deformation front, where the seawardmost thrust fault of the accretionary complex intersects the seafloor), the sediments that bury the eastern Juan de Fuca Ridge flank are approximately 2.7 km thick. At Site U1364 the accreted sedimentary section is nearly doubled to a thickness of approximately 5 km (Yuan et al., 1994). With tectonic thickening and compaction, pore fluids are expelled, and gas—primarily biogenic methane—is transported upward to contribute to the formation of gas hydrates in the upper few hundred meters of the sediment section (Davis et al., 1990; Hyndman and Davis, 1992; Haacke et al., 2007; Riedel et al., 2010).

The location for Site U1364 was chosen for the same reasons as Site 889. It lies at a position landward of the prism toe where the fluid expulsion rate, estimated on the basis of the rates of compaction and vertical growth of the prism, reaches a cross-margin maximum, and where a clearly developed bottom simulating reflector marks the base of the gas hydrate stability field (Davis et al., 1990). Other holes drilled earlier during ODP Leg 146 and IODP Expedition 311 (Westbrook et al., 1994; Riedel et al., 2010) have documented the nature of the incoming undeformed sediments, the compaction history during accretion, the details of the lithology, and the distribution and composition of gas hydrates across the area. This information, along with detailed site survey studies (Scherwath et al., 2006; Riedel et al., 2010), provided an excellent basis for planning the depth, location, and other details of the ACORK installation at Site U1364 and established a valuable context for ACORK observations.

Instrumentation

Hole U1364A was drilled to a total depth of 336 mbsf through roughly 90 m of gently deformed slope-basin deposits and underlying sediments of the accretionary prism that

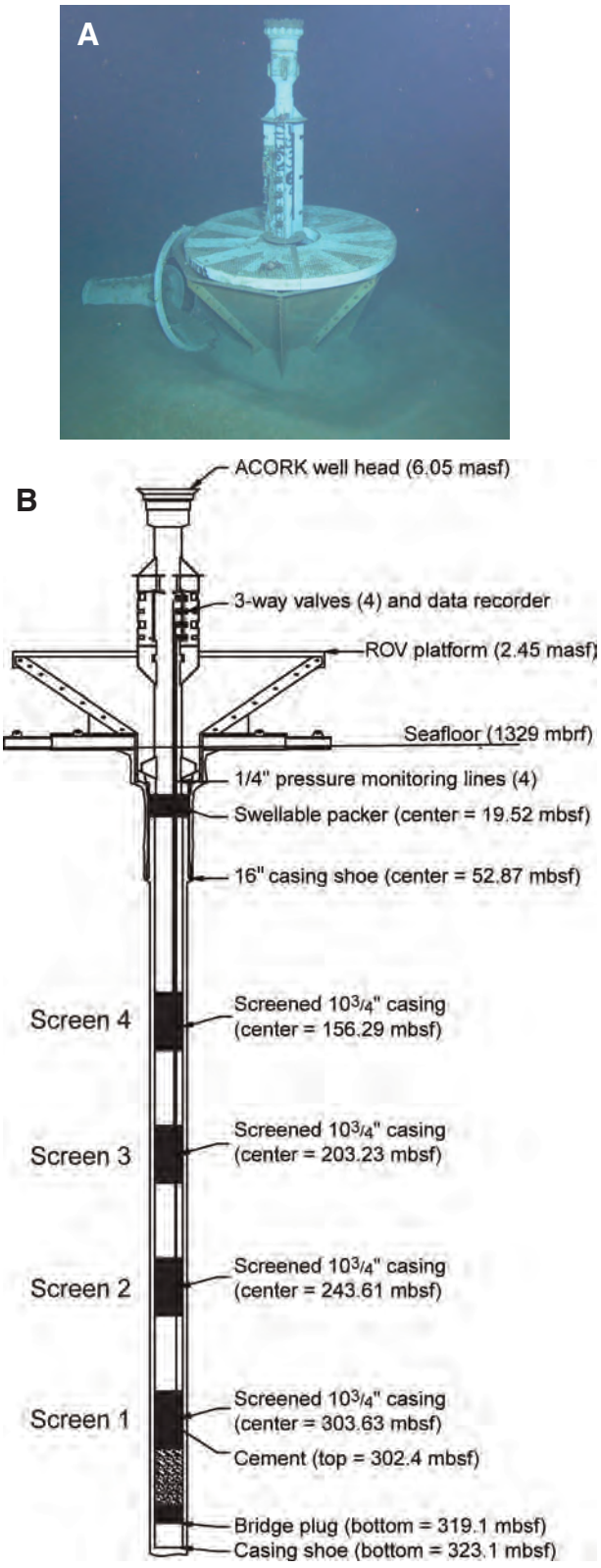

Figure 3. [A] The photograph of the reentry cone and ACORK wellhead (inset) was taken during the July NEPTUNE Canada servicing trip by the ROV ROPOS. The secondary cone seen lying on the seafloor to the left of the wellhead was intended to guide reentry into the casing for the bridge plug and cement installation, but it failed to land properly. Reentry was accomplished through the 24-inch diameter of the uppermost part of the ACORK structure. [B] Schematic illustration of the ACORK system installed in Hole U1364A, with component depths given in meters above and below seafloor (masf, mbsf).

are folded and faulted on a scale too small to be resolved in seismic reflection profiles (Fig. 2). The configuration of the ACORK, constructed around solid 10¾-inch casing and installed immediately after drilling, is shown schematically in Fig. 3b. Formation fluid pressures are transmitted to sensors at the wellhead (inset Fig. 3a) via 2.03-m-long circumferential sand-packed filter screens and 3-mm-diameter (1/8-inch i.d.) stainless steel hydraulic tubing mounted on the outside of the casing. The solid casing is open at the seafloor but sealed at the bottom with a bridge plug backed with cement, leaving the interior open to a depth of 302 mbsf for instruments requiring thermal or mechanical—but not direct—contact with the formation. Screens (numbered S1 to S4 from bottom to top) are positioned at depths of 304 mbsf, 244 mbsf, 203 mbsf, and 156 mbsf. The middle two pressure monitoring screens of the ACORK system (S2, S3) were positioned 14 m below and 27 m above the limit of gas hydrate stability at 230 mbsf to observe the effects of free gas and gas hydrate in the sediment matrix, and diffusive signals originating at the hydrate-gas boundary. The lowermost and uppermost screens (S1, S4) were placed 74 m below and above the boundary, a distance that was anticipated to be sufficient to avoid hydrologic complications originating at the boundary.

Instrumentation installed with the ACORK included five pressure sensors, four plumbed to be switchable between the formation screens and the ocean and the fifth plumbed permanently to the ocean, and a platinum thermometer sensing ocean temperature at the wellhead. Frequency output of the pressure sensors is measured with a low-power, high-precision (1 ppb) period counter. Data are stored in flash memory, and passed through to a communications port (i.e., to fiber-optic cable when connected). Under battery power, data are logged at one-minute intervals (programmable); under cable power, data are recorded at one sample per second. An on-board voltage detector automatically switches between the two modes. Calibration among sensors was done at the seafloor during deployment before the screens entered the hole, and will be done periodically to check for sensor drift though the use of three-way valves that can close the formation lines and connect the formation sensors to the open ocean. Temperature at the wellhead is determined with a highly stable platinum thermometer inside the instrument pressure case, and with one of the pressure sensors that contains a temperature-sensitive quartz oscillator. Further details about the instrumentation, the ACORK hardware, and the geologic setting are provided in Davis et al. (2010).

Early Data

Connection of the instrumentation at Hole U1364A to the NEPTUNE Canada fiber-optic cable system is planned for 2013; in the meantime, data are being logged autonomously using on-board battery power. The site was first visited with the remotely operated vehicle *ROPOS* in 2011 July (dive

R1430) as part of a NEPTUNE Canada service cruise. The early portion of the downloaded record (with the full length of the ACORK assembly in the water column) is shown in Fig. 4. The 1-minute-interval data record of the deployment shows a highly aliased view of the effects of heave resulting from both depth variations and acceleration of the water in the hydraulic tubing. The latter produced sys-tematically increasing amplitudes from the uppermost to lowermost screens. Average values of the pressure difference between the various screens and the seafloor (SF) allow correction for inaccuracy of the sensor calibrations (see Fig. 4).

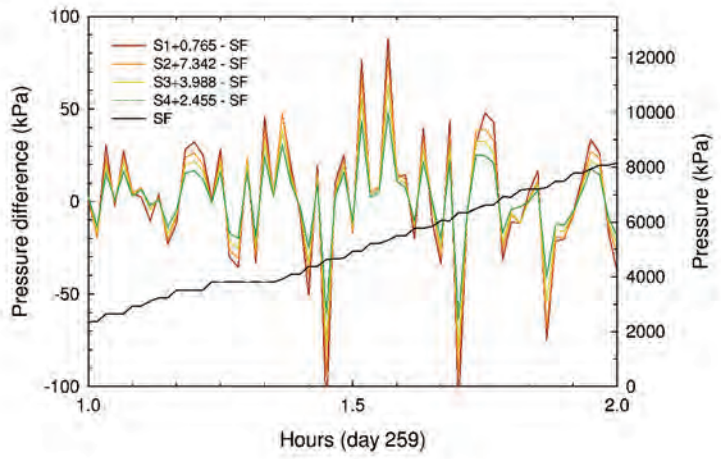

Figure 4. Pressure variations measured during the decent of the ACORK system. Screen pressures are shown relative to the seafloor sensor pressure (scale on left). Offsets given in legend are applied in this and other figures. Absolute pressure is shown for the seafloor sensor (scale on right). Units used for differential and absolute pressure in this and other plots are kPa, equivalent to a seawater head of 0.1 m..

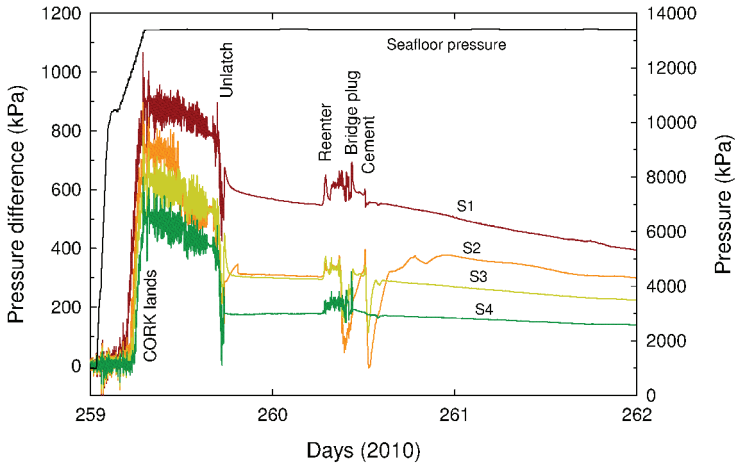

Figure 5. Record of pressure variations (screen pressures relative to seafloor, seafloor pressure absolute) measured during the Site U1364 ACORK installation, annotated with operational events.

Pressures recorded during the ACORK entry and installation (Fig. 5) show growing offsets and modest overpressures as the screens enter the hole. Peak pressures exceeded those that would be produced by the drilling mud used to prevent premature hole collapse (ρ=10.4 lb gal^{-1}=1200 kg m^{-3}) by 50%–80%. This may be a result of charging of the formation by water and mud pumped during drilling and casing installation. Pressure variations present during the early installation phase abated when the drill string was disconnected, and briefly returned after reentry for the bridge plug and cement installations. The drop in pressure at the time of cementing at screen S2, and to a lesser extent at screen S3, may have been caused by the temporary cooling effects of circulating drill mud during that operation, possibly with free gas being driven into solution.

After completion of the installation, pressures began a relatively smooth decay for roughly one week, then showed multiple, generally sympathetic perturbations (tentatively inferred to be the consequence of hole collapse) before entering a period of relative stability (Fig. 6). Hydrologic isolation between adjacent screens and between screens and the seafloor is apparent from the attenuation of the tidal load at the seafloor. Ratios of the formation to seafloor signal amplitudes, referred to as the tidal loading efficiency, were roughly 0.7, 0.5, 0.6, and 0.9 at screens S1–S4, respectively, early in the recording period (Fig. 7), and declined to roughly 0.6, 0.3, 0.4, and 0.7 by the end of the recording period. The value for screen S1 at 304 mbsf is comparable to values observed elsewhere in sediments of equivalent porosity (~50%; Davis and Villinger, 2006; Davis et al., 2009)

The greater degree of attenuation and phase lag of the signal at screen S2 relative to the loading at the seafloor is indicative of free gas in the sediments below the level of gas hydrate stability. Attenuated amplitude would result from the high compressibility of gas-bearing water in the sediment pore volume, and a change of phase would result from a diffusive signal generated by the large contrast in fluid and possibly matrix compressibilities at the gas/gas-hydrate boundary (Wang and Davis, 1996; Wang et al., 1998). Lack of a phase difference at screens S1 and S4 relative to the seafloor loading suggests that they are sufficiently far from the gas/gas-hydrate boundary for diffusive effects to be absent. The scale over which this is true depends on the period of the loading signal and the hydraulic diffusivity (permeability and storage compressibility) of the formation. A full analysis of the nature of loading will be done once high-sampling-rate data are available via the connection to the NEPTUNE Canada cable system, and an examination over a broad frequency band (e.g., ranging from microseismic to seasonal) is possible.

The full history (Fig. 8a) reveals complexities that are currently not understood. During the first eighty days of the recording period, pressures varied over days to weeks. Variations are largest at the uppermost screen (S4) and smallest at the lowermost (S1), and variations at the lower three screens mirror those at the uppermost. Thermal perturbations that might be caused by vertical flow in the annulus outside the casing (warm water transported up, cool solids down) could produce this difference (i.e., with sediment settling into the lower part of the hole causing cooling and a temporary decline in pressure arising from thermal contraction of the fluid in the screens and hydraulic tubing, and expelled water warming the uppermost interval), although any heating above the uppermost screen would affect all hydraulic lines equally. Fortunately, towards the end of the initial 160-day recording period, pressures settled to levels similar to those prior to the first major perturbations, although an elevated level of "noise" persists, most notably at the upper two screens. Highest average pressures are present at the two screens immediately above and below the base of the gas-hydrate stability field, and lowest at the uppermost screen.

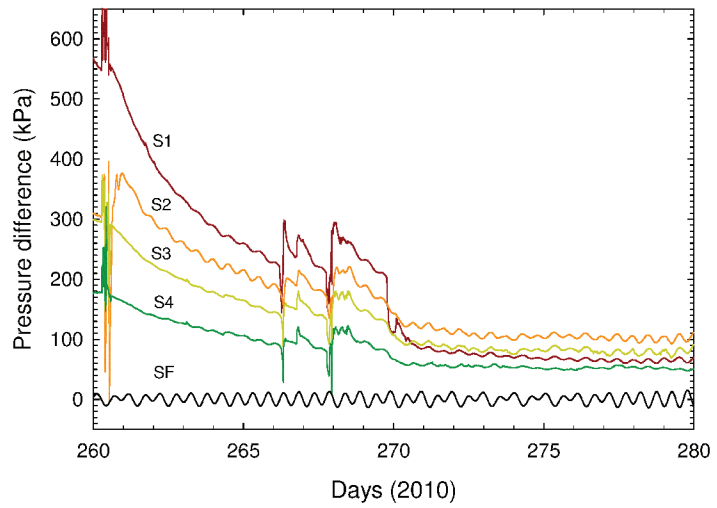

Figure 6. Three-week record of the decay of screen pressures (relative to seafloor) following the ACORK installation at Hole U1364A. Absolute seafloor pressure is shown with the same scaling as the relative pressures at screens but with the mean seafloor pressure removed.

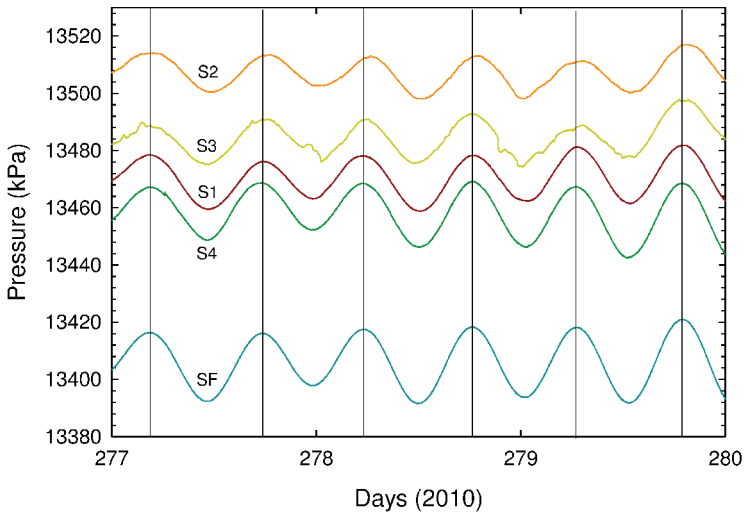

Figure 7. Three-day record of absolute seafloor and screen pressures, showing the dominant tidal component of variation. Differences in amplitudes and phases of pressure variations in the formation relative to pressure at the seafloor are discussed in the text. Lines at times of seafloor tidal peaks highlight the large phase lag of the signal at screen S2.

On 21 February (day 417 on plot), the seafloor pressure sensor suffered a failure possibly caused by crevice corrosion penetrating beneath the O-ring seal of its electrical connector. Excess current to the seafloor sensor was detected by the instrument, current was limited, and the problem was flagged in the stored data, but after roughly thirty minutes the leakage produced a short circuit, leaving all channels dysfunctional. On 24 July (*ROPOS* dive R1452) the cable to the faulty sensor was cut, which restored the system functionality. A brief interval of on-site logging showed the remaining sensors to be fully opera-tional and the formation pressure state to be similar to that seen in February.

Temperatures were measured throughout the history of the recording period with the temperature-dependent oscillator in the seafloor pressure sensor and with the platinum thermometer (Fig. 8b). Absolute accuracy is limited to a few tenths of a degree Celsius; calibration will be improved by comparing values to an accurately calibrated conductivity-temperature-depth (CTD) sensor during the next *ROPOS* visit. Precision of both sensors is much better than the accuracy; variations in the two records follow one another within a few milliKelvin. Small differences are primarily the consequence of the thermal time constant of the pressure sensor being longer than that of the platinum thermometer. Temporal variations are seen from diurnal to seasonal periods.

Summary and Discussion

Data from the first five months of seafloor and formation pressure recording at Hole U1364A at the toe of the Cascadia subduction zone accretionary prism have demonstrated that the IODP ACORK multi-level hydrologic monitoring system will provide well isolated hydrologic observations in the sedimentary formation via hole closure around external casing screens at relatively shallow levels (~300 mbsf). However, persistent noise, particularly at the uppermost screen (156 mbsf), suggests variable leakage in the annulus outside the casing. Borehole temperature monitoring, planned with other instrument installations inside the casing in 2013, will provide a sensitive test for any long-term or episodic vertical flow.

Formation pressures measured at the monitoring screens range from 40 kPa to 80 kPa above hydrostatic. These are significant but not high, i.e., a small fraction of the lithostatic potential at the deepest screen of roughly 2 MPa. High pressures are not expected at this relatively shallow level in the prism, given the relatively high formation permeability and the long time that has elapsed (~300 years) since the last large subduction earthquake when large contractional strain may have been produced in the outermost part of the prism. Highest pressures are observed at the screens immediately above and below the level of gas hydrate stability (marked both at this location and regionally by a clear bottom simulating seismic reflector). This may be a consequence of ongoing gas production.

While information about dynamic response to seafloor loading over a broad range of frequencies will not be available until the instrumentation is connected to the NEPTUNE Canada power and communications cable, variations in the amplitude and phase of loading at tidal frequencies provide some preliminary insights. There is a general decline in the tidal amplitude at all screens with time, suggesting a progressive increase in the degree of closure of the formation around the casing with time. At the deepest screen, formation pressure variations are in phase with the seafloor load throughout the record, demonstrating that there is no significant hydrologic diffusion or leakage at this level. The tidal loading efficiency (formation/seafloor = 0.6 late in the record) is consistent with observations in other sedimentary sections with similar porosity, and suggests that the formation is sufficiently rigid for volumetric strain to be detected with pressure (i.e., with a conversion efficiency of roughly 5 kPa μstrain^{-1}; Davis et al., 2009).

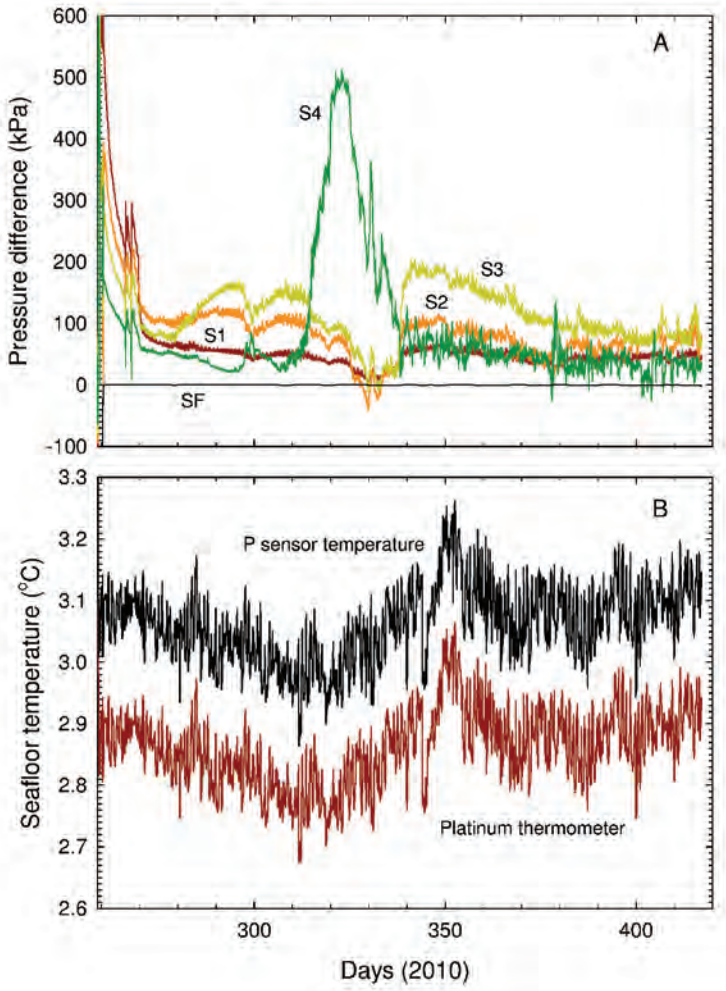

Figure 8. Full history of [A] seafloor (tides filtered) and relative formation pressures and [B] seafloor temperature observed prior to failure of the seafloor pressure sensor on 21 February 2011 (day 417). Scaling convention for pressures is the same as in Figs. 4–6. Temperatures (offset for plotting clarity; absolute values to be calibrated during the next *ROPOS* visit) are measured inside the main instrument pressure case with a platinum thermometer, and inside the seafloor pressure sensor with a quartz oscillator.

The tidal signal at the screen just below the hydrate stability boundary (S2) is anomalously low in amplitude (formation/seafloor = ~0.3 late in the record) and lags the seafloor load by roughly two hours. The low amplitude is probably the consequence of the high compressibility of interstitial free gas, and the large phase lag is likely the consequence of a diffusive signal propagating from the gas/gas-hydrate boundary, where there may be a sharp contrast in both matrix and interstitial fluid compressibilities.

Acknowledgments

Installation of the CORK observatory at Hole U1364A seemed like a routine operation as a result of the skilled help of IODP shipboard technical, operations, and engineering personnel and the crew on D/V *JOIDES Resolution*, led by Mitch Malone, Bill Rhinehart, and Bob Aduddell. Michael Riedel provided invaluable information about local seismic and lithologic structure. Zest was added to the short cruise by the energetic leaders and participants of the IODP School of Rock. Data downloading operations and remediation of the problem created by the seafloor pressure sensor failure were carried out by the crew of the remotely operated vehicle *ROPOS*, led by Keith Shepherd and assisted by Martin Scherwath and Reece Hasanen of NEPTUNE Canada. Support for the design and construction of the wellhead instrumentation prior to the expedition was provided by Robert Macdonald, Robert Meldrum, James Guenther, John Bennest, Jonathan Schmidt, and David Miles. Pressure sensors, sensor frequency counters, and the NEPTUNE-compatible data logger were provided by Paroscientific Inc., Bennest Enterprises Ltd., and Minerva Technologies Ltd., respectively.

The IODP Expedition 328 Scientists and School of Rock Educators

E. Davis, M. Malone, M. Heesemann, M. Riedel, D. Divins, J. Collins, K. Ludwig, S. Hovan, M. Reagan, and S. Slough

References

Davis, E., Becker, K., Wang, K., and Kinoshita, M., 2009. Co-seismic and post-seismic pore-fluid pressure changes in the Philippine Sea plate and Nankai decollement in response to a seismogenic strain event off Kii Peninsula, Japan. *Earth Planets Space*, 61:649–657.

Davis, E.E., and Hyndman, R.D., 1989. Accretion and recent deformation of sediments along the Cascadia subduction zone. *Geol. Soc. Am. Bull.*, 101:1465–1480. doi:10.1130/0016-7606(1989)101%3C1465:AARDOS%3E2.3.CO;2

Davis, E.E., and Villinger, H., 2006. Transient formation fluid pressures and temperatures in the Costa Rica forearc prism and subducting oceanic basement: CORK monitoring at ODP sites 1253 and 1255. *Earth Planet. Sci. Lett.*, 245:232–244.

Davis, E.E., Becker, K., Wang, K., and Carson, B., 1995. Long-term observations of pressure and temperature in Hole 892B, Cascadia accretionary prism. *In* Carson, B., Westbrook, G.K., Musgrave, R.J., and Suess, E. (Eds.), *Proc. ODP, Sci. Results*, 146 (Pt. 1): College Station, TX (Ocean Drilling Program), 299–311. doi:10.2973/odp.proc.sr.146-1.219.1995

Davis, E.E., Hyndman, R.D., and Villinger, H., 1990. Rates of fluid expulsion across the northern Cascadia accretionary prism: Constraints from new heat flow and multichannel seismic reflection data. *J. Geophys. Res.*, 95:8869–8889. doi:10.1029/JB095iB06p08869

Davis, E.E., Malone, M.J., and the Expedition 328 Scientists and Engineers, 2010. Integrated Ocean Drilling Program Expedition 328 Preliminary Report: Cascadia subduction zone ACORK observatory. *IODP Prel. Rept.*, 328. doi:10.2204/iodp.pr.328.2010

DeMets, C., Gordon, R.G., Argus, D.F., and Stein, S., 1990. Current plate motions. *Geophys. J. Int.*, 101:425–478. doi:10.1111/j.1365-246X.1990.tb06579.x

Haacke, R.R., Westbrook, G.K., and Hyndman, R.D., 2007. Gas hydrate, fluid flow and free gas: Formation of the bottom-simulating reflector. *Earth Planet. Sci. Lett.*, 261:407–420. doi:10.1016/j.epsl.2007.07.008

Hyndman, R.D., and Davis, E.E., 1992. A mechanism for the formation of methane hydrate and seafloor bottom-simulating reflectors by vertical fluid expulsion. *J. Geophys. Res.*, 97:7025–7041. doi:10.1029/91JB03061

Hyndman, R.D., Yorath, C.J., Clowes, R.M., and Davis, E.E., 1990. The northern Cascadia subduction zone at Vancouver Island: Seismic structure and tectonic history. *Can. J. Earth Sci.*, 27:313–319. doi:10.1139/e90-030

Riedel, M., Collett, T.S., and Malone, M., 2010. Expedition 311 synthesis: Scientific findings. *In* Riedel, M., Collett, T.S., Malone, M.J., and the Expedition 311 Scientists, *Proc. IODP*, 311: Washington, DC (Integrated Ocean Drilling Program Management International, Inc.). doi:10.2204/iodp.proc.311.213.2010

Scherwath, M., Riedel, M., Spence, G.D., and Hyndman, R.D., 2006. Data report: Seismic structure beneath the north Cascadia drilling transect of IODP Expedition 311. *In* Riedel, M., Collett, T.S., Malone, M.J., and the Expedition 311 Scientists, *Proc. IODP*, 311: Washington, DC (Integrated Ocean Drilling Program Management International, Inc.). doi:10.2204/iodp.proc.311.110.2006

Wang, K., and Davis, E.E., 1996. Theory for the propagation of tidally induced pore pressure variations in layered subseafloor formations. *J. Geophys. Res.*, 101:11483–11495. doi:10.1029/96JB00641

Wang, K., Davis, E.E., and van der Kamp, G., 1998. Theory for the effects of free gas in subsea formations on tidal pore pressure variations and seafloor displacements. *J. Geophys. Res.*, 103:12339–12354. doi:10.1029/98JB00952

Westbrook, G.K., Carson, B., Musgrave, R.J., et al., 1994. *Proc. ODP, Init. Repts.*, 146 (Pt. 1): College Station, TX (Ocean Drilling Program). doi:10.2973/odp.proc.ir.146-1.1994

Yuan, T., Spence, G.D., and Hyndman, R.D., 1994. Seismic velocities and inferred porosities in the accretionary wedge sediments at the Cascadia margin. *J. Geophys. Res.*, 99:4413–4427. doi:10.1029/93JB03203

Authors

Earl Davis, Pacific Geoscience Centre, Geological Survey of Canada, 9860 West Saanich Road, Sidney, BC V8L 4B2, Canada, e-mail: edavis@nrcan.gc.ca.

Martin Heesemann, NEPTUNE-Canada, University of Victoria, P.O. Box 1700 Stn CSC, Victoria, BC V8W 2Y2, Canada, e-mail: mheesema@uvic.ca.

and the IODP Expedition 328 Scientisits and Engineers

IODP Expedition 331: Strong and Expansive Subseafloor Hydrothermal Activities in the Okinawa Trough

by Ken Takai, Michael J. Mottl, Simon H.H. Nielsen and the IODP Expedition 331 Scientists

doi:10.2204/iodp.sd.13.03.2011

Abstract

Integrated Ocean Drilling Program (IODP) Expedition 331 drilled into the Iheya North hydrothermal system in the middle Okinawa Trough in order to investigate active subseafloor microbial ecosystems and their physical and chemical settings. We drilled five sites during Expedition 331 using special guide bases at three holes for reentry, casing, and capping, including installation of a steel mesh platform with valve controls for postcruise sampling of fluids. At Site C0016, drilling at the base of the North Big Chimney (NBC) mound yielded low recovery, but core included the first Kuroko-type black ore ever recovered from the modern subseafloor. The other four sites yielded interbedded hemipelagic and strongly pumiceous volcaniclastic sediment, along with volcanogenic breccias that are variably hydrothermally altered and mineralized. At most sites, analyses of interstitial water and headspace gas yielded complex patterns with depth and lateral distance of only a few meters. Documented processes included formation of brines and vapor-rich fluids by phase separation and segregation, uptake of Mg and Na by alteration minerals in exchange for Ca, leaching of K at high temperature and uptake at low temperature, anhydrite precipitation, potential microbial oxidation of organic matter and anaerobic oxidation of methane utilizing sulfate, and methanogenesis. Shipboard analyses have found evidence for microbial activity in sediments within the upper 10–30 m below seafloor (mbsf) where temperatures were relatively low, but little evidence in the deeper hydrothermally altered zones and hydrothermal fluid regime.

Introduction and Goals

Active seafloor hydrothermal systems at mid-ocean ridges, volcanic arcs, backarc basins, and hotspots are environments with extraordinarily high fluxes of energy and matter. The "subvent biosphere" is the subseafloor biosphere that is predicted to exist just beneath active hydrothermal vents and fluid discharge zones and is sustained from the hydrothermal energy and matter inputs (Deming and Baross, 1993; Takai et al., 2001). The existence of a subvent biosphere has been inferred from many microbiological and geochemical investigations of vent chimney structures and diffuse hydrothermal fluids (Nunoura and Takai, 2009; Nunoura et al., 2010; Takai et al., 2008; 2009; and references in Takai et al., 2006, and Huber and Holden, 2008). In the Iheya North field, a typical deep-sea hydrothermal system in the Okinawa Trough, it has been suggested that a variety of microbial communities based on different chemolithoautotrophic primary producers is present in subseafloor habitats (Nakagawa et al.,

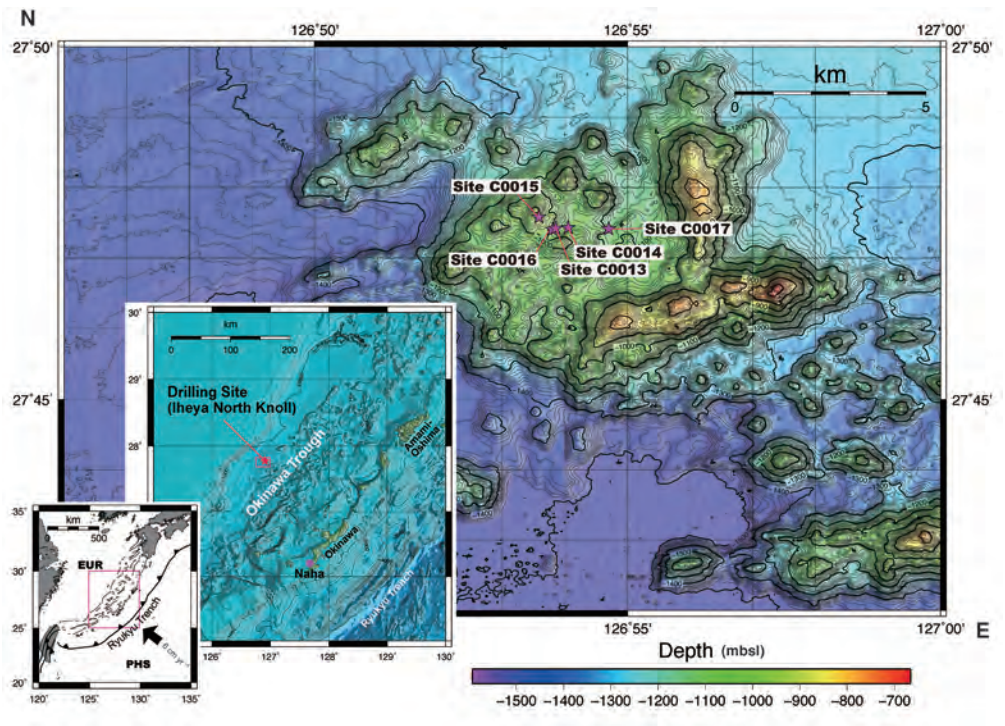

Figure 1. Area map of Iheya North Knoll showing Sites C0013–C0017 drilled during Expedition 331. Insets show the Iheya North Knoll in relation to Okinawa and Okinawa in relation to major tectonic components. EUR= Eurasian Plate, PHS = Philippine Sea Plate. Modified from Takai et al. (2011).

2005). Variability in potential subseafloor microbial communities is likely associated with physical and chemical variation of hydrothermal fluids, controlled by phase-separation and phase-partition of hydrothermal fluid beneath the seafloor. In addition, the overall hydrothermal environments associated with organic-rich sediments provide unusual amounts of C1 compounds (CO_2 and CH_4) in hydrothermal fluids as carbon sources, as well as unique microbial habitats affected by liquid CO_2 and gas hydrates (Nakagawa et al., 2005; Kawagucci et al., 2011). Thus, the abundant supply of energy and carbon and the richness of the habitats supported by physical and chemical variations in the Iheya North field provide an ideal setting for the formation of functionally and metabolically diverse subseafloor microbial communities associated with hydrothermal activity.

There were three major scientific objectives of Expedition 331 drilling were.

1. to test for the existence of a functionally active, metabolically diverse subvent biosphere associated with subseafloor hydrothermal activity;
2. to clarify the architecture, function, and impact of subseafloor microbial eco-systems and their relationship to physical, geochemical, and hydrogeologic variations within the hydrothermal mixing zones around the discharge area; and
3. to establish artificial hydrothermal vents in cased holes from potential subseafloor hydrothermal flows, and to prepare a research platform at each cased hole for later study of fluids tapped from various parts of the hydrothermal system and their associated microbial and macrofaunal communities.

Geological Setting and Earlier Work

The Okinawa Trough is a backarc basin extending for ~1200 km, between the Ryukyu arc-trench system and the Asian continent (Fig. 1; Lee et al., 1980; Letouzey and Kimura, 1986). Seismic reflection data suggest a typical backarc structure (Letouzey and Kimura, 1986) with a high-velocity mantle below ~6000 mbsf overlain by potentially young basalt with an average velocity of 5.8 km s^{-1} between ~3000 mbsf and 6000 mbsf, an igneous rock layer (4.9 km s^{-1}) between ~1000 mbsf and 3000 mbsf, and ~1000 m of sediment immediately beneath the seafloor. Since the discovery of submarine hydrothermal activity at Iheya Ridge and Izena Hole in the middle Okinawa Trough in 1988 (Halbach et al., 1989; Sakai et al., 1990), six active hydrothermal fields have been discovered—Minani-Ensei Knoll, Iheya North, Iheya Ridge, Izena Hole, Hatoma Knoll, and Yonaguni Knoll IV.

Characteristics of the tectonic setting in this active hydrothermal system are reflected in the chemical composition of sulfide deposits. Sulfide samples collected from the Iheya North field are distinctly more enriched with Pb than mid-oceanic-ridge sulfides (Fig. 2). The polymetallic Zn-Pb-Cu chemical signature of Iheya North sulfides is similar to that of Kuroko-type hydrothermal deposits formed during the Tertiary in northeast Japan.

The chemistry of hydrothermal fluids collected from active sulfide chimneys in the Okinawa Trough is characterized by higher concentrations of CO_2, CH_4, NH_4, I, and K and higher alkalinity than those in typical sediment-free mid-ocean-ridge hydrothermal fluids (Sakai et al., 1990; Gamo et al., 1991; Konno et al., 2006; Takai and Nakamura, 2010; Kawagucci et al., 2011). The distinctive hydrothermal fluid chemistry is strongly linked with the geologic setting and the thick terrigenous sediments of the Okinawa Trough. Philippine Plate subduction along the Ryukyu arc-trench system supplies dacitic-rhyolitic magma rich in K and volatile components to the Okinawa Trough (Sakai et al., 1990; Gamo et al., 2006). Organic-rich terrigenous sediment filling the Okinawa Trough (Narita et al., 1990) supplies not only the sedimentary chemical inputs (NH_4, I, etc.; Gamo et al., 1991; You et al., 1994), but also promotes the widespread occurrence of functionally active microbial communities that impact hydrothermal fluid chemistry and circulation (Nakagawa et al., 2005; Inagaki et al., 2006; Nunoura and Takai, 2009; Nunoura et al., 2010; Takai and Nakamura, 2010; Kawagucci et al., 2011). In addition to the chemical aspects, the relatively shallow water depth of many Okinawa Trough hydrothermal systems serves to induce subcritical phase separation (Suzuki et al., 2008) and subsequent phase segregation, as the boiling temperature of seawater decreases steeply with decreasing pressure at ~100 bar. Phase separation and segregation sometimes

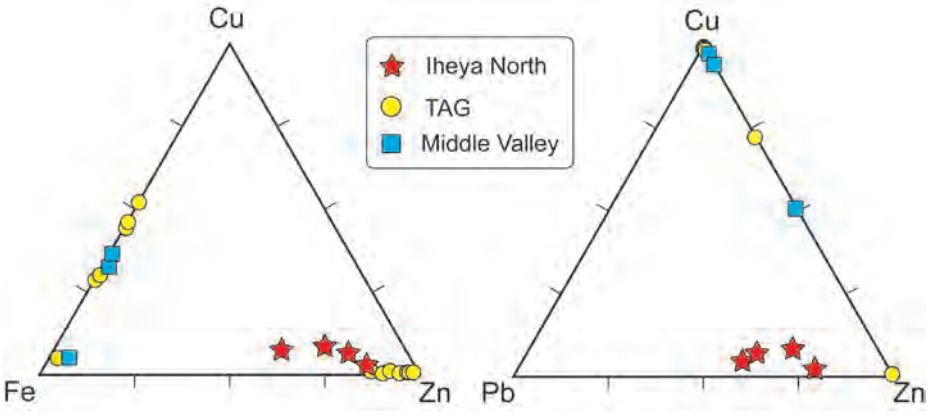

Figure 2. Ternary diagrams of the composition of sulfide samples from active hydrothermal fields. Iheya North data from Ueno et al. (2003). TAG = TAG mound, Mid-Atlantic Ridge, Middle Valley = Middle Valley, Juan de Fuca Ridge. Modified from Takai et al. (2011).

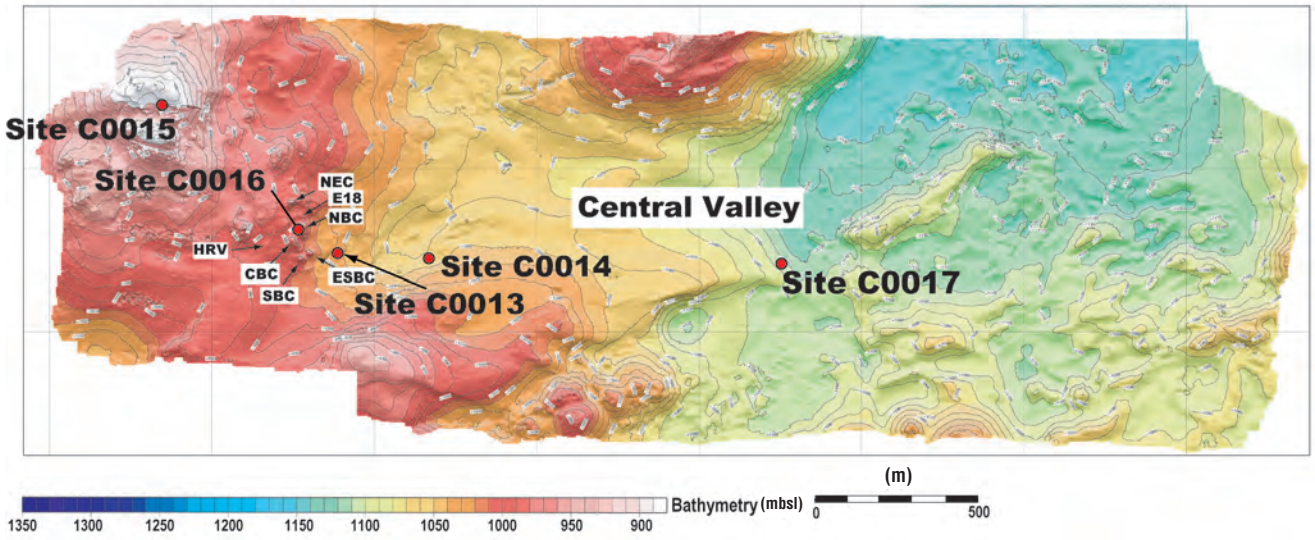

Figure 3. Detailed bathymetry of the Iheya North hydrothermal field and the central valley at Iheya North Knoll, with the location of Sites C0013–C0017 drilled during Expedition 331. HRV=High Radioactive Vent mound, CBC=Central Big Chimney mound, SBC=South Big Chimney mound, NEC=North Edge Chimney mound, E18=event Marker 18 mound, NBC = North Big Chimney mound, ESBC="Ese" South Big Chimney mound. Modified from Takai et al. (2011).

produce hydrothermal fluids of quite different chemical composition at different vent sites in the same hydrothermal field, even though they are derived from the same source fluid (Kawagucci et al., 2011).

Drilling, Temperature Measurement, Sampling, and Installation of Vents

We drilled five sites during Expedition 331: the active hydrothermal vent site and sulfide-sulfate mound at North Big Chimney (NBC) (Site C0016, Fig. 3), three sites east of NBC at distances of ~100 m (C0013), 450 m (C0014), and 1550 m (C0017) from the active vents, and one site (C0015) on a hill ~600 m northwest of the active vents that represents a potential migration path for hydrothermal fluid.

The NBC hydrothermal mound at Site C0016 is 20 m high and 6 m in diameter. When we attempted to core this active high-temperature (311°C) vent at its summit, the pipe broke, and core recovery failed (Hole C0016A). We drilled a second hole 20 m away, immediately at the base of the mound on its western side (Hole C0016B). We used conventional hard rock drilling equipment supplied by Baker-Hughes Inteq (BHI) specifically for Expedition 331 due to high temperatures and expectation of hard rock. The BHI system collects 4-inch diameter core in aluminum liners in lengths of 9 m, 18 m, or 27 m, but requires a time-consuming pipe trip for each core. It penetrated to 45 mbsf in three runs of 9 m, 18 m, and 18 m. Each run recovered several large pieces of core, but the total recovery was only 2.095 meters, nearly all of it hard rock. The only evidence for the actual depths of the recovered rock thus comes from the drilling records. Hole C0016B was not cased, but it was fitted with a corrosion cap with 3 m of 5.5-inch pipe hanging beneath and extending 0.4 m into the seafloor (Fig. 4). ROV video images showed vigorous black smoker discharge from the corrosion cap outlet immediately after its deployment. This hydrothermal emission began only after the third coring run, which penetrated 27–45 mbsf, and was probably derived from a depth below 38 mbsf.

At Sites C0013, C0014, and C0017, we drilled the relatively high, moderate, and low heat flow areas, respectively, to the east of the Iheya North hydrothermal field to investigate subseafloor microbial habitats and communities within broad gradients of physical and chemical variation, both laterally and vertically, that could be affected by mixing between discharging hydrothermal solutions and recharging ambient bottom seawater. These sites were drilled using the hydraulic piston coring system (HPCS) to first refusal and then again in any softer intervals encountered deeper in the hole, alternating as necessary with the extended punch (EPCS) and extended shoe (ESCS) coring systems, and, for one run at Site C0013, the BHI system, to penetrate the harder layers. Both the EPCS and ESCS systems were able to penetrate the harder layers, with a slight advantage to the ESCS for the hardest layers, though the EPCS was generally much better at core recovery. We penetrated the margin of the local discharge-recharge zone to depths of 55 mbsf (C0013), 137 mbsf (C0014), and 151 mbsf (C0017), coring variably hydrothermally altered sediment and pumiceous deposits (Figs. 5, 6). We were able to measure *in situ* temperature at two of these sites using the advanced piston corer temperature tool (APCT3) shoe (upper calibration limit = 55°C) as part of the HPCS, combined with commercial thermoseal strips (Nichiyu Giken Co., Ltd.) taped to the outer surface of the core liner. We were not able to measure temperature at proximal flank Site C0013, but the gradient was likely higher than at the other two flank sites.

Eight holes (C0013A–C0013H) were drilled at Site C0013, and core was recovered from all but Hole C0013A. Hole C0013E was the deepest (54.5 mbsf) and was cased down to 40.2 mbsf and fixed with a corrosion cap (open outlet pipe) mounted on the guide base (Fig. 4). During drilling and coring operations at Site C0013, we encountered many operational and sample handling problems. These problems were due to the unexpectedly high temperature gradient at the site and the presence of repeated hard layers that appear to behave as cap rocks alternating with soft and sticky clay-rich layers. Porosity measurements on the core clearly document the repeated occurrence of low-porosity harder layers (e.g., 0–2 mbsf, 7–10 mbsf, and 20–30 mbsf). We observed at several depths that when a hard cap rock was drilled through into softer underlying layers, subseafloor hydrothermal fluid began to outflow from the hole, where it was imaged by the ROV video camera. To tap this fluid, we used slotted, perforated casing pipe over the depth interval 21–39.8 mbsf in Hole C0013E (Fig. 4). Immediately after casing and capping this hole, we observed in the ROV video image strong hydrothermal fluid discharge from the casing pipe that was hung in the guide base. Thermoseal temperature-sensitive strips on the corrosion cap outlet pipe showed in the ROV video imagery that the discharging water temperature was >250°C.

Seven holes were drilled at Site C0014 (Holes C0014A–C0014G). Hole C0014G was the deepest (136.7 mbsf) and was cased down to 117.8 mbsf and fixed with a corrosion cap (open outlet pipe) mounted on the guide base. As at Site C0013, we encountered repeated hard layers that behaved as cap rock, and discharge from the holes, beyond what may be only expelled drilling fluid, after penetrating these layers (35–44.5 mbsf in Hole C0014B, 25.5–35 mbsf in Hole C0014E, and 37.7–47.2 mbsf and 89.2–93.7 mbsf in Hole C0014G). We again cored multiple low-porosity layers (e.g., in Holes C0014B, C0014E, and C0014G). Based on pore water chemistry, density, and porosity (and indicated by low recovery during drilling), we inferred lateral hydrothermal flow at 31–42.5 mbsf and 90–95 mbsf at Site C0014. We therefore installed slotted, perforated casing pipe at 29.8–49.2 mbsf, 78.3–97.8 mbsf, and 107.5–117.2 mbsf in Hole C0014G (Fig. 4). After casing and capping, we saw in the ROV-mounted video diffuse hydrothermal fluid discharge, not from the corrosion cap outlet but from the seafloor, through the annulus, the space between the wall of the hole and the casing pipe. The temperature of the diffusing fluids was found to be >240°C based on exposure of thermoseal strips mounted on the corrosion cap outlet pipe. We measured temperature at Site C0014 using the APCT3 temperature shoe on the HPCS core barrel for lower temperatures (0°C–55°C) and thermoseal temperature-sensitive strips for higher temperatures (75°C–250°C). The temperature-depth profile at Site C0014 is shown in Fig. 7a. Temperature increases nearly linearly at 3°C m^{-1} to 145°C ± 5°C at 47 mbsf and then increases abruptly to >210°C at 50 mbsf, below a hard layer near that depth. The drilled sequence at Site C0014 comprises interbedded, variably altered, and consolidated volcaniclastic gravels and breccias, as well as hemipelagic mud (Fig. 5). Given the location of the site on the upper flank of an active volcanic complex, mass wasting and debris flows are likely to be important sedimentary processes, potentially leading to high rates of redeposition of hemipelagic and volcaniclastic material. The deeper portion of the rock volume cored has been hydrothermally altered. Differing degrees and styles of hydrothermal alteration form the basis for the division of Site C0014 sediments and lithologies into lithostratigraphic units.

Hole C0017D is the deepest (150.7 mbsf) of four holes drilled at Site C0017 and is located 1550 m east of the high-temperature vents. Based on its low heat flow, it was inferred to be a location of probable recharge of the hydrothermal system. We observed no evidence for discharge of water from any of these holes, but the concave-upward tempera-

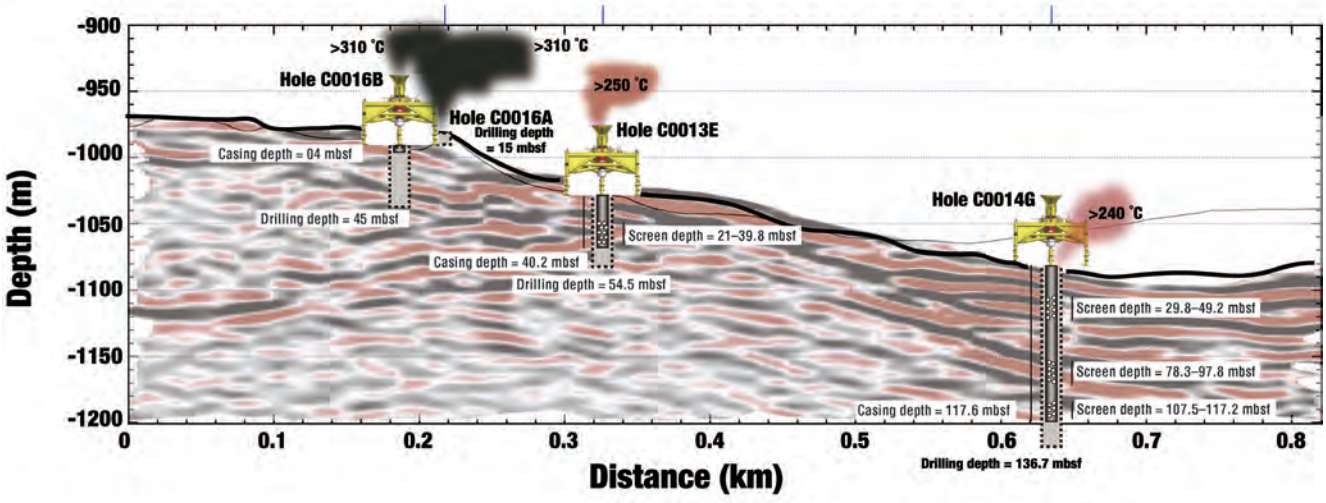

Figure 4. Schematic illustration of post-drilling natural and artificial hydrothermal vents created during Expedition 331. Outflow temperatures measured by ROV (Hole C0013E) and thermal stickers (Holes C0014G and C0016B). Modified from Takai et al. (2011).

ture profile we measured (Fig. 7b) can be fit reasonably well with an exponential function and is consistent with overall downwelling, with distinct perturbations in the temperature gradient that suggest localized lateral flow that may be influenced by the variable lithologies we cored (Fig. 6). We measured temperature successfully at seven depths in Holes C0017B–C0017D over the interval 18.3–150.7 mbsf; combined with the ocean bottom water temperature at the site of 4.9°C ± 0.5°C, our profile is defined by eight points. Six of the downhole measurements were made using the APCT3 temperature shoe on the HPCS. The seventh and deepest measurement, at 150.7 mbsf, was made in triplicate using three identical thermoseal temperature-sensitive strips with chemically impregnated beads for 75°C, 80°C, 85°C, 90°C, and 95°C taped to the bottom outer surface of the plastic core liner. These beads were darkened and thus exposed at maximum temperatures of 85°C, 90°C, and 90°C on the three strips, which we reported as 90°C ± 5°C. The APCT3 shoe recorded a temperature in excess of its maximum range of 55°C for this core. Down to ~50 mbsf, where we encountered a hard layer that was probably pumice (no core was recovered, Fig. 6), temperature remained low, <15°C. Beneath this hard layer, temperature jumped to 25°C–39°C at 69–85 mbsf and then appeared to level off for a short interval, reaching only 44°C at 112 mbsf before increasing nearly exponentially to 90°C at the bottom of Hole C0017D at 150.7 mbsf.

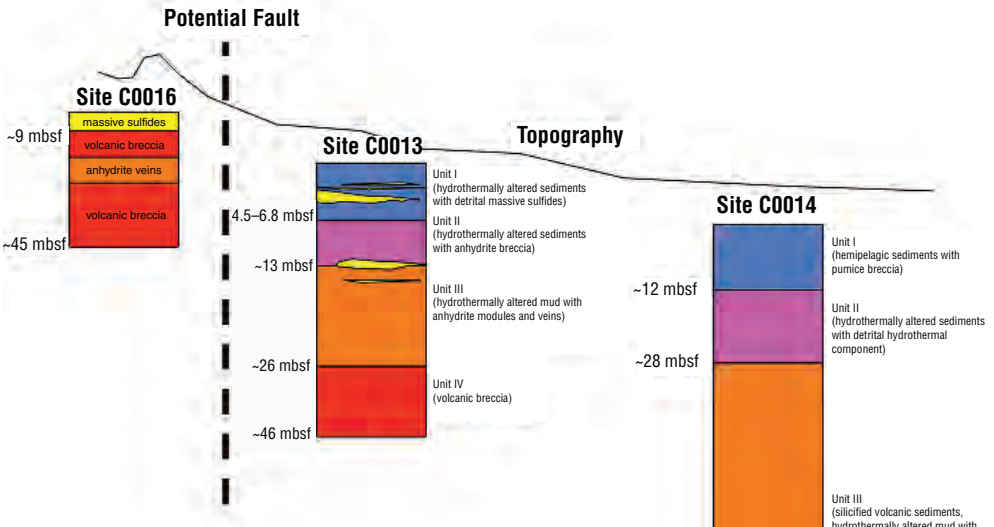

Figure 5. Lithostratigraphic characteristics in Sites C0013, C0014, and C0016. The colored lithostratigraphic units (Units I, II, III and IV) represent the main correlative markers between the sites. The sudden change in dip between Site C0016 and the other sites is consistent with potential faulting. Modified from Expedition 331 Scientists (2010).

Three holes were drilled at Site C0015 (Holes C0015A–C0015C). Although a relatively short interval was cored (0–9.5 mbsf), a broad diversity of sediment types was drilled, with coarse pumiceous gravel and grit, siliciclastic sand, hemipelagic mud, bioclastic gravel, and foraminiferal sediment all recovered. In contrast to the other sites, the samples of Site C0015 do not have any significant hydrothermal input, nor do they appear at present to support a robust microbial community associated with hydrothermal activity. Thus, Site C0015 is excluded from further description and discussion.

Preliminary Scientific Results

Drilling and coring operations during Expedition 331 provided insight into the hydrothermal flow regime at Iheya North Knoll. While the thermal gradient was known to be high at Site C0016 at NBC mound, Sites C0013 and C0014 have steeper thermal gradients than we expected. Site C0013 was located 100 m east of the vigorous high-temperature vents and mounds (Fig. 3). Drilling to our maximum depth of 54.5 mbsf, we penetrated several hard, low-porosity layers that could function as a cap rock and found thick, porous sediment hydrothermally altered at high temperature between the harder, less permeable layers. The interstitial water showed large changes in composition both laterally and vertically over short distances, suggesting chaotic lateral flow in permeable horizons separated by impermeable barriers. The lithostratigraphy, physical properties of the sediment and rock, and interstitial water chemistry thus all provided insight into the hydrothermal flow regime at Site C0013.

Site C0014 was located ~450 m east of the high-temperature vents and mounds (Fig. 3). The temperature gradient was roughly linear from 0 mbsf to 47 mbsf, increasing from the bottom water temperature of 4.5°C to 145°C over that depth range, but it deviated greatly from this line at 0–9 mbsf and 47–50 mbsf, where it was clearly affected by high-temperature fluid pooling or lateral flow. Interstitial water chemistry demonstrated vertical stratification, from water with seawater chloride values at 0–25 mbsf, to a vapor at 29–38 mbsf, and to a brine from 48 mbsf to the deepest sample at 114 mbsf. Within the upper sediments, which consisted of pelagic sediments and pumiceous gravel, there was considerable lateral variability in the intensity of microbial sulfate reduction between the four holes that were only a few meters apart; clearly there was a functionally robust and metabolically diverse subseafloor biosphere here. At 20 mbsf, where the temperature was ~70°C, and to the bottom of the deepest Hole C0014G at 137 mbsf, where a linear fit would have the

temperature exceed 400°C, the sediment and rock we recovered was intensely hydrothermally altered. As at Site C0013, chaotic flow should be occurring through permeable formations and along fault structures, and was likely separated vertically by impermeable beds that behave as cap rocks.

Site C0017 was located 1550 m east of the high-temperature vents of the Iheya North hydrothermal field, in an area of low heat flow (Fig. 3). The overall temperature profile was exponential and concave upward, consistent with downwelling of cold water, implying that this was an area of recharge to the hydrothermal system. We reached a maximum temperature of 90°C ± 5°C at the bottom of the deepest Hole C0017D at 151 mbsf. Deviations from a smooth temperature profile indicated the presence of a discrete zone of cold water recharge, consistent with interstitial water chemistry and the presence of a highly oxidized layer at 26–35 mbsf that supported a microbial community. We found only a small amount of hydrothermally-altered sediment deep in Hole C0017D. These results, taken together, provided a more detailed look at the large-scale hydrogeology of the Iheya North Knoll hydrothermal system than previously observed at subseafloor hydrothermal systems elsewhere (Takai et al., 2011). The hydrological regime at Iheya North Knoll was characterized by large-scale hydrothermal alteration, deposition, and fluid migration within permeable rocks and sediments hosted by the Iheya North Knoll volcanic complex. Prior to Expedition 331, we knew little about the spatial and temporal scales and patterns of hydrothermal circulation in subseafloor hydrothermal systems, particularly those in subduction zone settings such as volcanic arcs and backarc spreading centers.

Much of the sediment and rock we cored at Sites C0013, C0014, and C0016 was intensely hydrothermally altered, and mineralized (Fig. 5). Exceptional among the disseminated and vein, stockwork-type sulfide we recovered was the massive sphalerite-rich ore we cored in Hole C0016B. This marked the first time this type of massive sulfide, which closely resembles the Kuroko black ore, has been recovered from the subseafloor environment of an active deep-sea hydrothermal system. We recovered only 2.1 meters of core from 45 m of penetration in this hole, which made reconstruction of the lithostratigraphy impossible, but the recovered core included a wide diversity of lithologies that were typically associated with volcanic-hosted massive sulfide (VHMS) mineralization. In addition to the sphalerite-rich black ore, recovered core included a boulder-sized, coarsely crystalline piece of anhydrite veined by sphalerite-pyrite, as well as pyrite-veined and pyrite-altered volcanic rock.

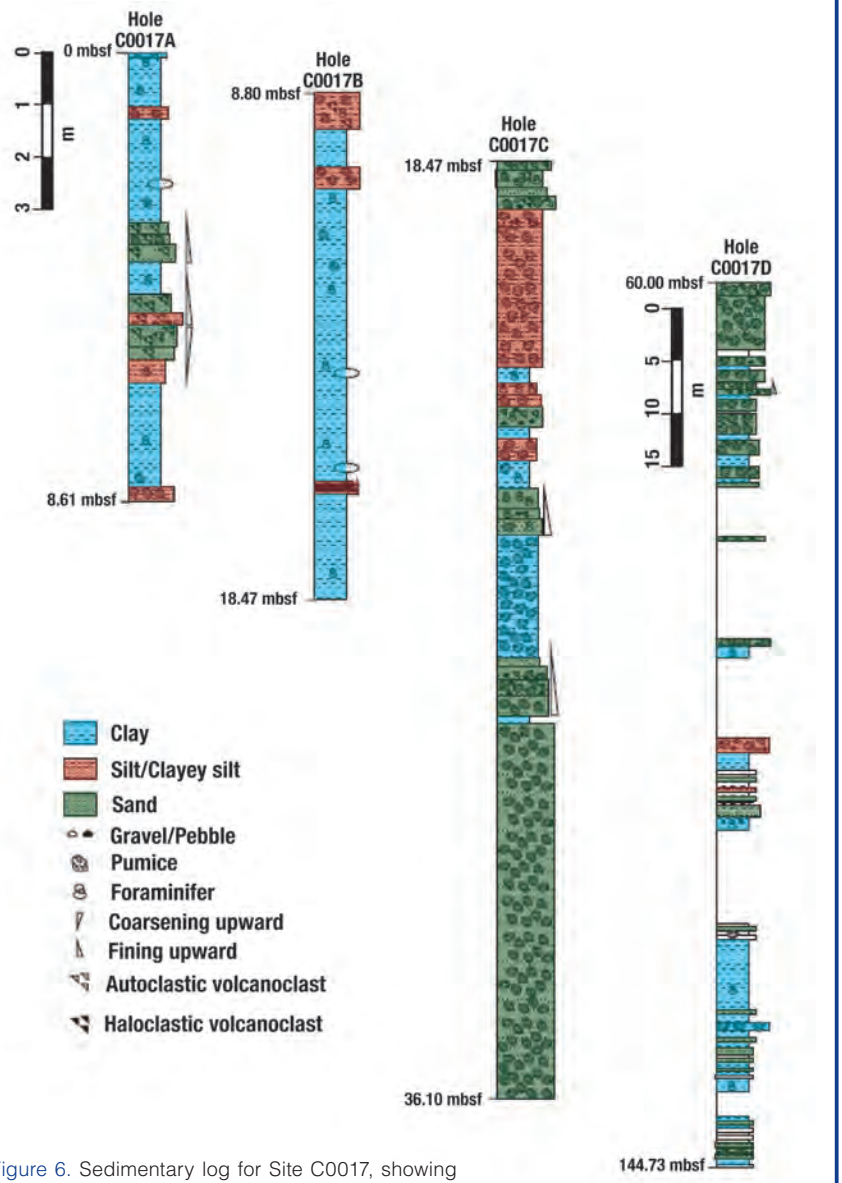

Figure 6. Sedimentary log for Site C0017, showing sediment types. Modified from Takai et al. (2011).

The shipboard microbiological analyses and experiments provided little evidence for the existence of a hot subvent biosphere beneath the Iheya North hydrothermal field, though direct microscopic cell count and cultivation from a colder, diffusely venting site and a site of lateral recharge provided evidence for subseafloor psychrophilic to mesophilic microbial communities. Prior to this expedition, it was hypothesized that subseafloor mixing between hydrothermal fluids and recharging seawater was sustained by a fine-scale network of narrow hydrothermal fluid flow paths within the subseafloor along the eastern flank of the hydrothermal system. The hydrothermal regimes we intersected by drilling, including the permeable reservoirs and flow paths, appeared to be larger

in scale than we had envisioned. Most of the sediment and rock we cored at Sites C0013, C0014, and C0016 were exposed to much higher temperatures than the microbiologically habitable temperature range (<122°C). However, smaller and more limited zones that were habitable by microbes were sampled, as well as a larger one at the hydrothermal recharge zone at Site C0017. Recharge zones were, of course, an essential part of all hydrothermal systems.

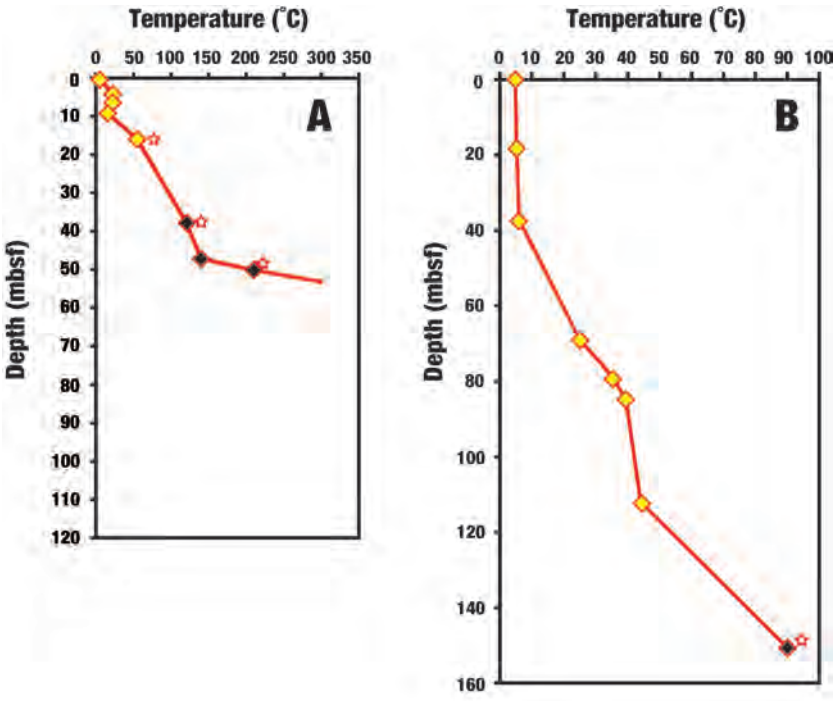

Figure 7. Depth profile of temperature in the subseafloor at Sites [A] C0014 and [B] C0017 as measured by the APCT3 shoe and thermoseal chemically impregnated temperature-sensitive strips. Yellow=APCT3, black=thermoseal strip. Stars=minimum values. Modified from Takai et al. (2011).

Plans for Future Investigations

A total of twenty-four holes were drilled during Expedition 331, of which twenty-one resulted in recovered cores. We drilled 708 m and recovered 312 meters of core from 560 m attempted, yielding an overall recovery of 56%. This compares highly favorably with the only other attempt to drill a submarine felsic-hosted hydrothermal system during ODP Leg 193, which recorded an overall core recovery of 10.7% at the PACMANUS site in the Eastern Manus Basin, Papua New Guinea (Shipboard Scientific Party, 2002). The improved core recovery during Expedition 331 will provide excellent opportunities to assess the existence of a functionally active, metabolically diverse subvent biosphere and to clarify the architecture and function of subseafloor microbial ecosystems and the physical, geochemical, and hydrogeologic variations.

Holes C0013E and C0014G were cased with stainless steel pipe and capped with stainless steel corrosion caps with open outlets, and Hole C0016B was capped but not cased above a 3-m insertion pipe. Four post-drilling natural and artificial hydrothermal vents were created in Holes C0013E, C0014G, C0016A, and C0016B, in which hydrothermal fluid formerly trapped in the subseafloor ascended up the hole and exited into the ocean (Fig. 4). Temperature at all hydrothermal vent emissions was confirmed to be >240°C. These newly created hydrothermal vents will serve as windows into the subseafloor and will facilitate post-drilling, long-term studies of any associated microbial communities, fluid composition and flow, and *in situ* microbial and macrofaunal colonizations.

Interstitial water collected during Expedition 331 suggested that the subseafloor hydrothermal fluid regime of Iheya North field is chemically stratified with respect to chloride concentration. Pore water near the seafloor had the chloride concentration of seawater. It was underlain by a thin and possibly discontinuous vapor-rich layer at ≥5 mbsf at Site C0013 and at 29–38 mbsf at Site C0014. Beneath the vapor-rich layer lays a chloride-enriched brine, at least to the maximum depth of the holes drilled at these two sites. Previous surveys of the Iheya North hydrothermal vents always found that the discharging fluids were low in chloride but rich in vapor (Kawagucci et al., 2011). It was a puzzle where the complementary brines resided. Several theoretical calculations predicted that the greater densities of brines caused them to sink to greater depths within subseafloor hydrothermal reservoirs (Fontaine and Wilcock, 2006). Expedition 331 provided tentative evidence of subseafloor stratification of hydrothermal fluids that had separated phases. The post-drilling investigation of the hydrothermal fluids discharging from the natural and artificial hydrothermal vents may provide further evidence of the chemically stratified subseafloor hydrothermal fluid regime of Iheya North field.

At Site C0016, drilling at the summit of the active hydrothermal mound failed to recover core, and drilling at the base of the mound yielded only 2.1 meters of core from 45 m of penetration, but the core included the first Kuroko-type, sphalerite-rich black ore ever recovered from the modern subseafloor. The other four sites yielded interbedded hemipelagic and strongly pumiceous volcaniclastic sediment, along with volcanogenic breccias that are variably hydrothermally altered and mineralized, in the zeolite to greenschist facies. Detailed studies of these lithologies, in the context of all that is known about the active hydrothermal system at Iheya North Knoll, will provide direct evidence of how VHMS mineral deposits in general, and the Kuroko ores in particular, are formed.

Shipboard analyses did not confirm the presence of an active deep hot biosphere. Cell abundances were much lower than those found in previous Ocean Drilling Program/IODP sites on continental margins (8.7×10^5–2.4×10^7 cells mL^{-1} sediment at Site C0013, 1.3×10^6–4.1×10^8 cells mL^{-1} sediment at Site C0014 and 5.8×10^5–2.4×10^7 cells mL^{-1} sediment at Site C0017; Takai et al., 2011), and attempts at culturing (hyper)thermophiles were generally unsuccessful. In fact, we found evidence for microbial activity in sediments within the upper 10–30 mbsf where temperatures were relatively low but little evidence in the deeper hydrothermally altered zones and hydrothermal fluid regime. Future shore-based, more detailed investigations may provide multiple lines of evidence for functionally active, metabolically diverse subseafloor microbial communities within the environments of the Iheya North hydrothermal system. In addition, the future investigations will seek to clarify the depth limits for the existence of microbial cells, metabolic activities, and living and fossil organic biomarkers in the subseafloor environment. These limits may represent a realistic boundary between the habitable and the uninhabitable zones in the subseafloor environments, namely a thermal barrier of the subseafloor biosphere.

Acknowledgements

We thank the captains, offshore installation managers, operation superintendents, and all the crew, expedition staff and technicians on *Chikyu* from Mantle Quest Japan and CDEX, JAMSTEC, who assisted us in drilling, sampling, installation, and measurements during Expedition 331. We also thank the proponents and all involved in preparation of IODP Proposal 601. Without their cooperation, this expedition could have never been fulfilled. The curatorial team provided us with their support during the expedition and upon the post-expedition sample requests.

The IODP Expedition 331 Scientists

K. Takai (Co-Chief Scientist), M.J. Mottl (Co-Chief Scientist), S.H. Nielsen (Expedition Project Manager), J.L. Birrien, S. Bowden, L. Brandt, A. Breuker, J.C. Corona, S. Eckert, H. Hartnett, S.P. Hollis, C.H. House, A. Ijiri, J. Ishibashi, Y. Masaki, S. McAllister, J. McManus, C. Moyer, M. Nishizawa, T. Noguchi, T. Nunoura, G. Southam, K. Yanagawa, S, Yang, and C. Yeats.

References

Deming, J.W., and Baross, J.A., 1993. Deep-sea smokers: Windows to a subsurface biosphere? *Geochim. Cosmochim. Acta*, 57(14):3219–3230. doi:10.1016/0016-7037(93)90535-5

Expedition 331 Scientists, 2010. Deep hot biosphere. *IODP Prel. Rept.*, 331. doi:10.2204/iodp.pr.331.2010

Fontaine, F.J., and Wilcock, W.S.D., 2006. Dynamics and storage of brine in mid-ocean ridge hydrothermal systems. *J. Geophys. Res.*, 111(B6):B060102. doi:10.1029/2005JB003866

Gamo, T., Ishibashi, J., Tsunogai, U., Okamura, K., and Chiba, H., 2006. Unique geochemistry of submarine hydrothermal fluids from arc-back-arc settings of the Western Pacific. *In* Christie, D.M., Fisher, C.R., Lee, S.-M., and Givens, S. (Eds.), *Back-arc Spreading Systems: Geological, Biological, Chemical, and Physical interactions*. Geophys. Monogr., 166:147–161. doi:10.1029/166GM08

Gamo, T., Sakai, H., Kim, E.-S., Shitashima, K., and Ishibashi, J., 1991. High alkalinity due to sulfate reduction in the CLAM hydrothermal field, Okinawa Trough. *Earth Planet. Sci. Lett.*, 107(2):328–338. doi:10.1016/0012-821X(91)90080-2

Halbach, P., Nakamura, K., Wahsner, M., Lange, J., Sakai, H., Käselitz, L., Hansen, R.-D., et al., 1989. Probable modern analogue of Kuroko-type massive sulfide deposits in the Okinawa Trough back-arc basin. *Nature*, 338(6215):496–499. doi:10.1038/338496a0

Huber, J.A., and Holden, J.F., 2008. Modeling the impact of diffuse vent microorganisms along mid-ocean ridges and flanks. *In* Lowell, R.P., Seewald, J.S., Metaxas, A., and Perfit, M.R. (Eds.), *Magma to Microbe: Modeling Hydrothermal Processes at Oceanic Spreading Centers*. Geophys. Monogr., 178:215–231. doi:10.1029/178GM11

Inagaki, F., Kuypers, M.M.M., Tsunogai, U., Ishibashi, J.-I., Nakamura, K.-I., Treude, T., Ohkubo, S., et al., 2006. Microbial community in a sediment-hosted CO_2 lake of the southern Okinawa Trough hydrothermal system. *Proc. Natl. Acad. Sci. U.S.A.*, 103(38):14164–14169. doi:10.1073/pnas.0606083103

Kawagucci, S., Chiba, H., Ishibash, J., Yamanaka, T., Toki, T., Muramatsu, Y., Ueno, Y., et al., 2011. Hydrothermal fluid geochemistry at the Iheya North field in the mid-Okinawa Trough: Implication for origin of methane in subseafloor fluid circulation systems. *Geochemical. J.*, 45(2):109–124.

Konno, U., Tsunogai, U., Nakagawa, F., Nakaseama, M., Ishibashi, J., Nunoura, T., and Nakamura, K., 2006. Liquid CO_2 venting on the seafloor: Yonaguni Knoll IV hydrothermal system, Okinawa Trough. *Geophys. Res. Lett.*, 33(16):L16607. doi:10.1029/2006GL026115

Lee, C.-S., Shor, G.G., Jr., Bibee, L.D., Lu, R.S., and Hilde, T.W.C., 1980. Okinawa Trough: Origin of a back-arc basin. *Mar. Geol.*, 35(1–3):219–241. doi:10.1016/0025-3227(80)90032-8

Letouzey, J., and Kimura, M., 1986. The Okinawa Trough: Genesis of a backarc basin developing along a continental margin. *Tectonophysics*, 125(1–3):209–230. doi:10.1016/0040-1951(86)90015-6

Nakagawa, S., Takai, K., Inagaki, F., Chiba, H., Ishibashi, J., Kataoka, S., Hirayama, H., Nunoura, T., Horikoshi, K., and Sako, Y., 2005. Variability in microbial community and venting chemistry in a sediment-hosted backarc hydrothermal system: Impacts of subseafloor phase-separation. *FEMS Microbiol. Ecol.*, 54(1):141–155. doi:10.1016/j.femsec.2005.03.007

Narita, H., Harada, K., and Tsunogai, S., 1990. Lateral transport of sediment particles in the Okinawa Trough determined by natural radionuclides. *Geochem. J.*, 24:207–216. doi:10.2343/geochemj.24.207

Nunoura, T., and Takai, K., 2009. Comparison of microbial communities associated with phase-separation-induced hydrother-

mal fluids at the Yonaguni Knoll IV hydrothermal field, the Southern Okinawa Trough. *FEMS Microbiol. Ecol.*, 67:351–370. doi:10.1111/j.1574-6941.2008.00636.x

Nunoura, T., Oida, H., Nakaseama, M., Kosaka, A., Ohkubo, S.B., Kikuchi, T., Kazama, H., et al., 2010. Archaeal diversity and distribution along thermal and geochemical gradients in hydrothermal sediments at the Yonaguni Knoll IV hydrothermal field in the southern Okinawa Trough. *Appl. Environ. Microbiol.*, 76(4):1198–1211. doi:10.1128/AEM.00924-09

Sakai, H., Gamo, T., Kim, E.-S., Shitashima, K., Yanagisawa, F., Tsutsumi, M., Ishibashi, J., et al., 1990. Unique chemistry of the hydrothermal solution in the mid-Okinawa Trough backarc basin. *Geophys. Res. Lett.*, 17(12):2133–2136. doi:10.1029/GL017i012p02133

Shipboard Scientific Party, 2002. Leg 193 summary. *In* Binns, R.A., Barriga, F.J.A.S., Miller, D.J., et al., *Proc. ODP, Init. Repts.*, 193: College Station, TX (Ocean Drilling Program). doi:10.2973/odp.proc.ir.193.101.2002

Suzuki, R., Ishibashi, J., Nakaseama, M., Konno, U., Tsunogai, U., Gena, K., and Chiba, H., 2008. Diverse range of mineralization induced by phase separation of hydrothermal fluid: Case study of the Yonaguni Knoll IV hydrothermal field in the Okinawa Trough back-arc basin. *Res. Geol.*, 58(3):267–288. doi:10.1111/j.1751-3928.2008.00061.x

Takai, K., and Nakamura, K., 2010. Compositional, physiological and metabolic variability in microbial communities associated with geochemically diverse, deep-sea hydrothermal vent fluids. *In* Barton, L., Mendl, M., and Loy, A. (Eds.), *Geomicrobiology: Molecular and Environmental Perspective:* New York (Springer), 251–283. doi:10.1007/978-90-481-9204-5_12

Takai, K., Komatsu, T., Inagaki, F., and Horikoshi, K., 2001. Distribution of archaea in a black smoker chimney structure. *Appl. Environ. Microbiol.*, 67(8):3618–3629. doi:10.1128/AEM.67.8.3618-3629.2001

Takai, K., Mottl, M.J., Nielsen, S.H., and the Expedition 331 Scientists, 2011. *Proc. IODP, 331*: Washington, DC (Integrated Ocean Drilling Program Management International, Inc.). doi:10.2204/iodp.proc.331.2011

Takai, K., Nakagawa, S., Reysenbach, A.L., and Hoek, J., 2006. Microbial ecology of mid-ocean ridges and backarc basins. *In* Christie, D.M., Fisher, C.R., Lee, S.M., and Givens, S. (Eds.), *Back-Arc Spreading Systems: Geological, Biological, Chemical and Physical Interactions*. Geophys. Monogr., 166:185–213. doi:10.1029/144GM23

Takai, K., Nunoura, T., Horikoshi, K., Shibuya, T., Nakamura, K., Suzuki, Y., Stott, M., et al., 2009. Variability in microbial communities in black smoker chimneys at the NW caldera vent field, Brothers Volcano, Kermadec arc. *Geomicrobiol. J.*, 26(8):552–569. doi:10.1080/01490450903304949

Takai, K., Nunoura, T., Ishibashi, J., Lupton, J., Suzuki, R., Hamasaki, H., Ueno, Y., et al., 2008. Variability in the microbial communities and hydrothermal fluid chemistry at the newly discovered Mariner hydrothermal field, southern Lau Basin. *J. Geophys. Res.*, 113:G02031. doi:10.1029/2007JG000636

Ueno, H., Hamasaki, H., Murakawa, Y., Kitazono, S., and Takeda, T., 2003. Ore and gangue minerals of sulfide chimneys from the North Knoll, Iheya Ridge, Okinawa Trough, Japan. *JAMSTEC J. Deep Sea Res.*, 22:49–62, http://docsrv.godac.jp/MSV2_DATA/23/22_06.pdf.

You, C.-F., Butterfield, D.A., Spivack, A.J., Gieskes, J.M., Gamo, T., and Campbell, A.J., 1994. Boron and halide systematics in submarine hydrothermal systems: Effects of phase separation and sedimentary contributions. *Earth Planet. Sci. Lett.*, 123(1–3):227–238. doi:10.1016/0012-821X(94)90270-4

Authors

Ken Takai, Subsurface Geobiology Advanced Research (SUGAR) Project, Japan Agency for Marine-Earth Science & Technology (JAMSTEC), 2-15 Natsushima-cho, Yokosuka 237-0061, Japan, e-mail: kent@jamstec.go.jp.

Michael J. Mottl, Department of Oceanography, School of Ocean and Earth Science and Technology (SOEST), University of Hawaii at Manoa, 1000 Pope Road, Honolulu, HI 96822, e-mail: mmottl@soest.hawaii.edu.

Simon H.H. Nielsen, Center for Deep Earth Exploration (CDEX), Japan Agency for Marine-Earth Science & Technology (JAMSTEC), 3173-25 Showa-machi Kanazawa-ku, Yokohama 236-0001, Japan, e-mail: micropora@gmail.com.

and the IODP Expedition 331 Scientists

Related Web Link

http://www.jamstec.go.jp/chikyu/eng/Expedition/okinawa/exp331.html

IODP Expedition 335: Deep Sampling in ODP Hole 1256D

by Damon A.H. Teagle, Benoit Ildefonse, Peter Blum and the IODP Expedition 335 Scientists

doi:10.2204/iodp.sd.13.04.2011

Abstract

Observations of the gabbroic layers of untectonized ocean crust are essential to test theoretical models of the accretion of new crust at mid-ocean ridges. Integrated Ocean Drilling Program (IODP) Expedition 335 ("Superfast Spreading Rate Crust 4") returned to Ocean Drilling Program (ODP) Hole 1256D with the intention of deepening this reference penetration of intact ocean crust a significant distance (~350 m) into cumulate gabbros. Three earlier cruises to Hole 1256D (ODP 206, IODP 309/312) have drilled through the sediments, lavas, and dikes and 100 m into a complex dike-gabbro transition zone.

Operations on IODP Expedition 335 proved challenging throughout, with almost three weeks spent re-opening and securing unstable sections of the hole. When coring commenced, the comprehensive destruction of the coring bit required further remedial operations to remove junk and huge volumes of accumulated drill cuttings. Hole-cleaning operations using junk baskets were successful, and they recovered large irregular samples that document a hitherto unseen sequence of evolving geological conditions and the intimate coupling between temporally and spatially intercalated intrusive, hydrothermal, contact-metamorphic, partial melting, and retrogressive processes.

Hole 1256D is now clean of junk, and it has been thoroughly cleared of the drill cuttings that hampered operations during this and previous expeditions. At the end of Expedition 335, we briefly resumed coring before undertaking cementing operations to secure problematic intervals. To ensure the greatest scientific return from the huge efforts to stabilize this primary ocean lithosphere reference site, it would be prudent to resume the deepening of Hole 1256D in the nearest possible future while it is open to full depth.

Why Study Ocean Crust Forming at Fast Spreading Rates?

The vast majority (~70%) of magma derived from the mantle is brought into the Earth's crust at the mid-ocean ridges, and approximately two-thirds of that magma cools

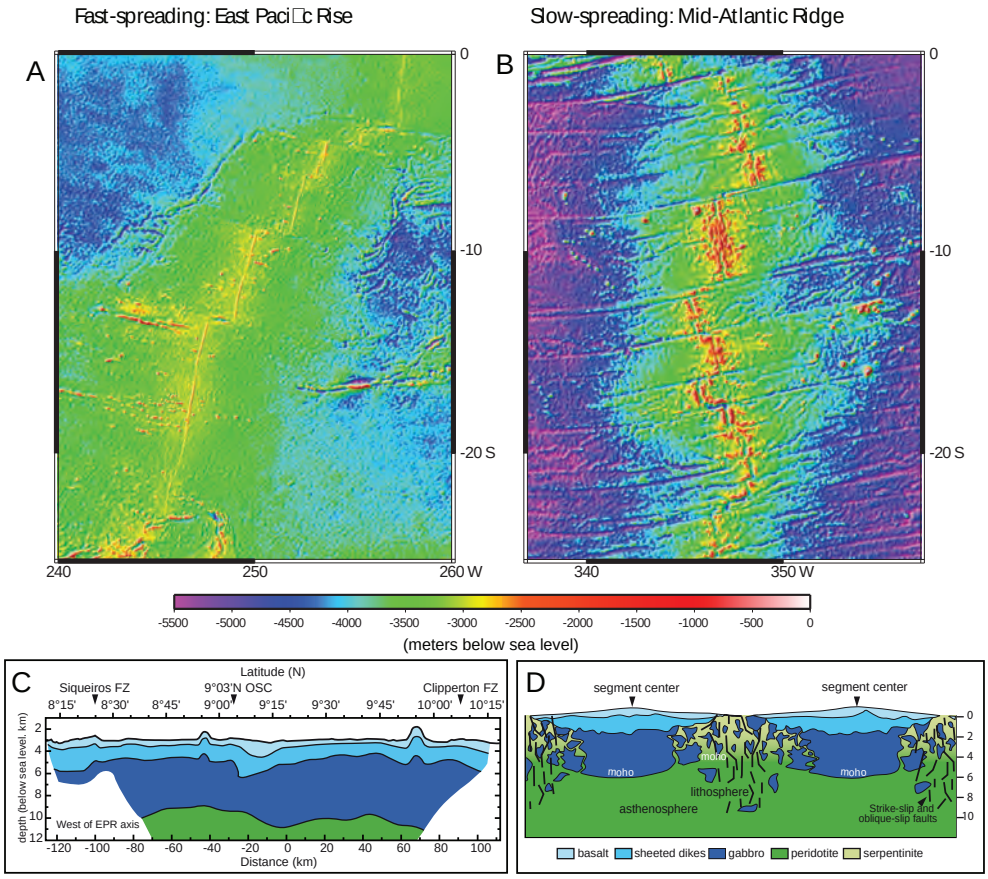

Figure 1. Bathymetric maps of the [A] fast spreading southern East Pacific Rise (EPR) compared to the [B] slow spreading Mid-Atlantic Ridge (MAR) from the equator to 25°S. Note the more pronounced bathymetric relief and axial graben along the MAR as well as the more closely spaced transform faults. Interpreted along-axis sections for the [C] EPR from ~8° to 10° N (after Canales et al., 2003) and [D] MAR (after Cannat et al., 1995).

and crystallizes in the lower portion of the ocean crust. Seismic, bathymetric, and marine geological observations indicate that ocean crust formed at fast spreading rates (full rate >80 mm yr^{-1}) is much less variable than crust formed at slow spreading rates (<40 mm yr^{-1}; Fig. 1) and is closer to the ideal "Penrose" pseudo-stratigraphy developed from ophiolites. Hence, understanding fast-spreading accretion processes at a few sites might reasonably be extrapolated to describe a significant portion of the Earth's surface. Although <20% of modern ridges are moving apart at fast spreading rates (Fig. 2), nearly 50% of present-day ocean crust and ~30% of the Earth's surface were produced by this pace of spreading. The great majority of crust that subducted back into the mantle over the past ~200 m.y. formed at fast-spreading ridges (Müller et al., 2008), making characterizing this style of crust most relevant for understanding the recycling of crustal and ocean-derived components back into the mantle.

The rate of spreading of the oceanic lithosphere has profound effects on the style of accretion at mid-ocean ridges due to changing balances between plate motion, magma production, conductive and hydrothermal cooling, detachment tectonics, and serpentinization of the upper mantle (Fig. 1c vs. 1d; Dick, 1989; Cannat et al., 1995, 2004, 2009; Chen and Phipps Morgan, 1996; Dick et al., 2003; Escartin et al., 2008). Although insights on formation of intrusive crust at detachment-dominated, slow-spread lithosphere have been obtained (e.g., Holes 735B, U1309D, and other sites; ODP Legs 118, 153, 176, 209, and IODP Expeditions 304–305; Dick et al., 2000; Ildefonse et al., 2007; Kelemen et al., 2007), the thermal regime and the melt supply and delivery in these settings differ significantly from those of the axial zone in fast-spreading lithosphere. Detailed understanding of the relatively uniform mechanisms operating at fast spreading ridges would provide a vital benchmark against which heterogeneous accretion on slow-spreading ridges could be compared.

Geological Setting of Site 1256 and Science Objectives of IODP Expedition 335

IODP Expedition 335 (13 April to 3 June 2011) was the fourth scientific drilling cruise of the Superfast campaign, and it returned to ODP Hole 1256D (6°44.163′N, 91°56.061′W) to deepen this ocean crust reference penetration a significant distance into cumulate gabbros. ODP Hole 1256D is located on 15-Ma-crust in the eastern equatorial Pacific Ocean in oceanic basement that formed during a sustained episode of superfast ocean ridge spreading (>200 mm yr^{-1}; Wilson, 1996). Ocean crust formed at a superfast spreading rate was deliberately targeted because there is strong evidence from mid-ocean ridge seismic experiments that gabbros occur at shallower depths in intact ocean crust with higher spreading rates. Therefore, the often difficult-to-drill upper ocean crust should be relatively thin. Expedition 335 follows on from ODP Leg 206 in 2002 and IODP Expeditions

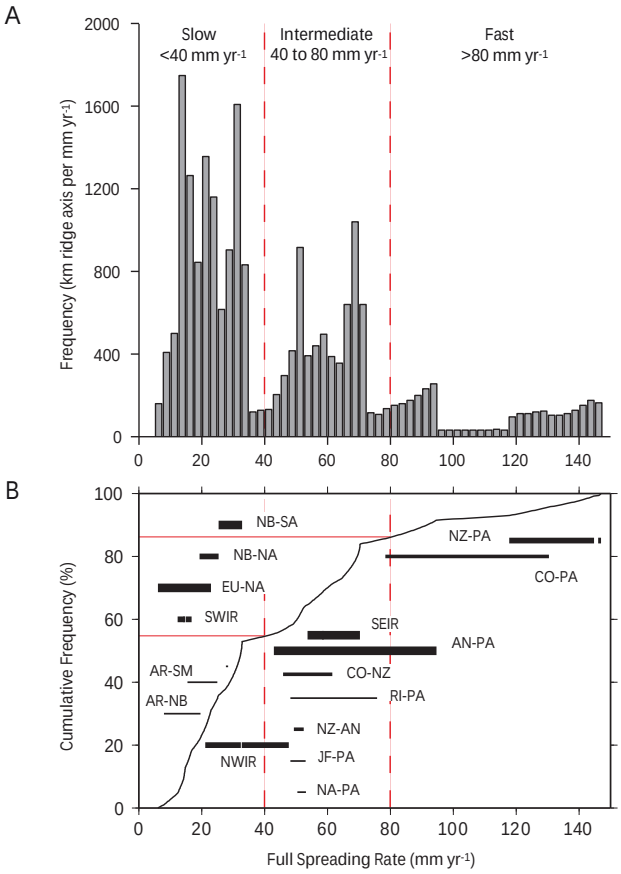

Figure 2. Distribution of spreading rates for major active plate boundaries, presented in [A] histogram form and as [B] cumulative distribution. The rates are the best-fit rates of the MORVEL model (DeMets et al., 2010), and ridge length is measured as the component perpendicular to spreading direction. Horizontal lines on the cumulative plot show the range of spreading rate for each plate pair, with line width scaled approximately to plate boundary length. Plate-pair labels follow the MORVEL convention, except in the Indian Ocean where the southeast, southwest, and northwest branches of the ridge system are grouped for 2–3 plate pairs to simplify labeling

309/312 in 2005 (Wilson et al., 2003; Teagle et al., 2006; Wilson et al., 2006) that prepared the first scientific borehole for deep drilling by installing a large reentry cone secured with almost 270 meters of 16-inch casing through the 250-m-thick sedimentary overburden and cemented into the uppermost basement. Hole 1256D was then deepened through a ~810-m-thick sequence of lavas and a thin (~346 m) sheeted dike complex, the lower 60 meters of which is strongly contact metamorphosed to granoblastic textures (Fig. 4). The first gabbroic rocks were encountered at 1407 meters below seafloor (mbsf) where the hole entered a complex dike-gabbro transition zone that includes two 20- to 50-m thick gabbro lenses intruded into granoblastic dikes. As of the end of Expedition 312 in December 2005, Hole 1256D had a total depth of 1507.1 mbsf, and it was open to its full depth.

It was expected that even with a shortened cruise (~6 weeks), coring on IODP Expedition 335 would be able to deepen Hole 1256D ~350 m, completely through the dike-gabbro transition zone and varitextured gabbros and a

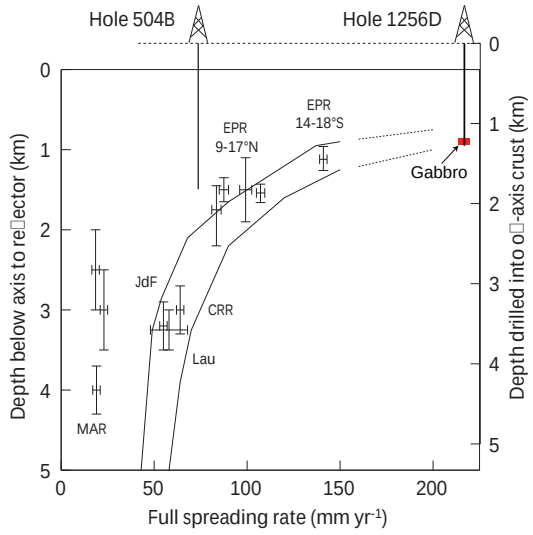

Figure 3. Depth to axial low-velocity zone plotted against spreading rate (Purdy et al., 1992; Carbotte et al., 1997). Depth versus spreading rate predictions from two models of Phipps Morgan and Chen (1993) are shown, extrapolated subjectively to 200 mm y^{-1}. Penetration to date in Holes 504B and 1256D is shown, with the depth at which gabbros were intersected indicated by the red box. Following core descriptions, a thickness of ~300 m of off-axis lava is shown for Hole 1256D and assumed for Hole 504B. EPR=East Pacific Rise, JdF=Juan de Fuca Ridge, Lau=Valu Fa Ridge in Lau Basin, CRR=Costa Rica Rift, MAR=Mid-Atlantic Ridge.

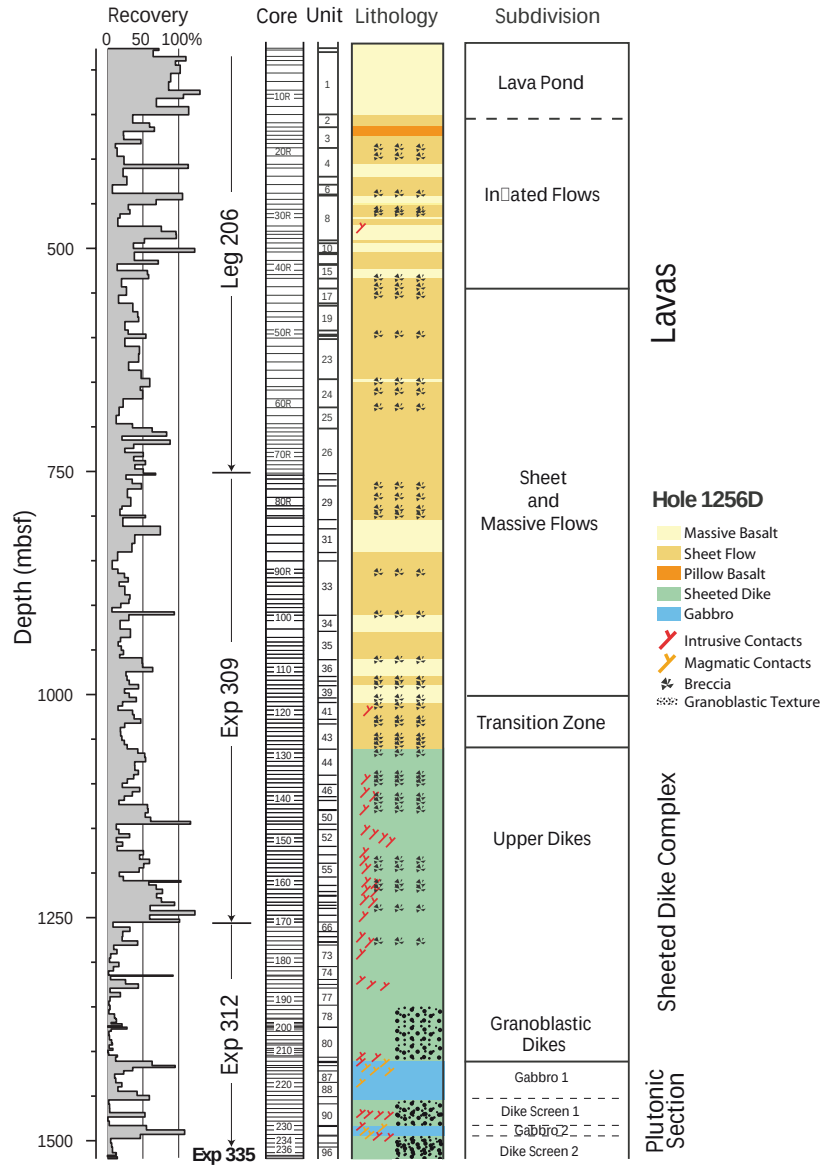

Figure 4. Stratigraphic column for Hole 1256D at the end of Expedition 335, showing the major and minor lithologic divisions of the upper ocean crust.

significant distance into true cumulate gabbros. Listed below are the specific scientific objectives of IODP Expedition 335 that were to be addressed by deepening Hole 1256D a significant distance into cumulate gabbros.

What is the major mechanism of magmatic accretion in crust formed at fast spreading rates? Is the lower crust formed by gabbro glaciers or sheeted sills (Korenaga and Kelemen, 1998; Fig. 5) or by some mixed or unknown mechanism?

How is heat extracted from the lower ocean crust? Specifically, what is the role of hydrothermal circulation in extracting latent heat from the lower ocean crust?

What is the geological significance of the seismic layer 2/3 boundary at Site 1256?

What is the magnetic contribution of the gabbro layer? Can the magnetic polarity structure of the lower crust be used to constrain cooling rates?

Operations

Expedition 335 reentered Hole 1256D more than five years after the last expedition to this site. The expedition encountered and overcame a series of significant engineering challenges, including a major obstruction at a depth of ~922 mbsf that had initially prevented reentry into the hole to its full depth of 1507 meters. At the bottom of the hole, coring resumed in the very hard granular rocks recovered during the previous Superfast expedition. Although there may only be a few tens of meters of these particularly tenacious granoblastic basalts formed by the contact metamorphism of sheeted dikes, their extreme toughness once more proved challenging to sample, resulting in the grinding down of one of the hardest formation coring bits (C9) into a smooth stump (Fig. 6a,b).

Action was then undertaken to clear the bottom of the hole of metal debris from the failed coring bit and drilling cuttings. These efforts returned hundreds of kilograms of rocks and drill cuttings (Fig. 6d), including large blocks (up to 3.5 kg) of the

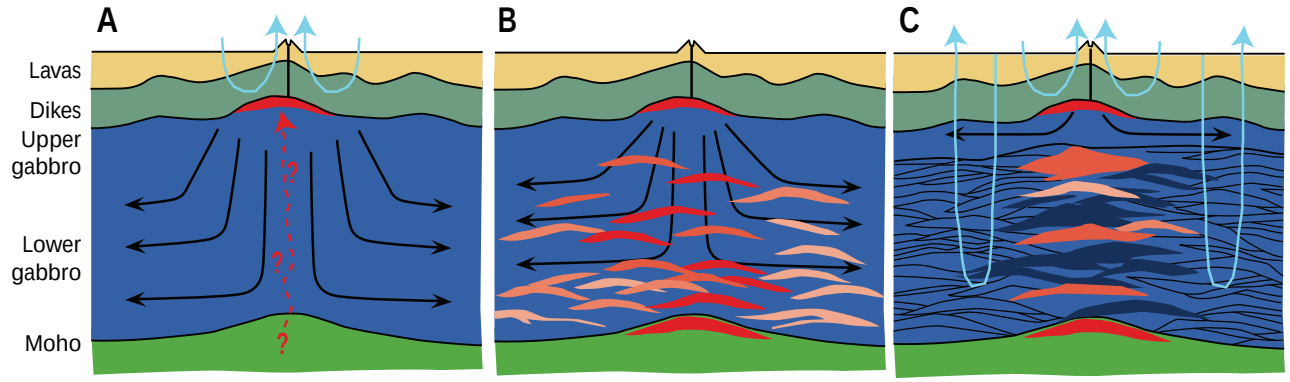

Figure 5. Diagrams of crustal accretion models (modified from Korenaga and Kelemen, 1998). Black arrows show the movement of the solid lower crust; blue arrows show the dominant zones where hydrothermal circulation will remove latent and sensible heat; red arrows show the movement of magma (unknown in all models). [A] Gabbro glacier ductile flow model (Henstock et al., 1993; Phipps Morgan and Chen, 1993; Quick and Denlinger, 1993). Ductile flow down and outward from a high level axial magma chamber constructs the lower crust. [B] A hybrid model of ductile flow with sill intrusions (Boudier et al., 1996). [C] "Sheeted" or "stacked" sill model of *in situ* formation of the lower crust by on-axis sill intrusions (Bédard et al., 1988; Kelemen et al., 1997; Kelemen and Aharonov, 1998; MacLeod and Yoauancq, 2000). (Original figure by Rosalind Coggon).

culprit granoblastic basalts that hitherto had only been very poorly recovered through coring . A limited number of gabbro boulders were also recovered, indicating again that we are tantalizingly close to breaking through into the gabbroic layer.

Scientific Results

Hole opening and remediation operations resulted in a major loss of time from the coring and wireline activities planned for Expedition 335. Coring on this expedition deepened Hole 1256D only modestly, from 1507.1 mbsf to 1521.6 mbsf (Fig. 4) at low rates of penetration (0.9 m hr^{-1}) and recovery (11%).

Hole cleaning operations at the bottom of Hole 1256D, particularly those runs that deployed the reverse-circulation junk basket, brought back a unique collection of large cobbles, angular rubble, and fine cuttings of principally strongly to completely recrystallized granoblastic basalt with minor gabbroic rocks and evolved plutonic rocks. The granoblastic basalts record high-temperature (granulite facies) metamorphism of previously hydrothermally altered sheeted dikes, with unequivocal evidence for hydrothermal alteration before and after the formation of granoblastic textures (Teagle et al., 2006; Koepke et al., 2008; France et al., 2009; Alt et al., 2010). The large blocks exhibit intrusive, structural, and textural relationships, and overprinting and cross-cutting hydrothermal alteration and metamorphic paragenetic sequences. Some of the rubble and ~30% of the fine cuttings recovered by fishing and cleaning operations most likely came from the lava sequences at the top of the hole on the basis of igneous textures and low-temperature alteration minerals (Mg-saponite, amorphous silica). In contrast, the high extent of metamorphic recrystallization exhibited by the granoblastic basalts, and operational factors (e.g., pipe movements), provide strong evidence that the granoblastic

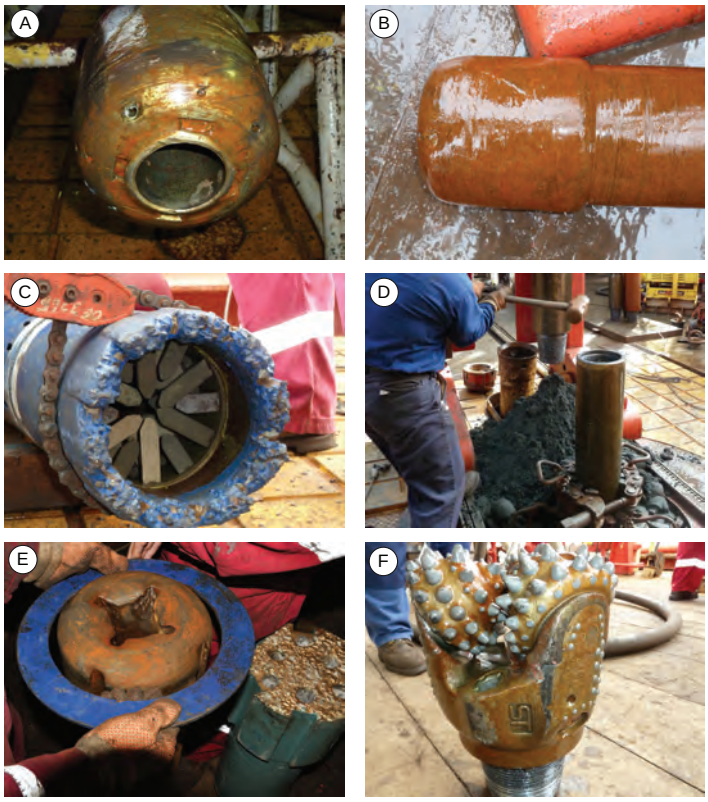

Figure 6. Photographs of some drilling, fishing, and milling tools illustrating the multiple operations achieved during IODP Expedition 335. [A] & [B] Remains of the Ulterra C9 RCB coring bit used during Run 9. The bit was probably used for ~10 h after it disintegrated, which resulted in this spectacularly abraded and sculptured bit ("Stumpy"), something never seen before by the drillers. [C] Bottom of the Bowen Reverse Circulation Junk Basket (RCJB), showing its hard-facing structure and the junk catcher spring fingers inside. This tool recovered a series of large-scale cobbles (up to 5 kg) of granoblastic basalt. [D] A series of RCJB runs returned a bottom hole assembly packed by fine-grained cuttings. This contributed efficiently to cleaning Hole 1256D. [E] Heavily worn and under-gauge 9-inch flat-bottomed milling tool. This tool worked at the bottom of the hole for 12 h; its final state indicates the very abrasive nature of metal debris and/or rocks at the bottom of the hole and an under-gauge lowermost portion (tens of centimeters) of the hole. Note for comparison the hard-facing structure of the next milling tool on the right side of the picture. [F] 9-inch Smith FH3VPS tricone bit used for Run 16. This armored bit was efficient to ream and clean the under-gauge bottom of the hole.

basalts, minor gabbros, and evolved plutonic rocks were sourced from the lowermost reaches of Hole 1256D (1494.9–1521.6 mbsf), most probably from below the lower-most recovered gabbroic interval (Fig. 4). Hence, the rocks recovered during Expedition 335 represent a ~15-m interval of the upper crust/lower crust transition, occurring below the ~90-m section, recovered during Expedition 312, of two gabbroic bodies (Gabbro 1 and Gabbro 2) separated by Dike Screen 1 (Fig. 4).

When the textural and contact relationships exhibited by the rocks recovered from the junk baskets are placed in the geological context of the Hole 1256D stratigraphy, a vision emerges of a complex, dynamic thermal boundary layer zone. This region of the crust between the principally hydrothermal domain of the upper crust and the intrusive magmatic domain of the lower crust is one of evolving geological conditions. There is intimate coupling between temporally and spatially intercalated magmatic, hydrothermal, partial melting, intrusive, metamorphic, and retrograde processes.

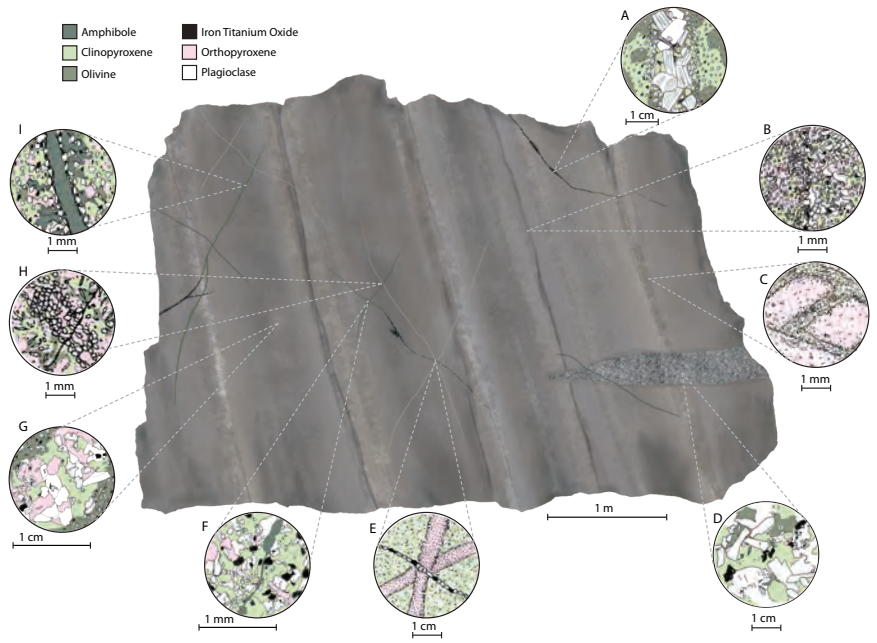

Figure 7. Sketch of a hypothetical outcrop in a future Site 1256 ophiolite of the dike-gabbro transition zone showing the contact relationships observed in the cores and junk basket rocks recovered during Expedition 335. Small sketches are drawn from sample and thin-section descriptions done during Expedition 335. [A] Diorite dikelet, comprised predominantly of primary igneous amphibole and plagioclase, cross-cutting granoblastic basalt. [B] Fine-grained dike chilled against coarser grained dike. The entire sample is recrystallized to granoblastic assemblages of plagioclase, orthopyroxene, clinopyroxene, magnetite, and ilmenite. Later fine post-contact-metamorphic hydrothermal amphibole veins (not shown) cut across the contact and both dikes. [C] Chilled and brecciated dike margin recrystallized to granoblastic assemblages. Angular clasts consist of granoblastic plagioclase with minor orthopyroxene, clinopyroxene, ilmenite, and magnetite. They are recrystallized from chilled dike margin breccia protolith. Clast matrix is orthopyroxene rich with minor clinopyroxene, plagioclase, and oxides; it is recrystallized from hydrothermal minerals (amphibole and chlorite) that veined and cemented the breccia protolith. [D] Subophitic texture in gabbro. [E] Diorite vein cross-cutting a conjugate set of metamorphic orthopyroxene veins. [F] Post-contact-metamorphic hydrothermal hornblende vein cutting granoblastic basalt. [G] Granoblastic basalt with a diorite patch. [H] Granoblastic orthopyroxene vein, recrystallized from precursor hydrothermal vein, in granoblastic dike. Orthopyroxene vein is cut by small post-contact-metamorphic hydrothermal amphibole vein. [I] Post-contact-metamorphic hydrothermal amphibole vein cutting granoblastic basalt, with 1-mm-wide amphibole-rich alteration halo where pyroxenes are replaced by amphibole.

With only a minor depth advance in Hole 1256D, we are yet to recover samples of cumulate gabbros required to test models of ocean ridge magmatic accretion and the intensity of hydrothermal cooling at depth. The total vertical thickness of granoblastic basalts is over 114 m, and Dike Screen 2 is now about the same thickness (so far) as Dike Screen 1. Highly perched, isolated gabbro intrusions are uncommon in ophiolites. The energy requirements for the granoblastic recrys-tallization at granulite facies condition of a >114-m-thick zone of sheeted dikes massively exceeds the thermal capacity of Gabbros 1 and 2 (Coggon et al., 2008; Koepke et al., 2008) if a simple subhorizontal arrangement of these layers is assumed. The enormous heat requirements for such extensive granulite facies recrystallization, the evidence for partial melting, together with the tantalizing presence of minor but not uncommon gabbroic rocks and felsic intrusives, dikelets, and veins, strongly indicates that the layer of purely plutonic rocks should be at most only a few tens of meters deeper in the hole.

Conclusions

Although the extensive remedial operations on Expedition 335 precluded significant deepening of Hole 1256D, significant progress was made in improving the stability of the borehole. The most problematic out-of-gauge zone at ~920–960 mbsf that caused reentry problems on Expeditions 312 and 335 has been stabilized with cement. The bottom of the hole has been cleared of rubble and junk, and there appears to be only a short (<1 m) under-gauge zone. What is important is that the regular, large sweeps of high viscosity mud have finally overcome and expunged the vast amount of fine cuttings recirculating in the hole, some most likely resident since ODP Leg 206. This is shown by the absence of soft fill in the final ~5 reentries, compared to upwards of 50 meters of soft fill at the end of Expedition 312. The engineering efforts on Expedition 335 have repaired and prepared Hole 1256D for further deep drilling, following five years of neglect. Hole 1256D is 1500 m of hard rock coring closer to cumulate gabbros than any other options in intact ocean crust and once more poised to answer fundamental

questions about the formation of new crust at fast spreading mid-ocean ridges. This would be best achieved by a timely return to the site.

Acknowledgments

IODP Expedition 335 was not an easy cruise. Engineering difficulties throughout the expedition presented a continuous series of challenges. The Shipboard Science Party is extremely grateful for the immense efforts of the transocean crew aboard *JOIDES Resolution* for their perseverance, innovation, open discourse, and "can-do" attitude. This team was aboard when Hole 1256D was first spudded in and cased into basement on ODP Leg 206; they were not going to allow the hole to fail. The Texas A&M University (TAMU) Operations Superintendent Ron Grout has sailed on three of the four cruises to Hole 1256D, and his advice in testing situations proved invaluable. The proponents of the Superfast campaign thank the IODP Science Advisory Structure (SAS) for their extension of Expedition 335; without the extra two weeks there could have been the catastrophic loss of Hole 1256D, but this extra time allowed the clearing of junk and cuttings and preservation of the hole for future deepening into the cumulate gabbro layers.

IODP Expedition 335 Scientists

Damon A.H. Teagle (Co-Chief Scientist), Benoit Ildefonse (Co-Chief Scientist), Peter Blum (Staff Scientist), Natsue Abe, Bénédicte Abily, Yoshiko Adashi, Jeffrey C. Alt, Ryo Anma, Graham Baines, Jeremy Deans, Henry J.B. Dick, Daisuke Endo, Eric C. Ferré, Lydéric France, Marguerite Godard, Gilles Guérin, Michelle Harris, Yoon-Mi Kim, Juergen H. Koepke, Mark D. Kurz, C. Johan Lissenberg, Sumio Miyashita, Antony Morris, Ryo Oizumi, Betchaida D. Payot, Marie Python, Parijat Roy, Jessica L. Till, Masako Tominaga, Douglas S. Wilson, and Natalia Zakharova.

References

Alt, J.C., Laverne, C., Coggon, R.M., Teagle, D.A.H., Banerjee, N.R., Morgan, S., Smith-Duque, C.E., Harris, M., and Galli, L., 2010. Subsurface structure of a submarine hydrothermal system in ocean crust formed at the East Pacific Rise, ODP/IODP Site 1256. *Geochem., Geophys., Geosyst.* 11:Q10010–Q10038. doi:10.1029/2010GC003144

Bédard, J.H., Sparks, R.S.J., Renner, R., Cheadle, M.J., and Hallworth, M.A., 1988. Peridotite sills and metasomatic gabbros in the Eastern layered series of the Rhum complex. *J. Geol. Soc. London*, 145(2):207–224. doi:10.1144/gsjgs.145.2.0207

Boudier, F., Nicolas, A., and Ildefonse, B., 1996. Magma chambers in the Oman ophiolite: Fed from the top or from the bottom? *Earth Planet. Sci. Lett.*, 144:239–250. doi:10.1016/0012-821X(96)00167-7

Canales, J.P., Detrick, R.S., Toomey, D.R., and Wilcock, W.S.D., 2003. Segment-scale variations in the crustal structure of 150-300 kyr old fast spreading oceanic crust (East Pacific Rise, 8 degrees 15' N-10 degrees 5' N) from wide-angle seismic refraction profiles. *Geophys. J. Int.*, 152:766–794.

Cande, S.C., and Kent, D.V., 1995. Revised calibration of the geomagnetic polarity timescale for the Late Cretaceous and Cenozoic. *J. Geophys. Res.*, 100: 6093–6095. doi:10.1029/94JB03098

Cannat, M., Cann, J.R., and Maclennan, J., 2004. Some hard rock constraints on the heat supply to mid-ocean ridges. *In* German, C., Lin, J., and Parson, L. (Eds.), *Mid-Ocean Ridges: Hydrothermal Interactions Between the Lithosphere and Oceans.* Geophys. Monogr. Ser., 148:111–150. Washington, D. C. (American Geophysical Union). doi:10.1029/148GM05

Cannat, M., Manatschal, G., Sauter, D., and Peron-Pinvidic, G., 2009. Assessing the conditions of continental breakup at magma-poor rifted margins: What can we learn from slow spreading mid-ocean ridges? *Compt. Rend. Geosci.* 341:406–427. doi:10.1016/j.crte.2009.01.005

Cannat, M., Mevel, C., Maia, M., Deplus, C., Durand, C., Gente, P., Agrinier, P., et al., 1995. Thin crust, ultramafic exposures, and rugged faulting patterns at Mid-Atlantic Ridge (22°–24°N). *Geology*, 23:49–52. doi:10.1130/0091-7613(1995)023%3C0049:TCUEAR%3E2.3.CO;2

Carbotte, S., Mutter, C., Mutter, J., and Ponce-Correa, G., 1997. Influence of magma supply and spreading rate on crustal magma bodies and emplacement of the extrusive layer: Insights from the East Pacific Rise at lat 16°N. *Geology*, 26: 455–458. doi:10.1130/0091-7613(1998)026<0455:IOMSAS>2.3.CO;2

Chen, Y.J., and Phipps Morgan, J., 1996. The effects of spreading rate, the magma budget, and the geometry of magma emplacement on the axial heat flux at mid-ocean ridges. *J Geophys. Res.*, 101:11475–11482. doi:10.1029/96JB00330

Coggon, R.M., Alt, J.C., and Teagle, D.A., 2008. Thermal history of ODP Hole 1256D lower sheeted dikes: Petrology, chemistry and geothermometry of the granoblastic dikes. *Eos, Trans. Am. Geophys. Union*, 89 (53, Suppl.): V44B-08 (Abstract) http://www.agu.org/meetings/fm08/waisfm08.html

DeMets, C., Gordon, R.G., and Argus, D.F., 2010. Geologically current plate motions, *Geophys. J. Int.*, 181:1–80. doi:10.1111/j.1365-246X.2009.04491.x

Dick, H.J.B., 1989. Abyssal peridotites, very slow spreading ridges and ocean ridge magmatism. *In* Saunders, A.D., Norry, M.J. (Eds.), *Magmatism in the ocean basins*. Geol. Soc. Spec. Pub., London, 42:71–105. Oxford (Blackwell Scientific Publications).

Dick, H.J.B., Lin, J., Schouten, H., 2003. An ultraslow-spreading class of ocean ridge. *Nature*, 426:405–412. doi:10.1038/nature02128

Dick, H.J.B., Natland, J.H., Alt, J.C., Bach, W., Bideau, D., Gee, J.S., Haggas, S., et al., 2000. A long *in situ* section of the lower ocean crust: Results of ODP Leg 176 drilling at the Southwest Indian Ridge. *Earth Planet. Sci. Lett.*, 179:31–51. doi:10.1016/S0012-821X(00)00102-3

Escartin, J., Smith, D.K., Cann, J., Schouten, H., Langmuir, C.H., and Escrig, S., 2008. Central role of detachment faults in accretion of slow-spreading oceanic lithosphere. *Nature*, 455:790–795. doi:10.1038/nature07333

France, L., Ildefonse, B., and Koepke, J., 2009. Interactions between magma and hydrothermal system in Oman ophiolite and in IODP Hole 1256D: Fossilization of a dynamic melt lens at fast spreading ridges. *Geochem. Geophys. Geosys.* 10:Q10O19. doi:10.1029/2009GC002652

Henstock, T.J., Woods, A.W., and White, R.S., 1993. The accretion of oceanic crust by episodic sill intrusion. *J. Geophys. Res.*, 98(B3): 4143–4161. doi:10.1029/92JB02661

Ildefonse, B., Blackman, D.K., john, B.E., Ohara, Y., Miller, D.J., MacLeod, C.J., and the IODP Expeditions 304–305 Party, 2007. Oceanic core complexes and crustal accretion at slow-spreading ridges. *Geology*, 35:623–626. doi:10.1130/G23531A.1

Kelemen, P.B., and Aharonov, E., 1998. Periodic formation of magma fractures and generations of layered gabbros in the lower crust beneath oceanic spreading ridges. *In* Buck, W.R., Delaney, P.T., Karson, J.A., and Lagabrielle, Y. (Eds.), *Faulting and Magmatism at Mid-Ocean Ridges*. Geophysical Monograph, 106:267–289. Washington, DC (American Geophysical Union). doi:10.1029/GM106p0267

Kelemen, P.B., Koga, K. and Shimizu, N., 1997. Geochemistry of gabbro sills in the crust-mantle transition zone of the Oman ophiolite: implications for the origin of the oceanic lower crust. *Earth Planet. Sci. Lett.*, 146:475–488.

Kelemen, P.B., Kikawa, E., Miller, D.J., and Shipboard Scientific Party, 2007. Leg 209 summary: Processes in a 20-km-thick conductive boundary layer beneath the Mid-Atlantic Ridge, 14°–16°N. *In* Kelemen, P.B., Kikawa, E., and Miller, D.J. (Eds.), *Proc. ODP, Sci. Results*, 209:1–33. College Station, TX (Ocean Drilling Program). doi:10.2973/odp.proc.sr.209.001.2007

Koepke, J., Christie, D.M., Dziony, W., Holtz, F., Lattard, D., Maclennan, J., Park, S., Scheibner, B., Yamasaki, T., and Yamazaki, S., 2008. Petrography of the dike–gabbro transition at IODP Site 1256 (equatorial Pacific): the evolution of the granoblastic dikes. *Geochem., Geophys., Geosyst.*, 9(7):Q07O09–Q07O37. doi:10.1029/2008GC001939

Korenaga, J., and Kelemen, P.B., 1998. Melt migration through the oceanic lower crust: A constraint from melt percolation modeling with finite solid diffusion. *Earth Planet. Sci. Lett.*, 156:1–11. doi:10.1016/S0012-821X(98)00004-1

MacLeod, C.J., and Yaouancq, G., 2000. A fossil melt lens in the Oman ophiolite: Implications for magma chamber processes at fast spreading ridges. *Earth Planet. Sci. Lett.*, 176:357–373. doi:10.1016/S0012-821X(00)00020-0

Müller, R.D., Sdrolias, M., Gaina, C., and Roest, W.R., 2008. Age, spreading rates, and spreading asymmetry of the world's ocean crust. *Geochem. Geophys. Geosys.*, 9:Q04006. doi:10.1029/2007GC001743

Phipps Morgan, J., and Chen, Y.J., 1993. The genesis of oceanic crust: Magma injection, hydrothermal circulation, and crustal flow. *J. Geophys. Res.*, 98:6283–6297. doi:10.1029/92JB02650

Purdy, G.M., Kong, L.S.L., Christeson, G.L., and Solomon, S.C., 1992. Relationship between spreading rate and the seismic structure of mid-ocean ridges. *Nature*, 355:815–817. doi:10.1038/355815a0

Quick, J.E., and Denlinger, R.P., 1993. Ductile deformation and the origin of layered gabbro in ophiolites. *J. Geophys. Res.*, 98:14015–14027. doi:10.1029/93JB00698

Teagle, D.A.H., Alt, J.C., Umino, S., Miyashita, S., Banerjee, N.R., Wilson, D.S., and Expedition 309/312 Scientists, 2006. *Proc. IODP*, 309/312: Washington, DC (Integrated Ocean Drilling Program Management International, Inc.). doi:10.2204/iodp.proc.309312.2006

Wilson, D.S., 1996. Fastest known spreading on the Miocene Cocos-Pacific Plate Boundary. *Geophys. Res. Lett.*, 23:3003–3006. doi:10.1029/96GL02893

Wilson, D.S., Teagle, D.A.H., Acton, G.D., et al., 2003. *Proc. ODP, Init. Repts.*, 206: College Station, TX (Ocean Drilling Program). doi:10.2973/odp.proc.ir.206.2003.

Wilson, D.S., Teagle, D.A.H., Alt, J.C., Banerjee, N.R., Umino, S., Miyashita, S., Acton, G.D., et al., 2006. Drilling to gabbro in intact ocean crust. *Science*, 312(5776):1016–1020. doi:10.1126/science.1126090

Authors

Damon A.H. Teagle, National Oceanography Centre, Southampton, University of Southampton Waterfront Campus, European Way, Southampton SO14 3ZH, U.K., e-mail: Damon.Teagle@southampton.ac.uk.

Benoit Ildefonse, Géosciences Montpellier, CNRS, Université Montpellier 2, CC 60, 34095 montpellier cédex 05, France.

Peter Blum, Integrated Ocean Drilling Program, Texas A&M University, 1000 Discovery Drive, College Station, TX 77845-9547, U.S.A.

and the IODP Expedition 335 Scientists

Photo Credit

Fig. 6: Photos [A] to [D], and [F]: Benoit Ildefonse, CNRS; Photo [E]: Johan Lissenberg, Cardiff University.

Operational Review of the First Wireline *In Situ* Stress Test in Scientific Ocean Drilling

by Moe Kyaw Thu, Takatoshi Ito, Weiren Lin, Mai-Linh Doan, David Boutt, Yoshihisa Kawamura, Chee Kin Khong, Lisa McNeill, Timothy Byrne, Demian Saffer, Eiichiro Araki, Nobu Eguchi, Ikuo Sawada, Peter Flemings, Yasuyuki Kano, Casey Moore, Masataka Kinoshita, and Harold Tobin

doi:10.2204/iodp.sd.13.06.2011

Introduction

Scientific ocean drilling's first *in situ* stress measurement was made at Site C0009A during Integrated Ocean Drilling Program (IODP) Expedition 319 as part of Nankai Trough Seismogenic Zone Experiment (NanTroSEIZE) Stage 2. The Modular Formation Dynamics Tester (MDT, Schlumberger) wireline logging tool was deployed in riser Hole C0009A to measure *in situ* formation pore pressure, formation permeability (often reported as mobility=permeability/viscosity), and the least principal stress (S3) at several isolated depths (Saffer et al., 2009; Expedition 319 Scientists, 2010).

The importance of *in situ* stress measurements is not only for scientific interests in active tectonic drilling, but also for geomechanical and well bore stability analyses. Certain *in situ* tools were not previously available for scientific ocean drilling due to the borehole diameter and open hole limits of riserless drilling. The riser-capable drillship, D/V *Chikyu*, now in service for IODP expeditions, allows all of the techniques available to estimate the magnitudes and orientations of 3-D stresses to be used. These techniques include downhole density logging for vertical stress, breakout and caliper log analyses for maximum horizontal stress, core-based anelastic strain recovery (ASR, used in the NanTroSEIZE expeditions in 2007–2008), and leak-off test (Lin et al., 2008) and minifrac/hydraulic fracturing (NanTroSEIZE Expedition 319 in 2009). In this report, the whole operational planning process related to *in situ* measurements is reviewed, and lessons learned from Expedition 319 are summarized for efficient planning and testing in the future.

Background

Borehole studies can provide information about vertical stress by downhole density logging, about minimum horizontal stress by extended leak-off test and hydraulic fracturing, and about maximum horizontal stress by breakout analyses (Zoback et al., 2003). During the expeditions of NanTroSEIZE Stage 1, a transect of eight sites was drilled in the regions of the frontal thrust, the midslope megasplay fault, and the Kumano forearc basin using a full suite of Measurement While Drilling - Logging While Drilling (MWD-LWD), coring, and downhole measurements (Kinoshita et al., 2009; Moe et al., 2009). The overarching objective of the LWD program was to provide borehole data that will be used in conjunction with cores to document the geology, physical properties, mechanical state, fluid content, and stress conditions at the drill sites (Kinoshita et al., 2009). Preliminary experiments to determine the orientations and magnitudes of principal stresses in the Nankai Trough were undertaken during the NanTroSEIZE Stage 1 expeditions using borehole image analysis (stress-induced breakouts and tensile fractures; Kinoshita et al., 2008) and indirect, core-based methods such as anelastic strain recovery about three-dimensional stress (Lin et al., 2006; Byrne et al., 2009). An extensive logging program at Site C0009A as part of NanTroSEIZE Stage 2 (Fig. 1) included conventional wireline logging in riser mode with formation stress measurements and a wide-angle Walkaway Vertical Seismic Profile (VSP) with the longest offset in scientific ocean drill-

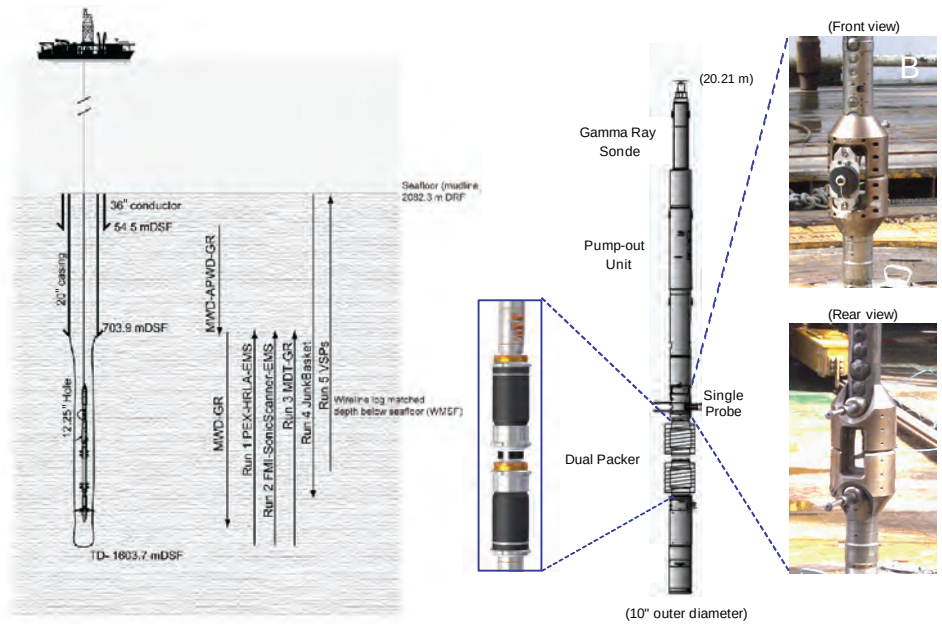

Figure 1. Modular Formation Dynamics Tester (MDT) in operation and illustration of all logging runs from Expedition 319. Measurement While Drilling to total-depth was followed by five runs of wireline toolstrings.

ing (30 km) to improve velocity information of the deep plate boundary and mega-splay faults—the ultimate targets of the project (Moe et al., 2009; Saffer et al., 2009; McNeill et al., 2010; Expedition 319 Scientists, 2010). In a vertical borehole, the orientation of breakouts is a well-established indicator of the orientation of the horizontal maximum principal stress in the present-day stress field (Zoback et al., 2003). Borehole breakouts have been used for stress estimation in NanTroSEIZE Stage 1 and previous expeditions on the Nankai margin (McNeill et al., 2004; Ienaga et al., 2006; Chang et al., 2010). This is the case for stress orientation but not for stress magnitude. Thus, for further understanding the state of stress, the hydraulic fracturing (HF) method was used to measure stress magnitude in Expedition 319 (Ito et al., 2009; Saffer et al., 2009; McNeill et al., 2010; Expedition 319 Scientists, 2010).

Data taken from HF measurements are not only scientifically important but also necessary for operational planning of deep riser holes. In this regard, *in situ* stress is useful for geomechanical and wellbore stability studies. The Center for Deep Earth Exploration (CDEX) has collaborated with GeoMechanics International, Inc. on such studies since 2007 in pore pressure estimation using seismic traces extracted from the high-resolution 3-D seismic data cube (Moore et al., 2009) and calibrated using LWD data as well as geomechanical studies using logging and core analyses data taken from the NanTroSEIZE Stage 1 expeditions (Kinoshita et al., 2009). The absence of leak-off and hydraulic fracturing information in this preliminary study increases the uncertainty in estimating the fracture gradient, and hence can be inconsistent with wellbore failure observations (Castillo et al., 2008).

In Situ Stress Measurement Methods

Stress magnitudes can be inferred from continuous logs (e.g., from sonic-based measurements), but these must be calibrated to obtain direct measurements of stress. At present, the only reliable and accurate measurements of *in situ* stress come from micro-fracturing (Thiercelin et al., 1996). There are several techniques to measure horizontal stress magnitudes and/or stress orientations through data obtained from a well bore. Core experiments include performing a variety of strain experiments. Checking with other results, such as from the micro-fracturing technique, provides a more reliable stress determination. Logging techniques rely on semi-empirical relationships between rock properties and stresses both existing at or near the well bore face, or the interference of stress via a mechanistic model which uses measurements of the borehole breakout (e.g., breakout width). Sonic-based measurements are perhaps the best known logging technique for obtaining stresses. Downhole techniques which fracture the formation are the Leak-Off Test (LOT) and the micro-fracturing technique. A wireline micro-fracturing tool can be used on a wireline (e.g., MDT) or on the drill pipe, where high performance gauges measure the packer internal pressure and the pressure of the fluid between the packers (Carnegie et al., 2002) (Fig. 1).

The importance of strict criteria on borehole conditions and selecting target depths should be noted. Limitations for the MDT wireline tool include the following.

- a hole diameter within 29.21 cm (11.5 inches) and 37.47 cm (14.75 inches) for easy packer insertion and efficient inflation
- hole ovality (Dmax/Dmin) <130% for efficient packer sealing
- expected permeability of <1 mD for the HF test by seawater injection using standard pump and >0.1 mD for the drawdown test (for formation pore pressure and permeability measurement) to prevent no pressure buildup and poroelastic disturbance within the formation caused by too large permeability and too long drawdown test from too small permeability (Note: Permeability derived in the Expedition 319 was ~ 0.1 mD (Boutt et al., in press).)
- zone thickness of >3 m for the HF and >2 m for the drawdown test
- avoidance of pre-existing fractures for both tests.
- good mud cake formation to avoid super-charging and enabling reliable pore pressure measurement and single probe permeability testing
- good borehole stability since the tool is significantly larger than usual logging tools

A classic stress test procedure consists of a series of injection stages or cycles as described below.

Packer inflation is meant to isolate the test interval and results in the pressure in the interval starting to rise after the tool has been properly positioned. A subsequent pressure decline is then observed to check the quality of the packer seal, with further pressurization if the seal is not satisfactory.

Leak-off cycles include injections of fluid into the interval at a constant flow rate. This pressurizes the wellbore below the breakdown of the formation to check that the downhole pump can deliver enough flow rate to overcome fluid diffusion through the mudcake and into the formation.

In the hydraulic fracturing cycles, fluid is again injected into the interval at a constant flow rate and up to the initiation of a tensile fracture, which is recognized either by a breakdown or a pressure plateau. The fracture is then extended for 1–5 minutes before the interval is isolated and the pump stopped (shut-in), the pressure decline then observed, and then followed by a series of injection/fall-off cycles (two to

five) to reopen, further propagate, and then close the fracture to both check the test is repeatable and possibly change the injection parameters (flow rate and injected volume).

Once the operator is satisfied that good quality data have been acquired, the packers are deflated, and the tool is moved to the next interval. A typical test can take from 20 minutes to 1.5 hours, depending on the number of injection cycles that are performed (Desroches and Kurkjian, 1998).

Logging Planning and Operations for Site C0009, Nankai Subduction Zone

A CDEX expedition team was formed in July 2008 following the scheduling of Expedition 319, and logging planning began with assessment of several new tools for scientific ocean drilling, such as MDT, Formation MicroImager (FMI), SonicScanner and High-Resolution Laterolog Array (HRLA), and walkaway VSP (utilizing the Vertical Seismic Imager tool). The call for participation left relatively little time between initiating operations and logging planning and the start of the expedition. An MDT test was agreed upon with the condition that the hole stability was first confirmed by the drilling and the logging results of two wireline runs.

In the process of preparing the MDT measurement plan, four major steps (before and during the expedition) were carried out. The first step was a series of seminars about the new tools and measurements, where expedition scientists attended and led the preparation for MDT draft measurement plan together with the CDEX Logging Staff Scientist (LSS) before expedition. The second step was working on details of measurement plan by logging scientists and Schlumberger engineers onboard with the LSS, Co-Chiefs (CCs), Expedition Project Manager (EPM), and operations geologists from CDEX. Daily updates were shared with the onshore LSSs, Co-chief Scientists, EPM and a Schlumberger MDT specialist. The third step was interpretation of wireline logs taken from logging runs prior to the MDT experiment. Caliper, FMI resistivity image, resistivity, gamma-ray, and sonic velocity logs were thoroughly examined to finalize the plan and select the target zones and depths for each test (Fig. 2). The fourth step was making final decisions on operational details in regard to safety among the onboard Executive Committee (i.e., Ship Captain, Operations Superintendent (OSI), EPM, CCs, and Offshore Installation Manager).

Major adjustments were made during steps onboard. From the cost factors, both dual packer HF tests and drawdown tests were reduced. For safety, the single probe tool was added to run together with the dual packer to reduce the risk of differential pressure sticking, for quick pore pressure and drawdown tests in the high or medium permeability formations, and for selection of dual packer test depths (ultimately providing further scientific data), This imposed a time limit for each MDT measurement.

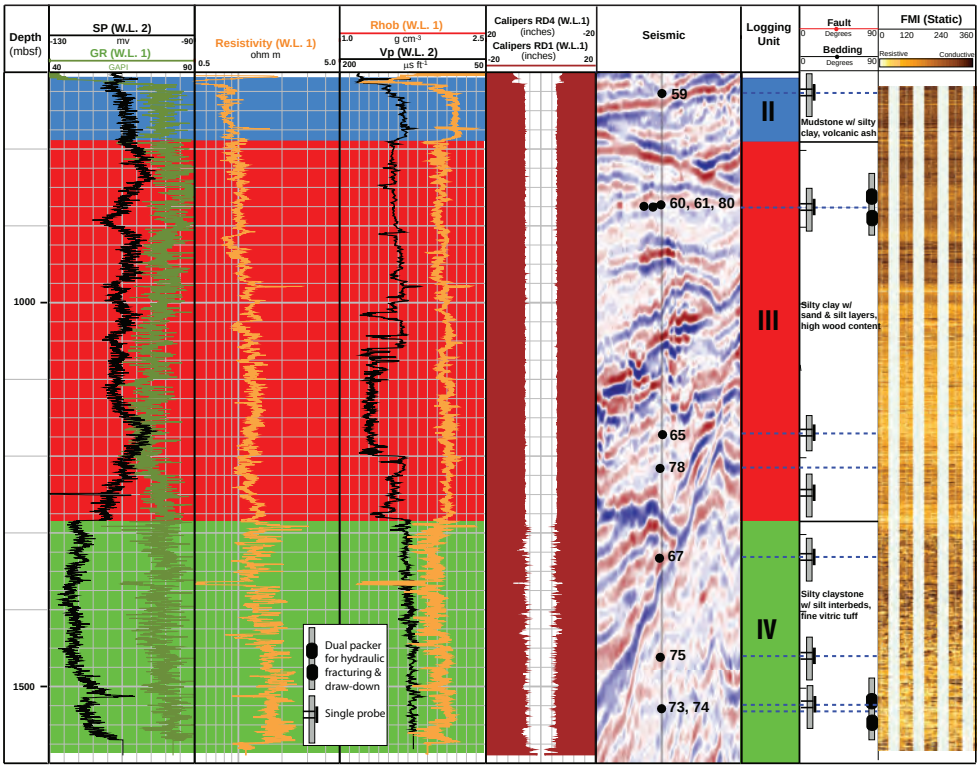

Figure 2. MDT test points on the seismic cross-section together with some important logging data and their interpretation. (From left to right) Depth (meter below seafloor, mbsf), wireline logging runs (W.L.) [spontaneous potential (SP), gamma-ray (GR)], resistivity, density (Rhob), p-wave velocity (Vp), EMS calipers, MDT test points on seismic, logging units from cuttings/core-log-seismic integration, dip picks from FMI data. and static-normalized FMI image.

After two runs of wireline logging, logging scientists and chief scientists identified test depths from logs during a short time of wiper trip in the hole. As a primary focus was making tests in the cored section at the bottom of the hole (where sample analyses would complement the *in situ* measurements), one HF and one drawdown test were made within the cored section at ~1500 mbsf with the dual packer. In addition, one HF test was conducted in the shallower part of the borehole, traveling to the bottom of the hole and four tests on return, and two tests were conducted at the depths of the dual packer tests as a

pre-test check on the site selection (Fig. 2). These sites are distributed throughout the borehole to give a range of data in different environments and formations. The single probe provided critical data for selecting the final MDT sites (both for HF and permeability) and in evaluating risks, as well as providing additional data on formation pore pressure and permeability.

Summary

Deployment of the MDT tool deeper within the forearc and in the vicinity of major fault zones in future riser holes will constitute a major breakthrough in understanding subduction zone fault mechanics, and it is a critical part of the NanTroSEIZE program (Araki et al., 2009; Saffer et al., 2009; McNeill et al., 2010). Operation of this tool was complex both in the planning and execution phase, but valuable experience has been gained by both CDEX and NanTroSEIZE scientists. Unlike other logging measurements, MDT requires considerable involvement of the scientists during planning stage, in decision making during the experiment through real-time monitoring, and constant communication with the MDT specialist, engineer, and drilling operations team. The following factors summarized from the experience and lessons learned from Expedition 319 should inform future MDT deployment on riser expeditions for efficient and scientifically reliable operations.

- A minimum of two LSSs are necessary for the logging operations of riser expeditions.
- Sufficient time is necessary for the dual packer test to generate useful results. A high-performance packer with auto retract mechanism may be an option for future experiments.
- Additional use of single probe at various depths was useful for range of scientific objectives: depth profile for hydrologic interpretation, evaluating the role of erosional and structural events on major transitions/unconformities, lithologic comparison, understanding how the deformation influences the permeability of accretionary prisms, and pore pressure estimation, which is a crucial parameter to understand the mechanics of the prism and décollement.
- Borehole imaging prior to and following the HF test is necessary to determine orientation of the fracture induced or activated by hydraulic fracturing.

Acknowledgements

Thanks are due to the marine and drilling crew of the *Chikyu* and many others for their hard work for the success of IODP Expedition 319. Funding from Ministry of Education, Culture, Sports, Science and Technology (MEXT), Japan, National Science Foundation (NSF), United States, and twenty-two other countries support this project as part of the Integrated Ocean Drilling Program (IODP) for successful drilling in the Nankai Trough.

References

Araki, E., Byrne, T., McNeill, L., Saffer, D., Eguchi, N., Takahashi, K., and Toczko, S., 2009. NanTroSEIZE Stage 2: NanTroSEIZE riser/riserless observatory. *IODP Sci. Prosp.,* 319. doi:10.2204/iodp.sp.319.2009.

Byrne, T.B., Lin, W., Tsutsumi, A., Yamamoto, Y., Lewis, J., Kanagawa, K., Kitamura, Y., Yamaguchi, A. and Kimura, G., 2009. Anelastic strain recovery reveals extension across SW Japan subduction zone. *Geophy. Res. Lett.*, 36:L23310. doi:10.1029/2009/GL040749

Boutt, D., Saffer, D., Doan, M-L., Lin, W., Ito, T., Kano, Y., Flemings, P., McNeil, L., Byrne, T., and Moe, K.T., in press. Scale dependence of *in situ* permeability measurements in the Nankai accretionary prism: The role of fractures. *Geophy. Res. Lett.*

Carnegie, A., Thomas, M., Efnik, M.S., Hamawi, M., Akbar, M., and Burton, M., 2002. An advanced method of determining *in situ* reservoir stresses: Wireline conveyed micro-fracturing. *Soc. Petrol. Eng. Conference Paper*, 78486-MS.

Castillo, D., Magee, M., and Dhakur, S., 2008. NanTroSEIZE Geomechanical analysis of the Stage 1 drilling and Data Acquisition Program: Phase 1. GeoMechanics International, Inc. (CDEX Internal Report).

Chang, C., McNeill, L.C., Moore, J.C., Lin, W., Conin, M., and Yamada, Y., 2010. *In situ* stress state in the Nankai accretionary wedge estimated from borehole wall failures. *Geochem. Geophys. Geosys.*, 11:Q0AD04. doi:10.1029/2010GC003261

Desroches, J., and Kurkjian, A.L., 1998. Applications of wireline stress measurements. *SPE Res. Eval. & Eng.*, 2(5):451–461.

Expedition 319 Scientists, 2010. Expedition 319 summary. *In* Saffer, D., McNeill, L., Byrne, T., Araki, E., Toczko, S., Eguchi, N., Takahashi, K., and the Expedition 319 Scientists, *Proc. IODP*, 319: Tokyo (Integrated Ocean Drilling Program Management International, Inc.). doi:10.2204/iodp.proc.319.101.2010

Ienaga, M., McNeill, L.C., Mikada, H., Saito, S., Goldberg, D., and Moore, J.C., 2006. Borehole image analysis of the Nankai accretionary wedge, ODP Leg 196: Structural and stress studies. *Tectonophysics*, 426:207–220. doi:10.1016/j.tecto.2006.02.018

Ito, T., Lin, W., Doan, M-L., Boutt, D., Kano, Y., Flemings, P., Ito, H., and IODP Expedition 319 Scientists, 2009. Outline of the in-situ stress tests using MDT tool at 2.7–3.6 km below sea level in the first riser hole on the NanTroSEIZE operation. [The 15th Formation Evaluation Symposium of Japan, 1–2 October 2009]. (extended abstract)

Kinoshita, M., Tobin, H., Moe, K.T., and the Expedition 314 Scientists, 2008. NanTroSEIZE Stage 1A: NanTroSEIZE LWD transect. *IODP Prel. Rept.,* 314. doi:10.2204/iodp.pr.314.2008

Kinoshita, M., Tobin, H., Ashi, J., Kimura, G., Lallemant, S., Screaton, E.J., Curewitz, D., Masago, H., Moe, K.T., and the Expedition 314/315/316 Scientists, 2009. NanTroSEIZE Stage 1 expeditions: Introduction and synthesis of key results. *Proc. IODP,* 314/315/316: Washington, DC (Integrated Ocean

Drilling Program Management International , Inc.).

Lin, W., Kwasniewski, M., Imamura, T., and Matsuki, K., 2006. Determination of three-dimensional *in situ* stresses from anelastic strain recovery measurement of cores at great depth. *Tectonophysics*, 426:221–238. doi:10.1016/j.tecto.2006.02.019

Lin, W., Yamamoto, K., Ito, H., Masago, H., and Kawamura, Y., 2008. Estimation of minimum principal stress from an extended leak-off test onboard the *Chikyu* drilling vessel and suggestions for future test procedures. *Sci. Drill.*, 6:43–47.

McNeill, L.C., Ienaga, M., Tobin, H., Saito, S., Goldberg, D., Moore, J.C., and Mikada, H., 2004. Deformation and *in situ* stress in the Nankai Accretionary Prism from resistivity-at-bit images, ODP Leg 196. *Geophys. Res. Lett.*, 31:L02602. doi:10.1029/2003GL018799

McNeill, L.C., Saffer, D., Byrne, T., Araki, E., Toczko, S., Eguchi, N., Takahashi, K., and Expedition 319 Scientists, 2010. IODP Expedition 319, NanTroSEIZE Stage 2: First IODP riser drilling operations and observatory installation towards understanding subduction zone seismogenesis. *Sci. Drill.*, 10:4–13.

Moe, K.T., Sanada, Y., Kido, Y., Kawamura, Y., Cukur, D., Doan, M.-L., Kano, Y., et al., 2009. Overview of the NanTroSEIZE riser logging: Operational planning and reality. [The 15th Formation Evaluation Symposium of Japan, 1–2 October 2009]. (extended abstract)

Moore, G.F., Park, J.-O., Bangs, N.L., Gulick, S.P., Tobin, H.J., Nakamura, Y., Sato, S., et al., 2009. Structural and seismic stratigraphic framework of the NanTroSEIZE Stage 1 transect. *In* Kinoshita, M., Tobin, H., Ashi, J., Kimura, G., Lallement, S., Screaton, E.J., Curewitz, D., Masago, H., Moe, K.T., and the Expedition 314/315/316 Scientists, *Proc. IODP,* 314/315/316. doi:10.2204/iodp.proc.314315316.102.2009

Saffer, D., McNeill, L., Araki, E., Byrne, T., Eguchi, N., Toczko, S., Takahashi, K., and the Expedition 319 Scientists, 2009. NanTroSEIZE Stage 2: NanTroSEIZE riser/riserless observatory. *IODP Prel. Rept.,* 319. doi:10.2204/iodp.pr.319.2009

Thiercelin, M.J., Plumb, R.A., and Desroches, J., 1996. A new wireline tool for *in situ* stress measurements. *SPE Format. Eval.*, 11(1):19–25.

Zoback, M.D., Barton, C.A., Brudy, M., Castillo, D.A., Finkbeiner, T. Grollimund, B.R., Moos, D.B., Peska, P., Ward, C.D., and Wiprut, D.J., 2003. Determination of stress orientation and magnitude in deep wells. *Int. J. Rock Mech. Min. Sci.*, 40(7–8):1049–1076. doi:10.1016/j.ijrmms.2003.07.001

Authors

Moe Kyaw Thu, **Nobu Eguchi**, **and Ikuo Sawada,** Center for Deep Earth Exploration (CDEX)—Japan Agency for Marine-Earth Science and Technology (JAMSTEC), 3173-25 Showa-machi, Kanazawa-ku, Yokohama, Kanagawa 236-0001, Japan, e-mail: moe@jamstec.go.jp.

Yoshihisa Kawamura, *Ippan Shadan Hojin* IODP-MI, Tokyo University of Marine Science and Technology, Office of Liaison and Cooperative Research, 3rd Floor, 2-1-6 Etchujima, Koto-ku, Tokyo, 135-8533 Japan.

Chee Kin Khong, ECA Services Techniques Schlumberger, Le Palatin 1, 1 cour du Triangle, 92936 La Defense –France.

Takatoshi Ito, Institute of Fluid Science, Tohoku University, 2-1-1 Katahira, Aoba-ku, Sendai, Miyagi 980-8577, Japan.

Weiren Lin, Kochi Institute for Core Sample Research, Japan Agency for Marine-Earth Science and Technology, 200 Mononobe-Otsu, Nankoku, Kochi 783-8502, Japan.

Mai-Linh Doan, ISTerre Université de Grenoble 1, CNRS, F-38041 Grenoble, France.

David Boutt, Department of Geosciences, University of Massachusetts Amherst, 611 North Pleasant Street, 233 Morrill Center, Amherst, MA 01002, U.S.A.

Lisa McNeill, School of Ocean and Earth Science, National Oceanography Centre, Southampton, University of Southampton, Southampton SO14 3ZH, U.K.

Demian Saffer, The Pennsylvania State University, 0310 Deike Building, University Park, PA 16802, U.S.A.

Eiichiro Araki, Earthquake and Tsunami Research Project for Disaster Prevention, Japan Agency for Marine-Earth and Technology, 2-15 Natsushima-cho, Yokosuka, Kanagawa 237-0061, Japan.

Timothy Byrne, Center for Integrative Geosciences, University of Connecticut, U-2045, 354 Mansfield Road, Storrs, CT 06269, U.S.A.

Yasuyuki Kano, Disaster Prevention Research Institute, Kyoto University, Gokasho, Uji 611-0011, Japan.

Peter Flemings, Institute for Geophysics, Jackson School of Geosciences, University of Texas at Austin, 10100 Burnet Road (R2200), Austin, TX 78758-4445, U.S.A.

Casey Moore, University of California Santa Cruz, 1156 High Street, Santa Cruz, CA 95064, U.S.A.

Masataka Kinoshita, Institute for Research on Earth Evolution, Japan Agency for Marine-Earth Science and Technology, 2-15 Natsushima-cho, Yokosuka, Kanagawa 237-0061, Japan.

Harold Tobin, Department of Geology and Geophysics, University of Wisconsin-Madison, 1215 West Dayton Street, Madison, WI 53706, U.S.A.

Related Web Links

http://www.jamstec.go.jp/chikyu/eng/Expedition/NantroSEIZE/exp319.html
http://publications.iodp.org/preliminary_report/319/index.html
http://publications.iodp.org/proceedings/319/103/103_.htm

Photo Credit

Fig. 1: Photo courtesy of T. Ito, Tohoku University

Kochi Core Center Provides New Information Services

by Lallan Gupta, Toshio Hisamitsu, and Noriaki Masui

doi:10.2204/iodp.sd.13.05.2011

Introduction

During the last four decades of scientific drilling of seafloor all over the world, an enormous amount (~360,000 m) of marine cores has been collected. These cores are being curated in the three Integrated Ocean Drilling Program (IODP) core repositories located in Germany, Japan, and the U.S.A.. The IODP core repository in Japan is housed in the Kochi Core Center (KCC), Kochi on the island of Shikoku. The total amount of IODP core currently being curated in the KCC is about 93,000 m. These cores were collected from the Indian and west Pacific Oceans, and they consist of a diverse range of geological material. Detailed description of the core material is available in preliminary reports of each drilling expedition. This report details three new services being offered through the KCC website (www.kochi-core.jp): Core Summary, Routine Microbiological Sample (RMS), and Virtual Core Library (VCL).

Core Summary

Cores contain a wide variety of material for the earth science community. Although much of the research is carried out by taking bulk samples from cores, some researchers have specific interests for subsamples, such as ash, calcite nodules, or plankton fossils. However, such detail was so far only provided in individual volumes of preliminary reports or proceedings of expeditions of the IODP core material. For an electronic access to these data, the KCC curatorial staff compiled major features of sample material recovered through Deep Sea Drilling Project (DSDP), Ocean Drilling Program (ODP) and IODP, and made the "Core Summary" information publically available through the KCC web page (http://www.kochi-core.jp/cs/).

The core summary web page lists basic parameters like expedition or leg number, site number, hole, geographical location of the drilled site, drilled interval depth, total length of recovered core, approximate geological age range covered by the core sediments, an overview of lithology, age model, and magnetostratigraphy, together with the link for the preliminary report or proceedings of each drilling expedition. The list can be filtered using various combinations of keywords and parameters. This action will facilitate short-listing of the information related to the core material, which is dispersed in the individual volumes of the preliminary report or proceedings of each leg/expedition. For quickly locating the drill site, a click on the site name takes the user to geographical map services with the site clearly marked on it. Lithological summary of core material recovered from each hole can be quickly viewed in a pop-up window or a new window. Age model, core recovery, and magnetostratigraphy information extracted from preliminary reports or proceedings of each leg/expedition are available in PDF format, which can easily be downloaded.

Routine Microbiological Samples (RMS)

Subsequent to the discovery of life and biosphere in subseafloor environments, the study of biomass, activity, and function of subseafloor life and its ecological roles in biogeochemical cycles has become one of the major scientific objectives in the IODP. In addition, biochemical analytical techniques based on DNA are rapidly developing. Therefore, IODP's Science Advisory Structure (SAS) recommended routine sampling for geomicrobiology, and core repositories were asked to develop the capabilities for storage of core samples at very low temperature. The Japanese Center for Deep Earth Exploration (CDEX) initiated routine collection of microbiological sub-samples of cores in 2009, and these samples are being curated in the KCC.

Storage of the RMS under deep-freezing conditions is critical for preventing degradation—caused by abiotic hydrolysis, enzymatic reactions, and possible contamination—of fragile bio-molecules such as DNA, RNA, enzymes, sugar chains, and intact polar lipids. Moreover, aseptic sub-sampling and distribution of the RMS without thawing is desired for quality assurance purposes. KCC is equipped with deep freezers (-80°C) and liquid nitrogen-cooled tanks (-160°C) for long-term storage and with an aseptic band saw system for "clean" processing of the frozen core sample (Masui et al., 2009). Using these geobiological sampling devices, aliquots of the RMS can be distributed to the science community worldwide according to IODP policy. To spread information about IODP and RMS, KCC prepared a leaflet and a handbill for distribution at academic meetings. In addition, an RMS promotion site has been added to the KCC website. Overview of RMS curation and a list of the RMS have been made available through this website. The list can be filtered for sample depth, expedition, and site name in order to find suitable RMS.

Virtual Core Library (VCL)

The drilling vessel *Chikyu* is equipped with an X-ray Computed Tomography (XCT) scanner, which provides the capability to visualize the internal structure of cores to aid in discerning important geological features prior to splitting and discrete sampling of the cored materials. Standard core flow on board *Chikyu* involves XCT scanning of cores before they are split and archiving of the digital core images (Fig. 1). These data are used by shipboard scientists to identify key features within a core section and to decide if whole round core (WRC) sampling and preservation of part of an unsplit core is necessary for future investigations. The XCT scanning of one core section produces a file that contains data for previewing a 2-D image and for reconstructing a 3-D image of the core section. The files are saved into a format known as DICOM (Digital Imaging and Communication in Medicine). The J-CORES data server stores all files related to the XCT-scanned images, and provides access to the files via the Internet. Files are freely available after the expedition moratorium period.

KCC designed a new web page named "Virtual Core Library" (VCL) that introduces and promotes use of the XCT data for researchers and educators, and displays digital 3-D images of typical core sections on the gallery page. Users can also access preliminary reports of *Chikyu* expeditions and understand scientific details related to a particular cruise, site, hole, etc. The VCL provides a link to the coronal images (2-D images) of core sections that can be quickly viewed. Researchers can then request a copy of DICOM files for core sections of interest. After examining details of the request, curatorial staff will provide the data either by copying them on a DVD or through a file transfer protocol (FTP) setup.

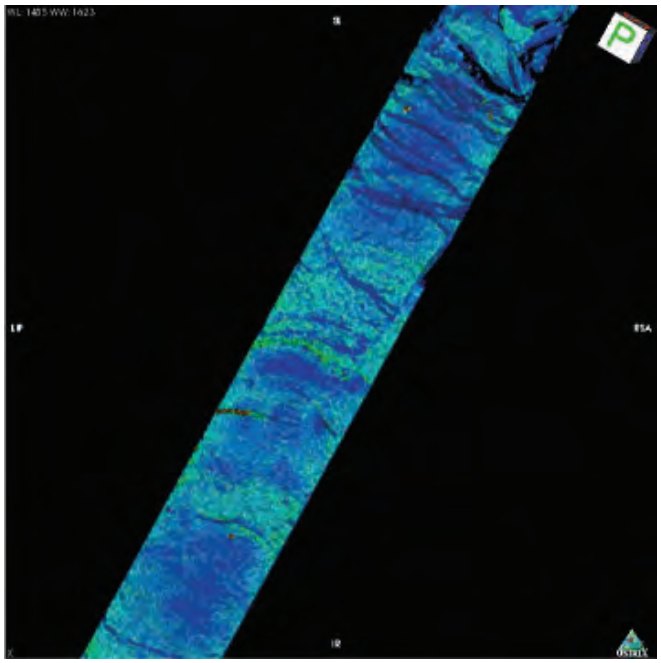

Figure 1. The OsiriX-rendered false colored image of a core section based on XCT scanning data. Fractures and gaps are easily visualized in this image. Change in color from light blue to red can be interpreted to be a reflection of change in density of core material, although calibration is a must to conclude about density.

Recently, DICOM viewing software has become freely available on the Internet (e.g., OsiriX, ApolloView Lite, Onis Viewer). Using such software, researchers can render 3-D images of core sections from DICOM files and can visualize the internal structure of cores by changing transparency and color and by rotating or slicing the image. General DICOM viewers have functions like rendering, cutting, or slicing 3-D images, and they provide an opportunity for users to "virtually sample". The VCL will be improved to accelerate use of the XCT data and promote new approaches in geological studies.

The KCC curatorial staff will continue to improve these Internet-based services to allow for the best possible utilization of IODP samples by researchers around the world, and thus contribute in enhancing our current understanding of the Earth and its environments.

References

Masui, N., Morono, Y., and Inagaki, F., 2009. Bio-Archive core storage and subsampling procedure for subseafloor molecular biological research. *Sci. Drill.*, 8:35–37. doi:10.2204/iodp.sd.8.05.2009

Authors

Lallan Gupta, **Toshio Hisamitsu**, **and Noriaki Masui**, Kochi Core Center, 200 Monobe Otsu, Nankoku, Kochi 783-8502, Japan, e-mail: gupta@jamstec.go.jp.

Related Web Links

http://www.kochi-core.jp/cs/
http://www.kochi-core.jp/rms/
http://www.kochi-core.jp/VCL/

Umbria-Marche Basin, Central Italy: A Reference Section for the Aptian-Albian Interval at Low Latitudes

by Rodolfo Coccioni, Luigi Jovane, Giuseppe Bancalà, Carla Bucci, Gerson Fauth, Fabrizio Frontalini, Liliane Janikian, Jairo Savian, Renato Paes de Almeida, Grasiane Luz Mathias, and Ricardo Ivan Ferreira da Trindade

doi:10.2204/iodp.sd.13.07.2011

Introduction

Within the Cretaceous Period, the Aptian-Albian interval (125–99.6 Ma, Ogg et al., 2008) was a critical time on a global scale. This is evident from 1) changes in the nature of the ocean-climate system brought about by increased ocean crust production coupled with active midplate and plate margin volcanism in a shifting paleogeography (Skelton et al., 2003); 2) cyclic deposition and preservation of common "black shales", some of them termed Oceanic Anoxic Events (OAE1a to OAE1d) (Schlanger and Jenkyns, 1976; Arthur et al., 1990); 3) periodic changes in redox conditions at the ocean bottom (Oceanic Red Beds, ORBs) (Wang et al., 2009); and 4) rapid biotic radiations and turnovers (Leckie et al., 2002). The Aptian-Albian time is also of interest for one of the most noteworthy geomagnetic events, namely the post-M0r "Cretaceous Quiet Zone". This long and constant normal polarity superchron without any convincing true reversal to date (Satolli et al., 2008) precludes usage of reversals magnetostratigraphy from the Aptian through the Santonian.

The Poggio le Guaine core was designed to provide a high-resolution age model and a high-resolution relative magnetic paleointensity reference curve for the Aptian-Albian interval of the long normal Cretaceous superchron; it was also designed to understand the causal linkages among geological, biogeochemical, oceanographic and climatic events as well as their consequences. The core was drilled at Poggio le Guaine, where the most continuous, complete, and best preserved Aptian-Albian succession is exposed throughout the Umbria-Marche Basin (UMB) of the northern Apennines of central Italy (Fig. 1). It represents a continuous record of fossiliferous pelagic rocks extending from the Albian-Cenomanian boundary down to the uppermost Barremian (99.6–126 Ma). In this progress report we present the first preliminary findings of this ongoing project.

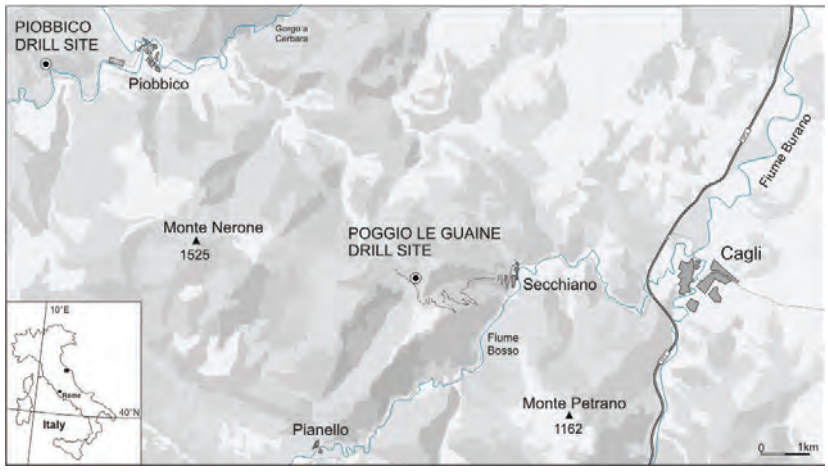

Figure 1. Location of the Poggio le Guaine drill site in the Umbria-Marche Basin (northern Apennines, central Italy). The location of the Piobbico drill site—where an 84-m-thick core extending from the upper Albian down to the uppermost Barremian was drilled in 1982—is also shown.

Geological and Stratigraphic Setting

After three decades of dedicated research, the Aptian-Albian pelagic succession of the UMB has become a classical reference section for studies at a regional to global scale. It deposited well above the calcite compensation depth at middle to lower bathyal depths (1000–1500 m) and at ~20°N paleolatitude over the southern margin of the western Tethys Ocean (Arthur and Premoli Silva, 1982; Coccioni et al., 1987, 1989, 1990, 1992; Erba, 1988, 1992; Cresta et al., 1989; Tornaghi et al., 1989; Coccioni, 1996; Coccioni and Galeotti, 1993; Satolli et al., 2008; Tiraboschi et al., 2009; Turchyn et al., 2009).

This succession extends from the uppermost part of the Maiolica Formation (Tithonian to lower Aptian) to the lower part of the Scaglia Bianca Formation (uppermost Albian to lowermost Turonian) and includes the entire Marne a Fucoidi Formation (Fig. 2). The uppermost part of the Maiolica Formation is represented by thin-bedded white to gray limestones interbedded with black shales. The lower part of the Scaglia Bianca Formation is characterized by thin-bedded yellowish-gray lime-stones with subordinate reddish limestones and some discrete thin black shales, which are the regional sedimentary expression of the latest Albian OAE1d (Fig. 2). Within the Cretaceous succession of the UMB, the Aptian-Albian Marne a Fucoidi Formation represents a distinctive varicolored interlude with more shale. This formation consists of thinly interbedded pale reddish to dark reddish, pale olive to dark reddish brown and pale olive to grayish olive marl-

stones and calcareous marlstones together with dark gray to black organic carbon-rich shales, usually with a low carbonate content, and yellowish-gray to light gray marly limestones and lime-stones (Fig. 2). Several distinctive organic-rich black shale and marl marker beds occur within the Aptian-Albian interval, some of which have been identified as the regional sedimentary expression of OAE1a to OAE1d (Coccioni et al., 1987, 1989, 1990; Coccioni, 1996, 2001).

Following the timescale of Ogg et al. (2008), the sediment accumulation rate is estimated to be ~0.24 cm kyr^{-1} and ~0.5 cm kyr^{-1} in the Aptian and Albian, respectively.

Drilling Site Location and Drilling Operations

The Poggio le Guaine succession was selected as the reference section for the Aptian-Albian interval following previous detailed stratigraphic investigations (Coccioni et al., 1987, 1989, 1990; Coccioni, 1996).

The Poggio le Guaine drill site (lat. 43°32'42.72"N; long. 12°32'40.92"E) is located on the Monte Nerone ridge at 888 m above sea level, 6 km west of the town of Cagli (Regione Marche, Italy) (Fig. 1). The outcropping beds show a strike of 310° and a dip of 30° to the northeast.

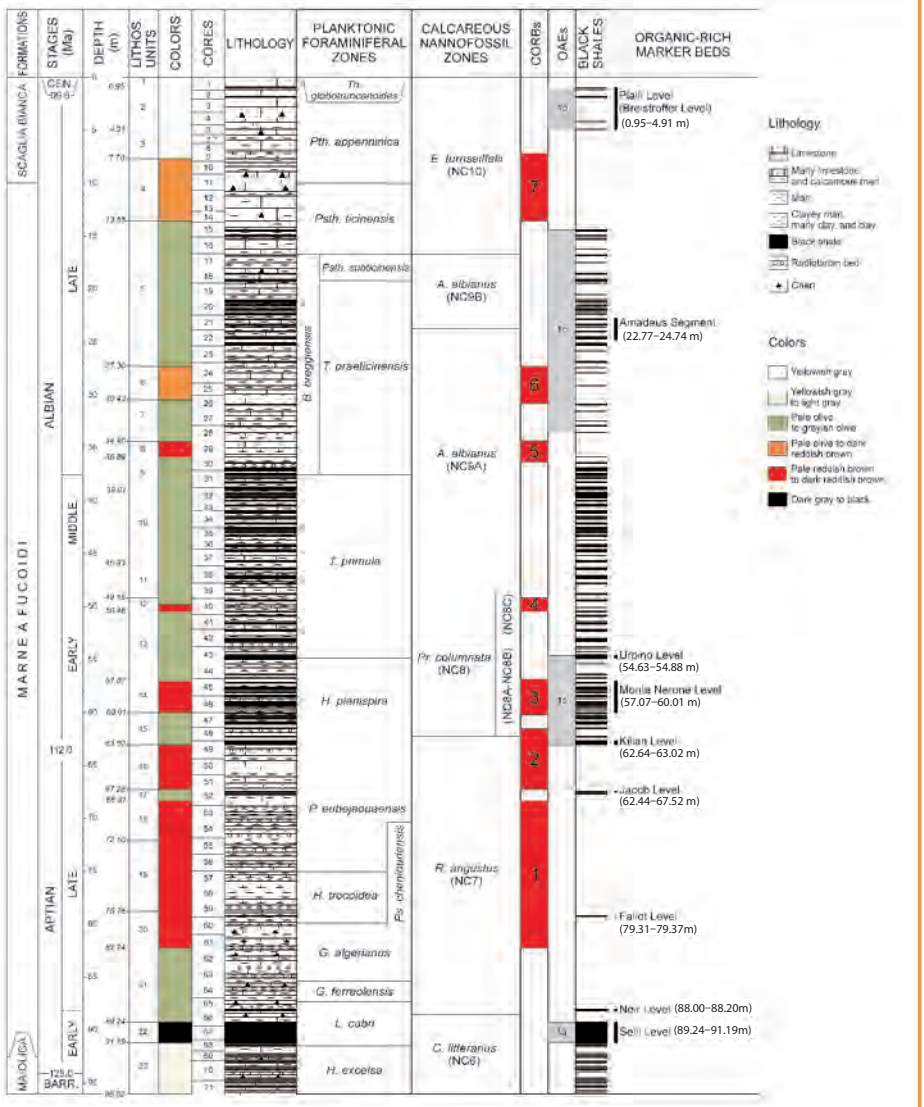

Figure 2. Stratigraphic framework of the Poggio le Guaine core with real stratigraphic depths according to bed dip measurements. Also shown are the occurrence and distribution of the organic-rich black shales including the marker beds resulting from Oceanic Anoxic Events (OAEs) and the discrete intervals where reddish colored beds become dominant (Cretaceous Oceanic Red Beds, CORBs). Integrated plankton biostratigraphy is adapted after Coccioni et al. (1987, 1989, 1990, 1992, 2007), Erba (1988, 1992), Tornaghi et al. (1989), Tiraboschi et al. (2009) and unpublished data. Abbreviations: Lithos.=Lithostratigraphic, Barr.=Barremian, Cen.=Cenomanian, H.=*Hedbergella*, L.=*Leupoldina*, G.=*Globigerinelloides*, P.=*Paraticinella*, Ps.=*Pseudoplanomalina*, T.=*Ticinella*, B.=*Biticinella*, Psth.=*Pseudothalmanninella*, Pth.=*Parathalmanninella*, Th.=*Thalmanninella*, C.=*Chiastozygus*, Pa.=*Parhabdolithus*, N.=*Nannoconus*, Pr.=*Predicosphaera*, A.=*Axopodorhabdus*, R.=*Rhagodiscus*, E.=*Eiffellithus*. Timescale is after Ogg et al. (2008). Following Huber and Leckie (2011), the Aptian-Albian boundary is placed at the highest occurrence of *Paraticinella eubejaouaensis*.

The drilling campaign took place on 1–14 September 2010. Drilling operations were performed with the Atlas Copco Mustang 5-F4 surface core drilling rig (Fig. 3). Coring was accomplished with a T2 double corer, using narrow-kerf, sawtoothed drill bits that cut a 10.1-cm-diameter hole and approximately 8-cm-diameter cores. The target interval was successfully encountered below the weathering zone, which is only a couple of decimeters thick. Lithologies were logged and digital color photographs taken, as each core section was recovered (Fig. 4). Later, the seventy-one cores drilled were packed, labeled, and put in PVC plastic boxes to prevent contamination and loss of moisture. During core packing, care was taken in collecting the fragments from the few fractured portions in plastic bags. The entire core is stored at the core repository of the Department of Earth, Life and Environmental Sciences, University of Urbino.

The Poggio le Guaine cored interval extends from the Albian-Cenomanian boundary down to the uppermost Barremian including the upper transition to the Scaglia Bianca Formation and the lower transition to the Maiolica Formation. The total length of the core is 98.72 m with essentially 100% recovery of excellent quality material throughout the drilling. For each core a set of dip measurements was taken directly at the drill site with four measurements on average for each meter of core. Marked changes of dip angle were observed in the uppermost and lowermost portions of

the core, the latter particularly affected by folding and minor faulting. Taking into account the dip measurements, the corrected thickness of the drilled section is 96.02 m, with 82.53 m corresponding to the Marne a Fucoidi Formation, 3.51 m corresponding to the underlying Maiolica Formation, and 9.98 m corresponding to the overlying Scaglia Bianca Formation (Fig. 2).

Litho-, Bio-, and Chronostratigraphy of the Poggio le Guaine Core

On the basis of dominant colors determined with the Munsell Rock Color Chart, the pattern of alternating colors, the calcium carbonate content, the occurrence of black shales, chert and radiolarian-rich beds, and by direct comparison with previous results from an adjacent outcrop (Coccioni et al., 1987, 1989, 1990), the Poggio le Guaine core was subdivided into twenty-three lithological units, which are recognizable on a regional scale (Coccioni, 1996; Fig. 2). Unit 1 to part of Unit 4 corresponds to the Scaglia Bianca Formation, and part of Unit 4 to the upper part of Unit 23 corresponds to the Marne a Fucoidi Formation. The Maiolica Formation is equated with most of Unit 23.

A total of two hundred forty organic-rich black shales and marls, millimeters to decimeters thick, is recorded in the cored sequence. These layers are not evenly distributed throughout the core. They are frequent to common in Units 2, 5 to 7, 9 to 15, 22 and 23 that are dominated by lithotypes that are pale olive to grayish olive and yellowish gray to light gray, and occasionally by pale olive and pale reddish brown to dark reddish brown (Fig. 2). Some of these organic-rich beds record OAE1a to OAE1d, namely the lower Aptian Selli Level (OAE1a, ~124 Ma), the uppermost Aptian Jacob Level, the lowermost Albian Kilian Level, the lower Albian Monte Nerone Level and the Urbino Level (all added to OAE1b, ~110–113 Ma), the upper Albian Amadeus Segment (equivalent to part of OAE1c, ~105 Ma) and the uppermost Albian Pialli Level (OAE1d, ~100.5 Ma). Some others are interpreted as regional equivalents of widely distributed OAEs, namely the lower Aptian Noir Level and the middle to upper Aptian Fallot Level (Herrle al., 2004; Figs. 2, 4).

Figure 3. Drilling operations at Poggio le Guaine.

Seven discrete intervals dominantly reddish are also recognized in the cored sequence, which correlate well with those identified as ORBs in the Aptian-Albian succession of the UMB (Hu et al., 2005; Fig. 2).

In agreement with previous detailed stratigraphic investigations from Aptian-Albian land-based sections throughout the UMB (Coccioni et al., 1987, 1989, 1990, 1992; Cresta et al., 1989; Coccioni and Galeotti, 1993; Coccioni 1996, 2001, 2002) and from an 84-m-thick core drilled at Piobbico (Fig. 1) in 1982 and extending from the upper Albian down to the uppermost Barremian (Erba, 1988, 1992; Tornaghi et al., 1989), the cored succession biostratigraphically represents the interval from the *Hedbergella excelsa* to the base of the *Thalmanninella globotruncanoides* planktonic foraminiferal zones and from the *Chiastozygus litterarius* (NC6) to the *Eiffellithus turriseiffelii* (NC10) calcareous nannofossil zones. Accordingly, from a chronostratigraphic point of view the Poggio le Guaine core encompasses the latest Barremian to earliest Cenomanian interval (Fig. 2).

Objectives

The Poggio le Guaine core, which can be considered as a reference section for the Aptian-Albian interval at low latitudes, is designated by a consortium of Italian and Brazilian researchers to provide high-ranking informative records for that critical time interval through high-resolution multiproxy studies. The studies already in progress include integrated stratigraphic and sedimentological analyses, multidisciplinary magneto-, bio-, and chemostratigraphy, as well as clay and organic geochemistry investigations.

The data set collected will supply the framework for the following three activities. 1) Computing a high-resolution magnetostratigraphy, in particular a relative paleointensity reference curve for the Aptian–Albian interval of the long normal Cretaceous superchron, will allow correlation of relative paleointensity curves from other places in the world. 2) A unique and original age model can be built up, at high-resolution and using absolute dating and astronomical tuning. Into this the sequence of the geological, biogeochemical, oceanographic and climatic events that are recorded throughout the Aptian–Albian critical time can be placed. 3) The causal linkages, as well as their consequences, among these events can be defined.

Acknowledgments

The Poggio le Guaine core is an integral part of the Magnetic Anomaly of Relative Intensity for the Aptian (MARIA) project. Coring was funded by Petróleo Brasileiro S.A. - Petrobras. The Università Agraria di Secchiano (Cagli, Regione Marche, Italy) generously granted access and facilitated drilling. We warmly thank Glen Hill, Thomas Wiersberg, Mika Saido and the Editor Kevin Johnson for their helpful comments.

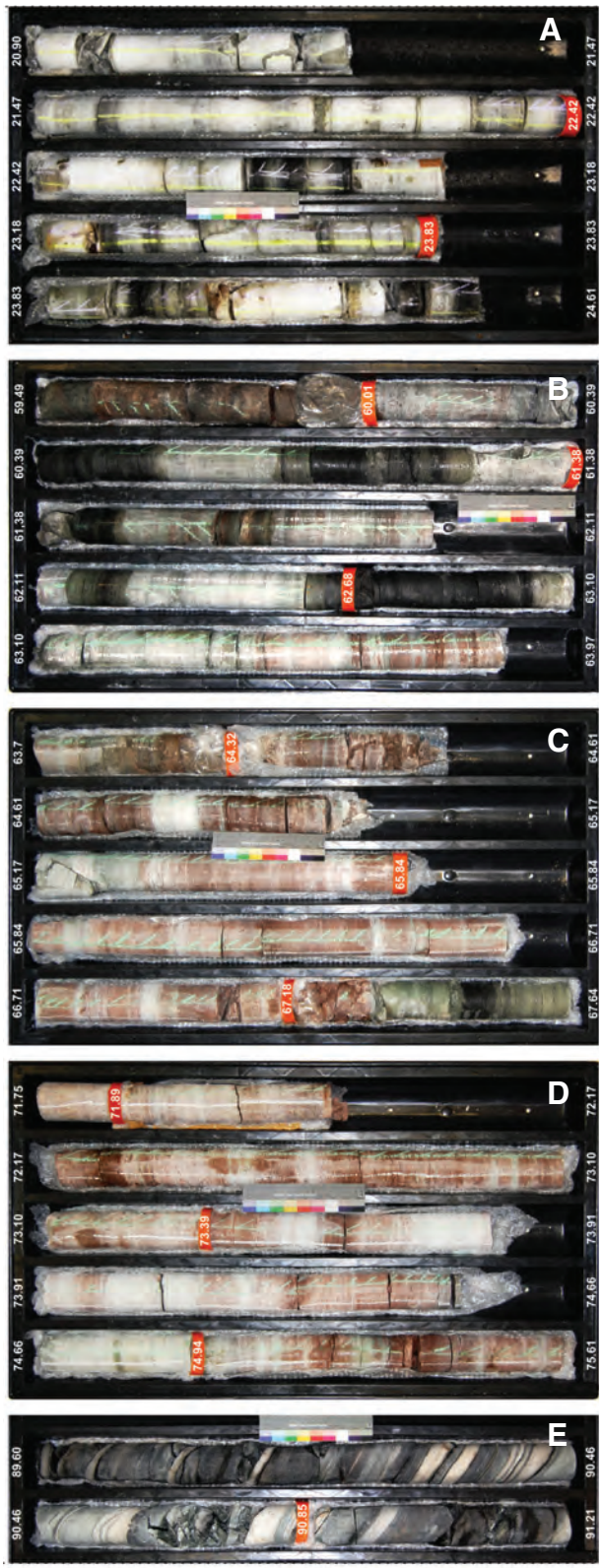

Figure 4. Photographs of selected cores recovered at Poggio le Guaine. [A] Cores 20 (20.90–22.45 m) to 22 (23.83–25.39 m) penetrated the marly limestones, marls, and black shales of the upper Albian Amadeus Segment (OAE1c); [B] Cores 46 (58.42–60.01 m) to 49 (62.68–64.33 m) recovered the marly clays, clays, marls, and black shales of the lower Albian Monte Nerone and Kilian Levels (OAE1b); [C] Cores 49 (62.68–64.33 m) to 52 (67.18–68.77 m) penetrated latest Aptian marls and calcareous marls together with the black shales of the uppermost Aptian Jacob Level (OAE1b); [D] Cores 54 (70.32–71.89 m) to 57 (74.94–76.45 m) recovered late Aptian marls, marly clays, and calcareous marls; [E] Cores 66 (88.00–89.60 m) to 68 (90.85–91.99 m) penetrated the lower Aptian Selli Level (OAE1a).

References

Arthur, M.A., and Premoli Silva, I., 1982. Development of widespread organic carbon-rich strata in the Mediterranean Tethys. *In* Schlanger, S.O., and Cita, M.B. (Eds.), *Nature of Cretaceous Carbon-Rich Facies*: San Diego (Academic Press), 7–54.

Arthur, M.A., Jenkyns, H.C., Brumsack, H.-J., and Schlanger, S.O., 1990. Stratigraphy, geochemistry, and paleoceanography of organic-carbon-rich Cretaceous sequences. *In* Ginsburg, R.N., and Beaudoin, B. (Eds.), *Cretaceous Resources, Events and Rhythms. NATO ASI Ser. 304*: Dordrecht, Netherlands (Kluwer Acad.), 75–119.

Coccioni, R., 2002. Stop 5 – The proposed global boundary stratotype section and point (GSSP) for the Barremian–Aptian boundary at Gorgo a Cerbara. In Santantonio, M. (Ed.), *General Field Trip Guidebook*. 6th International Symposium on the Jurassic System, 12–22 September 2002, Palermo, 239–241.

Coccioni, R., 1996. The Cretaceous of the Umbria-Marche Apennines (Central Italy). *Jost Wiedmann Symposium on Cretaceous Stratigraphy, Paleobiology and Paleobiogeography*, Tübingen, 7–10 March 1996, 129–136.

Coccioni, R., 2001. The "Pialli Level" from the latest Albian of the Umbria-Marche Apennines (Italy). *Federazione Italiana di Scienze della Terra, Geoitalia 2001*, 192–193.

Coccioni, R., and Galeotti, S., 1993. Orbitally induced cycles in benthonic foraminiferal morphogroups and trophic structures distribution patterns from the Late Albian "Amadeus Segment" (Central Italy). *J. Micropaleontol.*, 12:227–239. doi:10.1144/jm.12.2.227

Coccioni, R., Erba, E., and Premoli Silva, I., 1992. Barremian-Aptian calcareous plankton biostratigraphy from the Gorgo a Cerbara section (Marche, Central Italy) and implications for plankton evolution. *Cret. Res.*, 13:517–537. doi:10.1016/0195-6671(92)90015-I

Coccioni, R., Franchi, R., Nesci, O., Wezel, F.C., Battistini, F., and Pallecchi, P., 1989. Stratigraphy and mineralogy of the Selli Level (Early Aptian) at the base of the Marne a Fucoidi in the Umbro-Marchean Apennines, Italy. In Wiedmann, J. (Ed.), *Cretaceous of the Western Tethys. Proceedings 3rd International Cretaceous Symposium*, Stuttgart (E. Schweizerbart'sche Verlagsbuchhandlung), 563–584.

Coccioni, R., Franchi, R., Nesci, O., Perilli, N., Wezel, F.C., and Battistini, F., 1990. Stratigrafia, micropaleontologia e mineralogia delle Marne a Fucoidi delle sezioni di Poggio le Guaine e del Fiume Bosso (Appennino umbro-marchigiano). Atti 2° Convegno Internazionale "Fossili, Evoluzione, Ambiente", Pergola, 25–30 ottobre 1987, Tecnostampa, 163–201.

Coccioni, R., Nesci, O., Tramontana, M., Wezel, F.C., and Moretti, E., 1987. Descrizione di un livello–guida "radiolaritico-bituminoso-ittiolitico" alla base delle Marne a Fucoidi nell'Appennino umbro-marchigiano. *Boll. Soc. Geol. Italiana*, 106:183–192.

Coccioni, R., Premoli Silva, I., Marsili, A., and Verga, D., 2007. First radiation of Cretaceous planktonic foraminifera with radially elongate chambers at Angles (Southeastern France) and biostratigraphic implications. Rev. micropaléontologie, 50:215–224.

Cresta, S., Monechi, S., and Parisi, G., 1989. Stratigrafia del Mesozoico al Cenozoico nell'area Umbro-Marchigiana. *Mem. Descr. Carta Geol. Italia*, 34:185.

Erba, E., 1988. Aptian-Albian calcareous nannofossil biostratigraphy of the Scisti a Fucoidi cored at Piobbico (central Italy). *Riv. Ital. Paleont. Strat.*, 94:249–284.

Erba, E., 1992. Calcareous nannofossil distribution in pelagic rhythmic sediments (Aptian-Albian Piobbico core, central Italy). *Riv. Ital. Paleont. Strat.*, 97:455–484.

Herrle, J.O., Kössler, P., Friedrich, O., Erlenkeuser, H., and Hemleben, C., 2004. High-resolution carbon isotope records of the Aptian to Lower Albian from SE France and the Mazagan Plateau (DSDP Site 545): A stratigraphic tool for paleoceanographic and paleobiologic reconstruction. *Earth Planet. Sci. Lett.*, 218:149–161. doi:10.1016/S0012-821X(03)00646-0

Hu, X., Jansa, L., and Sarti, M., 2005. Mid-Cretaceous oceanic red beds in the Umbria-Marche Basin, central Italy: Constraints on paleoceanography and paleoclimate. *Palaeogeogr. Palaeoclimatol. Palaeoecol.*, 233:163–186. doi:10.1016/j.palaeo.2005.10.003

Huber, B.T., and Leckie, R.M., 2011. Planktic foraminiferal species turnover across deep-sea Aptian/Albian boundary sections. *J. Foram. Res.*, 41:53–95. doi:10.2113/gsjfr.41.1.53

Leckie, R.M., Bralower, T.J., and Cashman, R., 2002. Oceanic anoxic events and plankton evolution: Biotic response to tectonic forcing during the mid–Cretaceous. *Paleoceanogr.*, 17:13-1–13-29. doi: 10.1029/2001PA000623

Ogg, J.G., Ogg, G., and Gradstein, F.M., 2008. *The Concise Geologic Time Scale*: Cambridge (Cambridge University Press).

Satolli, S., Besse, J., and Calamita, F., 2008. Paleomagnetism of Aptian-Albian sections from the Northern Apennines (Italy): Implications for the 150–100 Ma apparent polar wander of Adria and Africa. *Earth Planet. Sci. Lett.*, 276:115–128. doi:10.1016/j.epsl.2008.09.013

Schlanger, S.O., and Jenkyns, H.C., 1976. Cretaceous oceanic anoxic events: Causes and consequences. *Geol. Mijnbouw*, 55:179–184.

Skelton, P.W., Spicer, R.A., Kelley, S.P., and Gilmour, I., 2003. *The Cretaceous World*: Cambridge (Cambridge University Press).

Tiraboschi, D., Erba, E., and Jenkyns, H.C., 2009. Origin of rhythmic Albian black shales (Piobbico core, central Italy): Calcareous nannofossil quantitative and statistical analyses and paleoceanographic reconstructions. *Paleoceanogr.*, 24:PA2222. doi:10.1029/2008PA001670

Tornaghi, M.E., Premoli Silva, I., and Ripepe, M., 1989. Lithostratigraphy and planktonic foraminiferal biostratigraphy of the Aptian-Albian "Scisti a Fucoidi" in the Piobbico core, Marche, Italy: Background for cyclostratigraphy. *Riv. Ital. Paleont. Strat.*, 95:223–264.

Turchyn, A.V., Schrag, D.P., Coccioni, R., and Montanari, A., 2009. Stable isotope analysis of the Cretaceous sulfur cycle. *Earth Planet. Sci. Lett.*, 285:115–123.

Wang, C., Hu, X., Huang, Y., Scott, R.W., and Wagreich, M., 2009. Overview of Cretaceous Oceanic Red Beds (CORBs): A window on global oceanic and climate change. *In* Hu, X., Wang, C., Scott, W., Wagreich, M., and Jansa, L. (Eds.), *Oceanic Red Beds: Stratigraphy, Composition, Origins, and Paleoceanographic and Paleoclimatic Significance. Society for Sedimentary Geology, Special Publication*, 91:13–33.

Authors

Rodolfo Coccioni, Dipartimento di Scienze della Terra, della Vita e dell'Ambiente dell'Università degli Studi "Carlo Bo," Campus Scientifico "E. Mattei", Località Crocicchia, 61029 Urbino, Italy, e-mail: rodolfo.coccioni@uniurb.it.

Luigi Jovane, Departamento de Oceanografia Física, Instituto Oceanográfico, Universidade de São Paulo, 05508-900 São Paulo, Brazil.

Giuseppe Bancalà, Dipartimento di Scienze della Terra, della Vita e dell'Ambiente dell'Università degli Studi "Carlo Bo," Campus Scientifico "E. Mattei", Località Crocicchia, 61029 Urbino, Italy.

Carla Bucci, Dipartimento di Scienze della Terra, della Vita e dell'Ambiente dell'Università degli Studi "Carlo Bo," Campus Scientifico "E. Mattei", Località Crocicchia, 61029 Urbino, Italy.

Gerson Fauth, Centro de Ciências Exatas e Tecnológicas, Área de Conhecimento e Aplicação de Geociências, Universidade do Vale do Rio dos Sinos, São Leopoldo, Brazil.

Fabrizio Frontalini, Dipartimento di Scienze della Terra, della Vita e dell'Ambiente dell'Università degli Studi "Carlo Bo," Campus Scientifico "E. Mattei", Località Crocicchia, 61029 Urbino, Italy.

Liliane Janikian, Departamento de Geofísica, Instituto de Astronomia, Geofísica e Ciências Atmosféricas, Universidade de São Paulo, 05508-090 São Paulo, Brazil.

Jairo Savian, Departamento de Geofísica, Instituto de Astronomia, Geofísica e Ciências Atmosféricas, Universidade de São Paulo, 05508-090 São Paulo, Brazil.

Renato Paes de Almeida, Departamento de Geologia Sedimentar e Ambiental, Instituto de Geociências, Universidade de São Paulo, 05508-090 São Paulo, Brazil.

Grasiane Luz Mathias, Departamento de Geofísica, Instituto de Astronomia, Geofísica e Ciências Atmosféricas, Universidade de São Paulo, 05508-090 São Paulo, Brazil

Ricardo Ivan Ferreira da Trindade, Departamento de Geofísica, Instituto de Astronomia, Geofísica e Ciências Atmosféricas, Universidade de São Paulo, 05508-090 São Paulo, Brazil.

Photo Credits

Figs. 3 and 4: Rodolfo Coccioni, Urbino University

Comparison of Rhizon Sampling and Whole Round Squeezing for Marine Sediment Porewater

by Heather N. Schrum, Richard W. Murray, and Britta Gribsholt

doi:10.2204/iodp.sd.13.08.2011

Introduction

The collection and chemical analysis of sedimentary porewater is central to many marine studies. Porewater alkalinity, dissolved inorganic carbon (DIC), sulfate, nitrate, and other dissolved ions are used to identify and determine rates of geochemical reactions and microbial respiration pathways, such as sulfate reduction and denitrification (Froelich et al., 1979; Berner, 1980; Gieskes et al., 1986; D'Hondt et al., 2004; Schulz, 2006; Martin and Sayles, 2007). Ammonium is critical for understanding microbial respiration and the nitrogen cycle (Blackburn, 1988). Chloride is used to reconstruct ocean salinity variations, constrain flow rates, and estimate gas hydrate concentrations (Paull et al., 1996; Adkins et al., 2002; Spivack et al., 2002). Each of these studies requires the recovery of porewater that is not compromised by sampling artifacts.

A number of methods are used to extract fluids from sediments. Here we report our experimental comparison of two methods used by the Integrated Ocean Drilling Program (IODP): extraction with Rhizon samplers and sediment squeezing (Seeberg-Elverfeldt et al., 2005; Manheim and Sayles, 1974).

Rhizon samplers are inserted directly into an intact sediment core; they collect porewater by vacuum filtration through a thin porous tube attached to a syringe (Seeberg-Elverfeldt et al., 2005; Dickens et al., 2007). Rhizons allow for high-resolution sampling because they may be spaced as closely as 2–3 cm apart. They also only minimally mechanically disturb the sediment and are typically time efficient. Porewater and soil moisture studies report that Rhizon sampling produces accurate results for dissolved ammonium, sulfate, chloride, and iron (Gribsholt and Kristensen, 2002; Song et al., 2003; Seeberg-Elverfeldt et al., 2005; Backman et al., 2006; Dickens et al., 2007). A disadvantage of Rhizon sampling is that it is often restricted to the upper portion of the sediment column (tens of meters, depending on lithology), where sediment is not too compacted. Also, the partial vacuum may lead to significant sampling artifacts for certain chemical species.

Whole round squeezing mechanically pressurizes a sediment sample, forcing the porewater through a sampling port. Squeezing has been shown to effectively collect porewater to depths of ~1600 m below seafloor (Saffer et al., 2010). Whole round squeezing also minimizes the contact of porewater with air. The disadvantages of squeezing include pressure-related additions through the destruction of particulate detritus or microbial cells (Bollinger et al., 1992), oxygen contamination (Robbins and Gustinis, 1976), and temperature artifacts (Bischoff et al., 1970; Fanning and Pilson, 1971). Many of these have been studied, however, and were deemed minimal (Gieskes, 1974). Dickens et al. (2007) compared Rhizon and squeezing methods for a suite of dissolved chemicals and concluded that the chemical concentrations did not vary significantly between methods.

We evaluated the use of Rhizon sampling and whole round squeezing for analyzing alkalinity, DIC, ammonium, sulfate, chloride, and nitrate in porewater from equatorial and South Pacific sites. In these experiments we directly compared the dissolved species collected by both methods in the same core and/or location and used these data to interpret potential sampling artifacts.

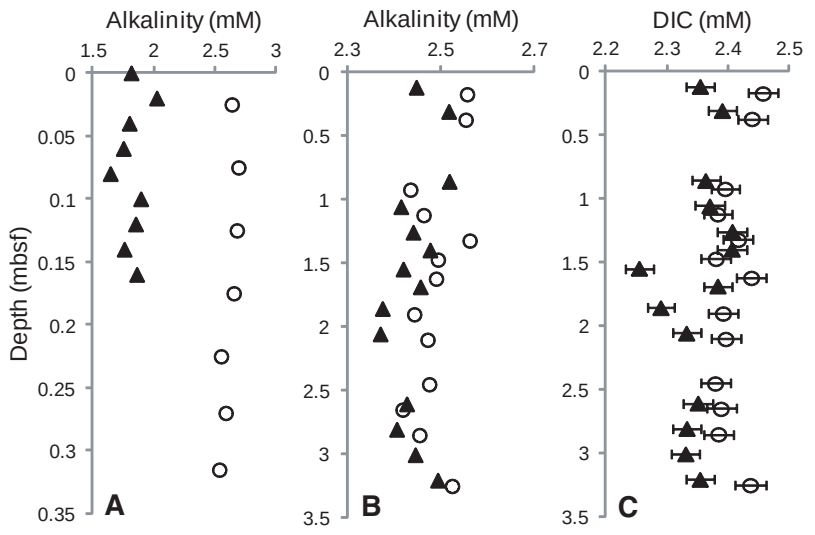

Figure 1. Alkalinity profiles at [A] SPG-9 and [B] EQP-9, and [C] DIC profile from EQP-9. Data from squeezing (open circles) and Rhizons (black triangles). Note differences in scales between sites. 0.5% error bars on alkalinity profiles are smaller than symbols. 1% error bars on DIC.

Materials and Procedures

We collected porewater from five sites in the Pacific Ocean with variable amounts of clay and biogenic ooze. At Site SPG-9 in the South Pacific Gyre we compared the Rhizon and squeezing method for alkalinity from sediment retrieved by a multi-core system, and we compared the porewater extraction methods for alkalinity and DIC from a gravity core at the Pacific Site EQP-9 (Fig. 1).

DIC, alkalinity, ammonium, sulfate, and chloride were measured from gravity cores at EQP-1, EQP-6, and EQP-6A (Fig. 2). Ammonium concentrations were compared for both extraction methods from samples at EQP-1. Two separate gravity cores at EQP-6 and -6A were retrieved at nearly the same location, and they have nearly identical lithologies. We compared both porewater extraction methods for sulfate and chloride at these two sites.

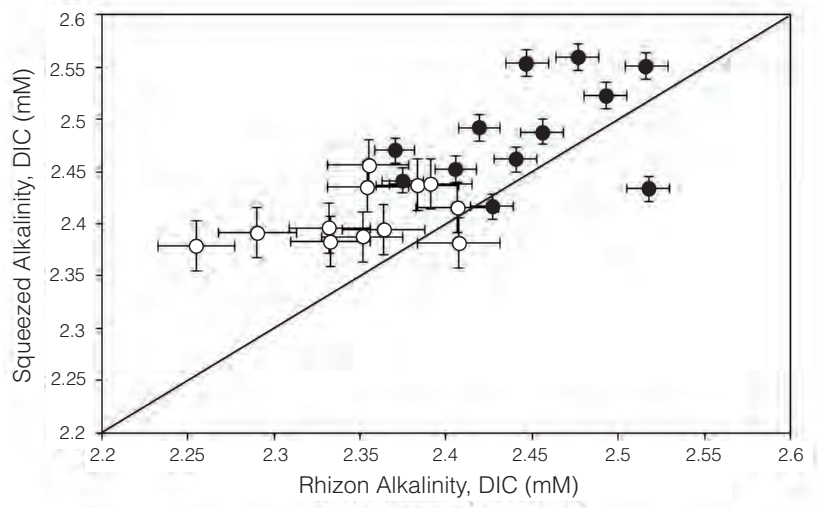

Figure 2. EQP-9 alkalinity (filled circles) and DIC (open circles) concentrations from Rhizon and squeezing methods. Line is 1:1. 0.5% and 1% error bars on alkalinity and DIC, respectively.

For SPG and EQP sites, Rhizon CSS-F 5-cm core solution samplers with 0.1µm microporous filters were used to collect porewater. The squeezing apparatus and method on both cruises were identical to those used by the Ocean Drilling Program (ODP) and Integrated Ocean Drilling Program (IODP) (see Methods in Backman et al., 2006).

For SPG and EQP samples, we measured alkalinity by Gran-titration following Gieskes et al. (1991). DIC was measured by acid extraction and infrared measurement of purged CO_2. Sulfate, chloride, and nitrate were quantified by ion chromatography. Dissolved ammonium was determined spectrophotometrically based on Solórzano (1969).

Comparative Assessment of Rhizon and Squeezing Protocols

At SPG-9 and EQP-9, alkalinities from porewater collected by Rhizon sampling are consistently lower than those measured from squeezed samples by approximately 0.8 mM and 0.06 mM, respectively. At EQP-9, DIC concentrations from Rhizons are approximately 0.06 mM on average less than squeezed concentrations (Fig. 1). These differences in alkalinity and DIC are larger than can be explained by analytical uncertainty.

Alkanity and DIC concentrations collected by Rhizon sampling have more scatter at SPG-9 and EQP-9. Rhizon alkalinities ranges from 1.64–2.02 mM and 2.37–2.52 mM at SPG-9 and EQP-9, respectively, while squeezed alkalinities range from 2.53–2.69 mM and 2.42–2.56 mM at these respective sites. Rhizon DIC values ranges from 2.25–2.41 mM versus 2.38–2.46 mM for squeezed samples at EQ-9.

In contrast to these findings, measured concentrations of ammonium, sulfate, and chloride are all within the error of the analytical methods, for both squeezing and Rhizon extraction at EQP-1, and EQP-6 and -6A (Fig. 3). This is consistent with results from Dickens et al. (2007) and Backman et al. (2006).

While neither the squeezing nor the Rhizon method for porewater extraction showed measurable sampling artifacts for ammonium, sulfate, and chloride, during the equatorial Pacific expedition we found repeated evidence that the squeezing method introduced nitrate contamination on the scale of tens of micromoles. We suspect that the Whatman #1 paper filters used inside the squeezer contained trace amounts of nitrate that were not removed even after soaking the filters in 18 MOhm water for ~24 hours and allowing them to dry. We filtered 18 MOhm water through the squeezer and found that a nitrate blank was present. Pressure-related destruction of cells may also have contributed to nitrate contamination during squeezing. Risgaard-Petersen et al. (2006) showed that there are considerable amounts of nitrate stored in foraminifera. These concentrations (~60 nmol cm^{-3} sediment) may not fully explain the contamination but may contribute to the erroneous nitrate values.

Discussion

Vacuum filtration is commonly used for fluid degassing. During Rhizon sampling into a low pressure headspace, subatmospheric pressure creates a pressure differential that forces the porewater through the filter. The filter creates a flow disturbance, causing minute bubbles of entrained gas to coalesce or to break the fluid into small droplets to provide a large surface-to-volume ratio for enhancing the effect of the vacuum degassing the fluid (Chambers et al., 1998).

CO_2 degassing during Rhizon sample extraction leads to alkalinity and DIC concentrations that are consistently lower than squeezed sample concentrations (Fig. 1). CO_2 degassing drives an increase in carbonate ion concentration, which increases the tendency for calcium car-bonate to precipitate, thereby decreasing alkalinity. In contrast, whole round squeezing applies pressure to the sediment sample, pushing the porewater out of the sediment into the filter-capped syringe, and it should have minimal impact on the carbonate system during sampling. It is possible, however, that pressure-related destruction of cells may cause some carbonate contamination during squeezing. When squeezing is used for sample extraction, care should be taken to store whole rounds at *in situ* temperature prior to squeezing, as carbonate saturation has retrograde solubility, and cation exchange between clay minerals and interstitial water is temperature dependent (Bischoff et al., 1970; Masuzawa et al., 1980).

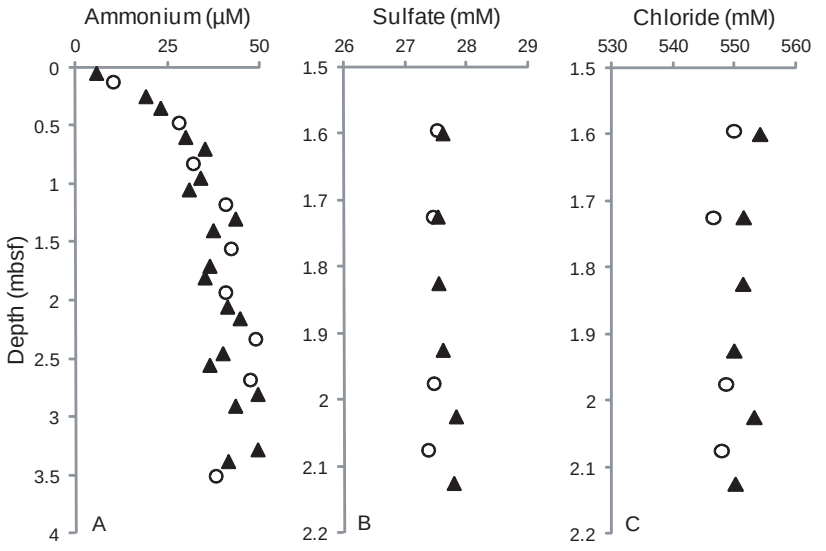

Figure 3. [A] Ammonium profiles at EQP-1 from squeezing (open circles) and Rhizons (black triangles). [B] Sulfate profiles at EQP-6 from squeezing (open circles) and at EQP-6A from Rhizons (black triangles). [C] Chloride profiles at EQP-6 from squeezing (open circles) and at EQP-6A from Rhizons (black triangles). EQP-6 and EQP-6A are nearly at the same location. Note differences in scales between sites. 3%, 0.15%, and 0.2% error bars on ammonium, sulfate and chloride profiles, respectively, are smaller than symbols.

The increased scatter in the alkalinity and DIC concentrations collected by Rhizon sampling also indicates compromised data. Based on visual inspection, if these concentrations were taken as true values, the data would lead to unrealistic concentration gradients in the sediment with improbable fluxes and rapidly changing sources and sinks (Fig. 1).

Our alkalinity results are not consistent with Backman et al. (2006), who convincingly reported no significant difference in alkalinity between samples collected by Rhizon and whole round squeezing. The differences in our findings are possibly due to sediment composition and porewater carbonate concentrations. Dissolved calcium carbonate concentrations are higher at most of the Pacific sites than in Arctic sediment collected by Backman et al. Porewater degassing during Rhizon sampling likely caused relatively greater calcium carbonate precipitation, which led to a greater decrease in alkalinity compared to squeezed samples. This is also the likely explanation for the greater difference in alkalinity concentrations between the Rhizon and squeezed samples at SPG-9 compared to EQP-9 (Fig. 1).

Recommendations

Our study shows that a combined sampling protocol of Rhizon sampling for ammonium (this study and Backman et al., 2006), nitrate, and metals (e.g., Mn, Backman et al., 2006) and squeezing for alkalinity, DIC, and pH will lead to a complete characterization of the dissolved chemical species in multiple environments. Future scientific coring and drilling expeditions that rely on high precision chemical profiles in marine sediment would greatly benefit from this combined sampling protocol.

While Seeberg-Elverfeldt et al. (2005) suggest that pH may be a viable measurement from Rhizon samplers, we argue that the degassing of CO_2 by Rhizons will produce higher than realistic pH and should be avoided. In this context, critical differences between soil systems and marine sediments appear to compromise comparison between soil-based and sediment-based studies. It is important that Rhizon samplers are employed to collect porewater that will be used to measure nitrate, as squeezing potentially introduces nitrate contamination on the scale of tens of micromoles.

Acknowledgements

We thank the captains and crew of the R/V *Roger Revelle* and R/V *Knorr*, and the Knox-02RR (South Pacific Gyre) and KNR 195-3 (equatorial Pacific) shipboard science party members. Special thanks to Steven D'Hondt and Arthur Spivack for their support and helpful comments and to Timothy Ferdelman, Benjamin Brunner, and Dennis Graham for fruitful conversations, sample collection, and chemical analyses. This project was funded by the NSF Biological Oceanography Program and the Integrated Ocean Drilling Program.

References

Adkins, J.F., McIntyre, K., and Schrag, D.P., 2002. The salinity, temperature, and $\delta^{18}O$ of the glacial deep ocean. *Science*, 298:1769–1773, doi:10.1126/science.1076252.

Backman, J., Moran, K., McInroy, D.B., Mayer, L.A., and the Expedition 302 Scientists., 2006. *Proc. IODP*, 302: Washington, DC (Integrated Ocean Drilling Program Management International, Inc.).

Berner, R.A., 1980. *Early Diagenesis: A Theoretical Approach:* Princeton, NJ (Princeton University Press).

Bischoff, J.L., Greer, R.E., and Luistro, A.O., 1970. Composition of interstitial waters of marine sediments: Temperature of squeezing effect. *Science*, 167(3922):1245–1246, doi:10.1126/science.167.3922.1245.

Blackburn, T.H., 1988. Chapter 8: Benthic mineralization and bacterial production, *In* Blackburn, T.H., and Sørensen, J. (Eds.), *Nitrogen Cycling in Coastal Marine Environments:* Chichester (John Wiley and Sons), 175–190.

Bollinger, R., Brandl, H., Höhener, P., Hanselmann, K.W., and Bachofen, R., 1992. Squeeze-water analysis for the determination of microbial metabolites in lake sediment - Comparison of methods. *Limnol. Oceanogr.*, 37:448–455, doi:10.4319/lo.1992.37.2.0448.

Chambers, A., Fitch, R.K., and Halliday, B.S., 1998. *Basic Vacuum Technology, second edition:* London (Institute of Physics Publ.), doi:10.1201/NOE0750304955.

D'Hondt, S., Jørgensen, B.B., Miller, D.J., Batzke, A., Blake, R., Cragg, B.A., Cypionka, H., et al., 2004. Distributions of microbial activities in deep subseafloor sediments. *Science*, 30:2216–2221, doi:10.1126/science.1101155.

Dickens, G.R., Koelling, M., Smith, D.C., Schneiders, L., and the IODP Expedition 302 Scientists, 2007. Rhizon sampling of pore waters on scientific drilling expeditions: An example from the IODP Expedition 302, Arctic Coring Expedition (ACEX). *Sci. Drill.*, 4:22–25.

Fanning, K.A., and Pilson, M.E.Q., 1971. Interstitial silica and pH in marine sediments: Some effects of sampling procedures. *Science*, 173:1228–1231, doi:10.1126/science.173.4003.1228.

Froelich, P.N., Klinkhammer, G.P., Bender, M.L., Luedtke, N.A., Heath, G.R., Cullen, D., Dauphin, P., Hammond, D., Hartman, B., and Maynard, V., 1979. Early oxidation of organic matter in pelagic sediments of the eastern equatorial Atlantic: Suboxic diagenesis. *Geochim. Cosmochim. Acta*, 43:1075–1090.

Gieskes, J.M., 1974. Interstitial water studies, Leg 25. *In* Simpson, E.S.W., Schlich, R., et al., *Init. Repts. DSDP,* 25: Washington, DC (U.S. Govt. Printing Office), 361–394.

Gieskes, J.M., Kastner, M., Erzinger, J., Boulegue, J., and Hart, S.R., 1986. Geochemical studies Hole 504B, Leg 92. *In* Leinen, M., Rea, D.K., et al., *Init. Repts. DSDP,* 92: Washington, DC (U.S. Govt. Printing Office), 547.

Gieskes, J.M., Gamo, T., and Brumsack, H., 1991. Chemical methods for interstitial water analysis aboard *JOIDES Resolution*. *ODP Tech. Note,*15.

Gribsholt, B., and Kristensen, E., 2002. Impact of sampling methods on sulfate reduction rates and dissolved organic carbon (DOC) concentrations in salt marsh sediment. *Wetlands Ecol. Manage.*, 10:371–379, doi:10.1023/A:1020940314010.

Manheim, F.T., and Sayles, F.L., 1974. Composition and origin of interstitial waters of marine sediments, based on deep sea drill cores. *In* Goldberg, E.D. (Ed.), *The Sea (Vol. 5): Marine Chemistry: The Sedimentary Cycle*. New York (Wiley-Interscience), 527–568.

Martin, W.R., and Sayles, F.L., 2007. The recycling of biogenic material at the seafloor. *In* Mackenzie, F.T. (Ed.), *Treatise on Geochemistry. Vol. 7: Sediments, Diagenesis, and Sedimentary Rocks:* Oxford (Elsevier Science), 37–65.

Masuzawa, T., Kanamori, S., and Kitano, Y., 1980. The reversible effect of temperature on the chemical composition of interstitial water of marine sediment. *J. Oceanogr. Soc. Jpn.*, 36:68–72, doi:10.1007/BF02209357.

Paull, C.K., Matsumoto, R., Wallace, P.J., and Expedition 164 Scientists, 1996. *Proc. ODP, Init. Repts.,* 164: College Station, TX (Ocean Drilling Program).

Risgaard-Petersen, N., Langezaal, A.M., Ingvardsen, S., Schmid, M.C., Jetten, M.S.M., Op den Camp, H.J.M., Derksen, J.W.M., et al., 2006. Evidence for complete denitrification in a benthic foraminifer. *Nature*, 443:93–96, doi:10.1038/nature05070.

Robbins, J.A., and Gustinis, J., 1976. A squeezer for efficient extraction of pore water from small volumes of anoxic sediment. *Limnol. Oceanogr.*, 21:905–909, doi:10.4319/lo.1976.21.6.0905.

Saffer, D., McNeill, L., Byrne, T., Araki, E., Toczko, S., Eguchi, N., Takahashi, K., and the Expedition 319 Scientists, 2010. *Proc. IODP,* 319: Tokyo (Integrated Ocean Drilling Program Management International, Inc.).

Schulz, H.D., 2006. Quantification of early diagenesis: Dissolved constituents in pore water and signals in the solid phase. *In* Schulz, H.D., and Zabel, M. (Eds.), *Marine Geochemistry, second edition:* Berlin (Springer-Verlag), 73–124.

Seeberg-Elverfeldt, J., Schlüter, M., Feseker, T., and Kölling, M., 2005. Rhizon sampling of porewater near the sediment-water interface of aquatic systems. *Limnol. Oceanogr.: Methods*, 3:361–371, doi:10.4319/lom.2005.3.361.

Solórzano, L., 1969. Determination of ammonia in natural waters by the phenolhypochlorite method. *Limnol. Oceanogr.*, 14:799–801, doi:10.4319/lo.1969.14.5.0799.

Song, J., Luo, Y.M., Zhao, Q.G., and Christie, P., 2003. Novel use of soil moisture samplers for studies on anaerobic ammonium fluxes across lake sediment-water interfaces. *Chemosphere*, 50(6):711–715, doi:10.1016/S0045-6535(02)00210-2.

Spivack, A.J., Kastner, M., and Ransom, B., 2002. Elemental and isotopic chloride geochemistry and fluid flow in the Nankai Trough. *Geophys. Res. Lett.*, 29:1661–1665, doi:10.1029/2001GL014122.

Authors

Heather N. Schrum, Massachusetts Maritime Academy, 101 Academy Drive, Buzzards Bay, MA 02532, U.S.A., e-mail: hschrum@maritime.edu

Richard W. Murray, Department of Earth Sciences, Boston University, 1 Silber Way, Boston, MA 02215, U.S.A.

Britta Gribsholt, Department of Biological Sciences, Center for Geomicrobiology, University of Aarhus, Ny Munkegade 114, DK-8000 Aarhus C, Denmark.

Climate Evolution in Central Asia during the Past Few Million Years: A Case Study from Issyk Kul

by Hedi Oberhänsli and Peter Molnar

doi:10.2204/iodp.sd.13.09.2011

Introduction

The lake Issyk Kul occupies a deep basin within the Earth's most active intracontinental mountain belt, the Tien Shan, far from any oceanic influence. It offers a record of continental climate spanning millions of years that is likely unmatched by any other source.

A three-day workshop, with the same title as this report and sponsored by the International Continental Drilling Project and German Science Foundation, was held on 12–17 June 2011 on the shore of Issyk Kul to discuss the scientific justification for and the logistical aspects of scientific drilling of the lake. A two-day geological field trip followed the workshop. Forty-five scientists from twelve countries discussed three obvious targets for paleoclimatic study, a related study of erosion, and a study of how microbial life has evolved within the basin. The conclusion was that these research topics justify further consideration of deep continental drilling at Issyk Kul.

The premise underlying the paleoclimate questions is that climates within continents need not follow that recorded by, and studied well with, marine sediment. A particularly clear example is that glaciation within alpine settings is not synchronized with that of continental ice sheets; maximum advances of alpine glaciers in many regions precede the last glacial maximum (LGM) at ~20 kyr BP.

The major outcome of the meeting was the identification of two drilling targets: one within the lake that would reach as deep into Quaternary time as possible and certainly as far as 100 kyr BP, and a second on shore that could penetrate sediment as old as 6–10 Ma.

Geologic Background

Issyk Kul (literally "hot lake" in Kyrgyz) occupies a deep topographic depression within the Tien Shan (Fig. 1). Observatories using GPS measurements (Fig. 2), modern seismicity, and active faulting indicate relatively rapid deformation and suggest that the Tien Shan is Earth's most active intracontinental mountain belt.

Seismicity in the Tien Shan is high, with four earthquakes since 1889 assigned magnitudes as large as 8 (Abdrakhmatov et al., 2002; Kondorskaya and Shebalin, 1977). Fault plane solutions of earthquakes consistently show reverse or thrust faulting. Evidence of active faulting is widespread (Abdrakhmatov et al., 2007; Chedia, 1986; Laverov and Makarov, 2005), and rates of slip on several faults exceed 1 mm yr^{-1} (Chen et al., 2007; Thompson et al., 2002).

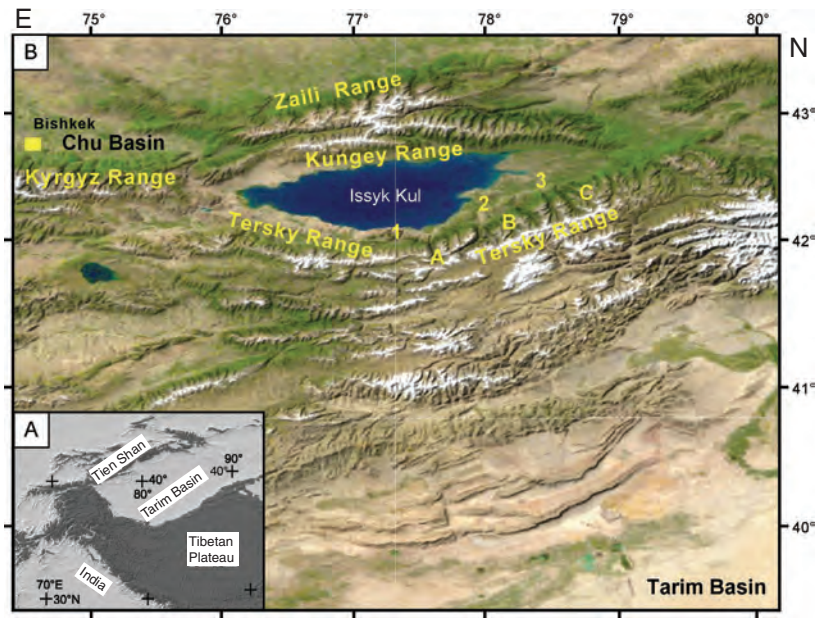

Figure 1. Topographic map of the Tien Shan showing the location of Issyk Kul and range-and-basin nature of the belt.

At present the Tarim Basin, which lies to the south of the Tien Shan, moves northward at 20 ± 2 mm yr^{-1} with respect to the Eurasian Plate to the north (Reigber et al., 2001; Zubovich et al., 2010). Deformation is not localized on the margins of the belt, but occurs throughout it, consistent with seismicity and studies of active faulting (Fig. 2). The present-day convergence rate between the Terskey Alatau south of Issyk Kul and the Kungey Alatau to its north is ~5 mm yr^{-1}.

Mineral cooling ages (Bullen et al., 2003) suggest accelerated exhumation of parts of the Tien Shan since ~10 Ma, and magnetostratigraphic dating of sediment in adjacent basins (Abdrakhmatov et al., 2001; Charreau et al., 2009; Ji et al., 2008;

Sun and Zhang, 2009) suggest accelerated deposition of sediment since that time. Both findings are consistent with enhanced erosion due to growing relief beginning near or shortly before 10 Ma. How deformation has developed since that time, either as an average across the belt or in individual mountain ranges within the Tien Shan, remains poorly constrained.

The Cenozoic stratigraphy of Kyrgyzstan is commonly divided into four units that overlie a surface that had little relief prior to deposition onto it (Abdrakhmatov et al., 2001; Burgette, 2008). At the bottom is the Kokturpak group, commonly tens of meters thick, fine-grained, deeply weathered, and typically dark red in color, perhaps deposited from Cretaceous to Eocene and possibly as young as Miocene. Disconformably overlying it is the Shamsi Group with thickness varying from hundreds of meters to ~2000 m. It is relatively well-sorted, reddish sediment, rich in quartz and feldspar with abundant conglomerate. Magnetostratigraphy suggests that deposition began 12–13 Ma ago. The Chu Group overlies the Shamsi group, with assigned dates ranging from 8 Ma to 4 Ma; in the Issyk Kul area, reported thicknesses range up to ~2800 m. It includes tabular beds with sandstone and conglomerate lenses interpreted as river channels of moderate size as well as lacustrine sediment and evaporites. Overlying the Chu group in many regions is coarse conglomerate of the Sharpyldak Formation. Thicknesses vary from tens to hundreds of meters to more than 1000 m in places. At the east end of the Issyk Kul basin, however, lacustrine sediment of Quaternary age is exposed.

At present, Issyk Kul sediment consists of a mixture of riverine sediment and endogenic carbonates (De Batist et al., 2001; Giralt et al., 2002). The steep northern and southern margins present evidence of slope failure, and mass-flow deposits are found at the foot of these steep slopes. Near the steep borders, only centimeter-thick fining-upwards sequences of small gravel and sand are present, whereas the central deep basin is filled with a mixture of carbonate hemipelagic sediment and fine terrigenous sediment that includes distal turbidite facies. The southern part of this deep central basin contains a topographic high, and available high-resolution seismic data and short gravity cores indicate that sedimentation there is dominated by bottom currents migrating up-slope towards the crest of the high. By contrast, deltaic sedimentation processes have dominated deposition on the eastern and western margins. Near the eastern and western shores, proximal deltaic sediment is found, whereas distal deltaic sediment (laminated silty-clay sediment) has been deposited closer to the central deep plain. Slope failure deposits dominate the fronts of both deltas.

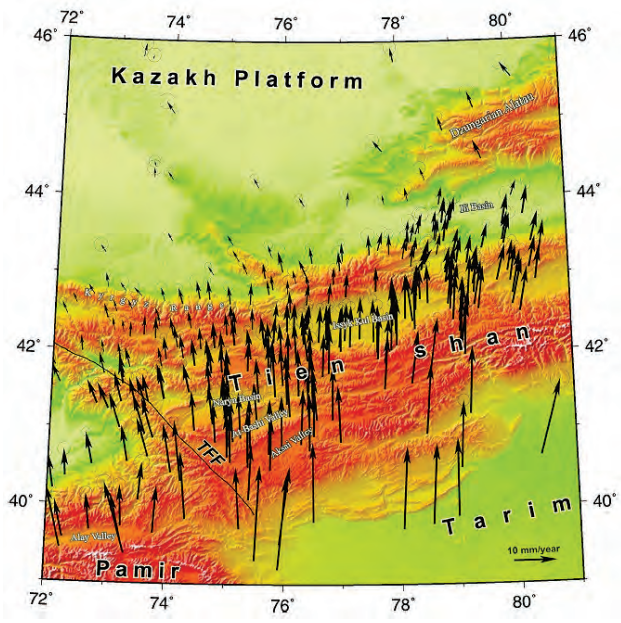

Figure 2. Map of GPS velocities across the Tien Shan. Error ellipses show 95% confidence. (from Zubovich et al., 2010).

Modern Climate

Issyk Kul and the Tien Shan lie within the mid-latitudes, far from the tropics where monsoons dominate climate, and where precipitation interacts profoundly with atmospheric circulation. At the same time, the Tien Shan is far from high-latitude conditions where extremes in the seasonal cycle play a crucial role, and where warming over the past century and a half has been most pronounced. Considerably more attention has been given to the Arctic than the mid-latitudes, and many view the study of mid-latitude climate as a gap in our understanding of climate dynamics.

The mid-latitudes, and the Issyk Kul region in particular, offer often under-appreciated features for climate study. For instance, changes in vegetation, either with continued global warming or on paleoclimate time scales, are much larger than in the tropics or high latitudes. Changes from forests to grassland, or vice versa, occur largely in mid-latitudes, and such changes affect both albedo and moisture availability. In the deep tropics, where changes in precipitation and the variability in temperature are small, large changes in vegetation are unlikely except in extreme climates. Similarly, at high latitudes, where trees are sparse, an expansion of woody vegetation is unlikely except in an extreme change in climate. Moreover, interannual variability of modern climate in and around the Tien Shan also is among the greatest on Earth (Aizen et al., 1997, 2001).

The Issyk Kul region offers some simple aspects that make its study attractive. For example, the most reliable part of General Circulation Models (GCMs) solves the Navier-Stokes equation to obtain the dynamics of flow, and although this solution depends on numerous parameterizations for local processes, such as latent and sensible heat transport from the surface, precipitation and latent heating of the remaining atmosphere, etc., many of these interactions can be described reliably. GCMs resolve well the physics of mid-latitude weather patterns and their associ-

ated mechanisms of precipitation. Precipitation in mid-latitudes results from advection of moisture by the large-scale flow and by the subsequent lifting of moisture in mid-latitude cyclones and by the flow incident on large topographical obstacles, all of which are governed by processes that are explicitly and well represented in climate models.

The Issyk Kul sedimentary archive represents a potential source of record from an intracontinental region whose climate neither responds directly to monsoons nor is forced by adjacent marine conditions, making it an attractive target for isolating mid-latitude atmospheric circulation components of past climate changes on a range of timescales. The climate of the Issyk Kul region is relatively simple but highly sensitive to vari-ations in the moisture supply, which affect both lake levels and the extent of Tien Shan alpine glaciation. It is possible to recover a long continuous sediment record from the Issyk Kul basin to test series of hypotheses at the junction of geomorphology, tectonics, paleoclimate, and biotic evolution.

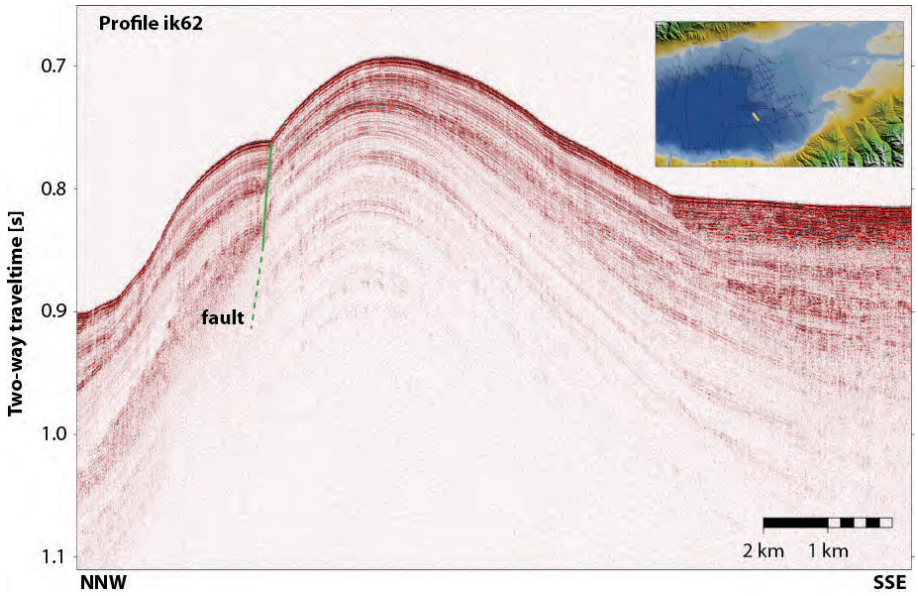

Figure 3. Seismic section that shows a subtle rise in bottom topography and with undisturbed sediment. (De Batist, M., unpublished; compiled by C. Gebhardt)

Scientific Questions That Merit Drilling of the Issyk Kul Basin

We first discuss five questions that motivate scientific drilling of the Issyk Kul Basin: three bear directly on climate, a fourth concerns the role that climate change plays in erosion of high terrain, and a fifth tackles microbiological properties in an old, possibly endemic lake, which, due to changes in its water chemistry, promoted halotolerant organisms and eventually endemism. These questions overlap to varying degrees, as each in part concerns differences between climates of high central Asia and global climate. We then pose other additional questions that deep drillholes will help resolve and thus will broaden the scope of a major scientific drilling effort at Issyk Kul.

Hypothesis 1. A semi-arid, continental climate characterizes the Issyk Kul watershed deep within a continental interior and far from large marine sources of water vapor. Today, its main moisture sources are the Mediterranean and the North Atlantic, with moisture arriving mostly during the spring. Issyk Kul is ideally suited to examine differing responses to advection of moisture from these sources and to direct temporal variations in insolation on an otherwise nearly pure continental climate.

Hypothesis 2. Seismic data (Fig. 3) from Issyk Kul reveal a bathymetric high that holds a stratigraphically continuous section, 150–200 m thick, of fine and at least partly laminated sediment. Based on prior stratigraphic studies in the basin (Giralt et al., 2002; Ricketts et al., 2001), it is likely that this sediment is calcareous and proxy-rich, with a sedimentation rate that will enable a high-resolution (roughly decadal to centennial) climate reconstruction back perhaps to 300–400 kyr BP. Turbidites, mass flow, and slumps seem not to have disturbed this section (Fig. 4). Millenial-scale abrupt climate climate changes, like Dansgaard-Oeschger (D-O) stadials whose origin seems to be in the North Atlantic, have been recoded well by speleothems in China, but recent work suggests that the connection is through the South Asian Monsoon (Pausata et al., 2011). The Issyk Kul region offers an ideal, intracontinental region to examine the direct response to such changes in the North Atlantic, without the strong modulation by the South Asian Monsoon.

Hypothesis 3. As noted earlier, alpine glaciers and continental ice sheets seem to respond differently to orbital scale forcing (Abramowski et al., 2006; Gillespie and Molnar, 1995; Owen et al., 2005), including the Tien Shan (Koppes et al., 2008; Xu et al., 2010), but such evidence, both global and specific to the Tien Shan, spans only the last glacial period, since ~100 kyr BP. In particular, due to the present-day aridity of the Issyk Kul region, glacial mass balance is most sensitive to amount of precipitation. A high-resolution, accurately dated history of glacial sediment input into the Issyk Kul basin will allow a reconstruction of the glacial history of its surroundings in the Tien Shan for several glacial cycles and hence an examination of how Alpine glaciers and continental ice sheets advance asynchronously over many cycles of orbital variability, if indeed they do. A detailed study of such asynchroneity could allow insights into how orbital

variations affect not just ice sheets but continental climate in general.

Hypothesis 4. The geomorphological, tectonic, and paleoclimate communities differ, both among each other and within each group, on the relative roles played by tectonics (whether active or dead) and climate (and climate change) in affecting erosion rates (Molnar and England, 1990; Willenbring and von Blanckenburg, 2010; Zhang et al., 2001). Tectonic movement is needed for terrain to lie above sea level, but present-day elevations need not be results of active tectonics. Erosive processes differ in different climates, and changing climates (especially in the statistics of precipitation variability) might alter erosion rates so that current landscapes are not in equilibrium with the present-day climate. Testing the relative importance of climate and tectonics as they manifest themselves in erosion requires finding a region where changes in both climate and tectonics can be dated well. Issyk Kul might provide an excellent archive not only to date changes in erosion rates, but also to evaluate the roles of tectonics and climate change in affecting such erosion rates.

Hypothesis 5. A variety kinds of evidence, such as the periodic alternation of endogenic Ca- and Mg-bearing carbonates and changes in the concentration of noble gases in sediment pore water (Brennwald et al., 2004), suggests that the Issyk Kul has alternated between being fresh and saline at many times in the past. Moreover, seismic surveys clearly show evidence of several dramatic lowstands of Issyk Kul, and historic records indicate repeated episodes of outflow from what is today a closed-basin lake. As various organisms thrive better in fresh than saline water, and vice versa, salinity changes may have profoundly affected taxonomic diversity in the basin and the development of endemism. At present, Issyk Kul is species-poor compared to most freshwater lakes and the oceans. Thus, Issyk Kul offers a field laboratory for studying how organisms respond to larger temporal variations in salinity, and perhaps evolve in response to such changes.

Other Questions Potentially Solved with Cores from the Issyk Kul Basin

The tectonics community at the workshop posed a number of questions that do not by themselves merit the high cost of drilling, but whose questions might be answered, or partly answered, with results from cores taken from the Issyk Kul basin. Moreover, some questions bear on local geology and local hazards, and all participants agreed that if a drilling program pokes holes into Kyrgyz territory, the Kyrgyz people ought to reap benefits from such a program.

Dating of sedimentary rock. As noted above, the Cenozoic stratigraphy of Kyrgyzstan is commonly divided into four units. Resolving when and how the Issyk Kul basin formed and when sedimentary facies changed is important for interpreting the contemporaneous climatic record archived within the basin.

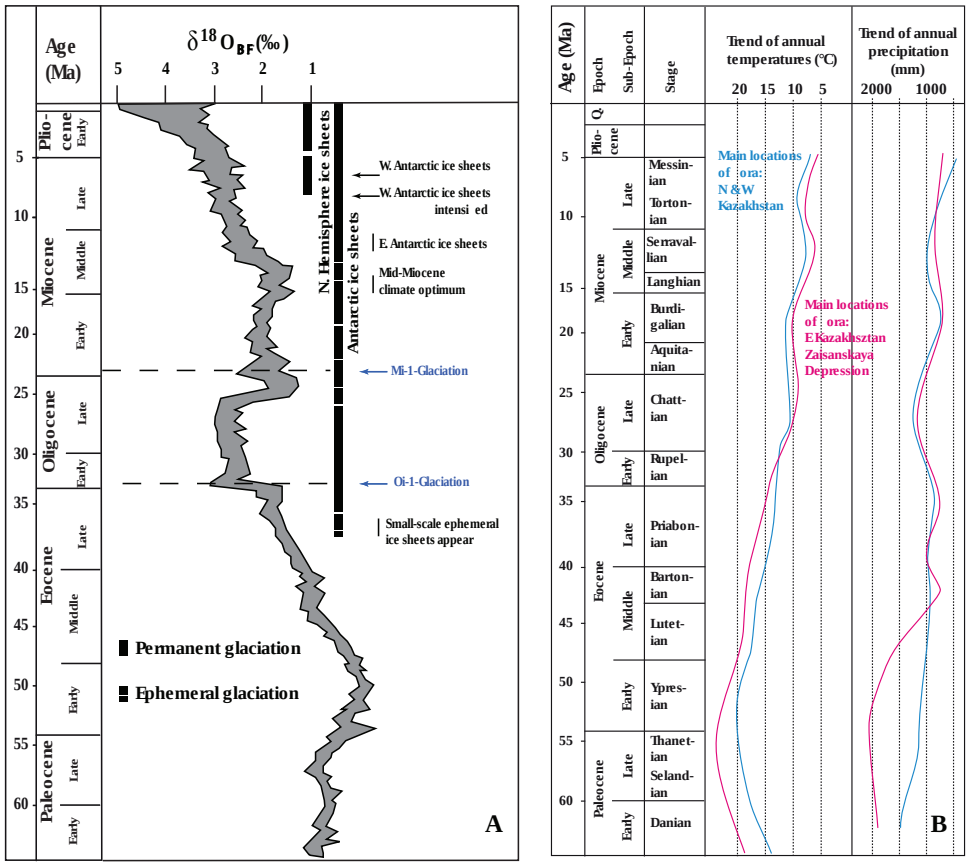

Figure 4. [A] The marine $\delta^{18}O$ synthesis of Zachos et al. [2001] compared with [B] the Central Asian climate history from Akhmetyev et al. (2005).

Seismites and paleoearthquakes. The Kyrgyz people live with a serious threat of earthquake disaster. For instance, in the northern Tien Shan of Kyrgyzstan and Kazakhstan, several major earthquakes occurred in historical times: in 1885 (Ms 6.9), 1887 (Ms 7.3), 1889 (Ms 8.3), and 1911 (Ms 8.1) (Abdrakhmatov et al., 2002). The latter two events are among the largest known intracontinental earthquakes worldwide, but the recurrence intervals of such earthquakes, which could be thousands to tens of thousands of years, are still unconstrained. If seismites can be found in lake sediment, they might provide a long record of earthquake

activity far beyond instrumental records and recorded history. If found, seismites from the Issyk Kul basin could significantly enhance our knowledge of the earthquake history of the Tien Shan, as well as serving as a case study for other low-strain regions worldwide.

Accurate measurements of heat flux. The state of the lower crust—brittle or ductile, and in other respects, too—depends largely on the temperature (but also on the degree of hydration) at relevant depths. Accurate measurements of temperatures in deep holes could address two quite different problems: one relevant to geodynamics and the other to climate over the past several thousand to one hundred thousand years.

Changes in the locus and rate of deformation. Finally, a topic that was discussed at some length and that interested many participants concerns the following questions. (1) How have changes in the locus and rate of deformation over the past 5–10 Ma both enabled sediment production and generated sediment accommodation space in the Issyk Kul basin, which thereby conditioned the landscape for climate-induced change? (2) Can we find evidence that Issyk-Kul surface processes have played an active role in shaping tectonic deformation, rather than just passively responding to it (Garcia-Castellanos, 2007; Whipple, 2009)?

Key Questions for Drill Site Selection

Several questions motivated the workshop discussion. What drilling targets allow the climate and tectonic-related questions to be answered most effectively? What are the geometry, depth, and timing of basin formation? What is the sedimentary architecture? Where in the stratigraphy are regressions and transgressions located? Preliminary data allow partial answers to these questions, but further seismic profiling planned for 2012 should answer at least some of these questions.

Available background data include bathymetric surveys and a detailed seismic survey carried out in 1982 and earlier in Soviet times. In addition, three seismic surveys were carried out in 1997, 2001, and 2002, using digital recording, with accompanying retrieval of several short cores (Giralt et al., 2002; Ricketts et al., 2001). In addition, 100 (or more) wells of up to 5-km depth have been drilled on land (Duchkov et al., 2001). Most of these cores are at least in part accessible. In addition to geologic maps made in Soviet times, a new atlas to be published soon and geologic maps of selected portions of the north slope of the range south of the lake (Burgette, 2008) are available. Furthermore, elevation data with 70-m horizontal resolution are digitally available for the region.

Given these data, the following additional scientific investigations have been deemed necessary.

- In selected areas, further bathymetric surveys are needed, particularly around the possible drill sites to acquire accurate water depths and bottom topographies. These surveys would help to delineate features of interest in the deepest basin.
- In regions with depths shallower than 120 m, which is the minimum drop in lake level during lowstands and where river incision may have removed sediment, denser seismic coverage than currently exists is needed.
- Seismic data from selected deeper parts and/or land is needed to extend existing coverage.
- Seismic refraction is necessary to determine seismic velocities and to define the geometry where layers are not flat in intervals between reflectors.
- A map of recent lake sediment based on cores that have been examined would be helpful.
- Finally, much data exists from drilling around the lake. Acquiring those data, digitizing them, and correlating them with seismic and outcrop data would help decide where a hole would be most likely to yield good results. A plan is underway to digitize logs from some such wells.

These pre-site surveys will help to define specific drilling locations and depths, as well as informing some the following questions.

- How deep is the basin and/or the bedrock?
- What are the geometry of the basin floor and timing of its formation?
- To what extent is the basin the result of recent or ancient tectonics?
- What is the nature of the infill; how much is terrestrial and how much lacustrine? What has been its stratigraphic development?
- Where has sediment that was transported by rivers been deposited? How much has been deposited by plumes and as turbidites?
- To what extent is the bathymetry the result of progradation from the east and the west? How have regressions, with possible lowering of the level down to 300 m, affected the bathymetry and sediment distribution?
- How large and when in the past were lake level fluctuations? Did any major incision/erosion remove sediment? Have there been catastrophic floods? Why are there high lake terraces? What are the ages and distribution of these lake high-stand terraces?

Possible Drill Sites

Four possibilities were discussed. They are listed below not in any order but along with the most important pros and cons.

Site A: In the deep abyssal plain. If the Drilling, Observation and Sampling of the Earth's Continental Crust (DOSSEC) rig were used, then with a water depth of 650 m, a penetration of a 850-m deep well, and a sedimentation rate of 0.3 mm yr^{-1} in this region, it could reach sediment with a maximum age of 2.8 Ma.

Virtues: Such a core could provide a complete record of undisturbed sediment since continental ice sheets first developed in North America.

Weaknesses: Such drilling will challenge existing drilling techniques, as the season for drilling is short. The dynamic positioning system would likely be required for the drilling platform to hold position. This would increase costs dramatically. Moreover, the core might contain thick layers of sand, deposited as turbidites, which would be hard to penetrate.

Site B: A well at a water depth of 300 m. Again, if sediment had been deposited at (only) 0.2 mm yr^{-1} (Vermeesch et al., 2004), a penetration of 1200 m, as with a DOSSEC rig, would reach a sediment with a maximum age of 6 Ma.

Virtues: Such a core might contain a long, complete but perhaps condensed record.

Weaknesses: Again, a short drilling season would challenge existing drilling techniques, and again anchoring of the drill rig would be required. Also again, there is the risk of drilling sand. Furthermore, the sedimentation rate might be much higher.

Site C: A well drilled on land on the plain just east of the lake. Penetration to 1500 m depth with sedimentation at a high average rate of 1 mm yr^{-1} would reach a maximum of 1.5 Ma, but at 0.2 mm yr^{-1}, it would reach 7.5 Ma. Such a well could penetrate farther, if a commercial rig rather than the DOSSEC rig were to be used.

Virtues: Logistics should be relatively easy, and costs should be relatively low. Other nearby wells drilled in Soviet times demonstrate feasibility. Moreover, downhole logging should be easier than on the lake.

Weaknesses: Potentially large stratigraphic gaps might exist, and sediment might be coarse. Before such an undertaking, seismic reflection profiling on land is needed.

Site D: A well sited on an anticline at 500 m water depth at the eastern end of the deep central basin. Assuming a DOSSEC rig is used, a penetration of 1000 m into sediment deposited at 0.3 mm yr^{-1} would reach a maximum age of 3.3 my.

Virtues: A long, complete but perhaps slightly condensed record would be obtained. The likelihood of drilling through coarse-grained material/turbidites is lowest among the sites considered.

Weaknesses: Again, a short drilling season would challenge existing drilling techniques, and again dynamic positioning system would likely be required for the drilling platform to hold position. This would increase costs dramatically. In addition, from the existing seismic profiling, a well might intersect a fault at depth.

The workshop participants did not discuss at length the virtues and weaknesses of all sites in detail, but the general consensus was that the best option for reaching sediment several million years old was Site C, and the best for paleoclimatic studies on the 100-ky timescales was Site D.

References

Abrakhmatov, K.E., Djanuzakov, K.E., and Delvaux, D., 2002. Active tectonics and seismic hazard of the Issyk-Kul basin in the Kyrgyz Tian-Shan, *In* Klerkx, J., and Imanackunov, B. (Eds.) *Lake Issyk-Kul: Its Natural Environment*: Dordrecht (NATO Science Series, Kluwer), 147–160.

Abdrakhmatov, K.E., Thompson, S., and Weldon, R., 2007. *Active Tectonics of the Tien Shan*: Bishkek, Kyrgyzstan (Ilim), in Russian.

Abdrakhmatov, K.E., Weldon, R., Thompson, S., Burbank, D., Rubin, Ch., Miller, M., and Molnar, P., 2001. Origin, direction, and rate of modern compression in the central Tien Shan, Kyrgyzstan. *Geologiya i Geofizika (Russian Geology & Geophysics)*, 42:1585–1609.

Abramowski, U., Bergau, A., Seebach, D., Zech, R., Glaser, B., Sosin, P., Kubik, P.W., and Zech, W., 2006. Pleistocene glaciations of Central Asia: Results from ^{10}Be surface exposure ages of erratic boulders from the Pamir (Tajikistan), and the Alay-Turkestan range (Kyrgyzstan). *Quat. Sci. Rev.*, 25:1080–1096. doi:10.1016/j.quascirev.2005.10.003

Aizen, E.M., Aizen, V.B., Melack, J.M., Nakamura, T., and Ohta, T., 2001. Precipitation and atmospheric circulation patterns at mid-latitudes of Asia. *Int. J. Climatology*, 21:535–556. doi:10.1002/joc.626

Aizen, V.B., Aizen, E.M., Melack, J., and Dozier, J., 1997. Climatic and hydrologic changes in the Tien Shan, Central Asia. *J. Climate*, 10:1393–1404. doi:10.1175/1520-0442(1997)010<1393:CAHCIT>2.0.CO;2

Akhmetyev, M.A., Dodoniv, A.E., Somikova, M.V., Spasskaya, I.I., Kremenetsky, K.V., and Klimanov, V.A., 2005. Kazakhstan and Central Asia (plains and foothills). In Velichko, A.A., and Nechaev, V.P. (Eds.), *Cenozoic Climatic and Environmental Changes in Russia, Geol. Soc. Am. Special Paper*, 382:139–161.

Brennwald, M.S., Peeters, F., Imboden, D.M., Giralt, S., Hofer, M., Livingstone, D.M., Klump, S., Strassmann, K., and Kipfer, R., 2004. Atmospheric noble gases in lake sediment pore water as proxies for environmental change. *Geophys. Res. Lett.*, 31:L04202. doi:10.1029/2003GL019153

Bullen, M.E., Burbank, D.W., and Garver, J.I., 2003. Building the northern Tien Shan: Integrated thermal, structural, and topographic constraints. *J. Geol.*, 111:149–165. doi:10.1086/345840

Burgette, R.J., 2008. Uplift in response to tectonic convergence: The Kyrgyz Tien Shan and Cascadia subduction zone [Ph.D. dissert.]. University of Oregon, Eugene, OR.

Charreau, J., Chen, Y., Gilder, S., Barrier, L., Dominguez, S., Augier, R., Sen, S., et al., 2009. Neogene uplift of the Tian Shan Mountains observed in the magnetic record of the Jingou River section (northwest China). *Tectonics*, 28:TC2008. doi:10.1029/2007TC002137

Chedia, O.K., 1986. Morphostructures and Neotectonism of the Tien Shan: Frunze (Ilim), in Russian.

Chen, J., Heermance, R., Burbank, D.W., Scharer, K.M., Miao, J., and Wang, C., 2007. Quantification of growth and lateral propagation of the Kashi anticline, southwest Chinese Tian Shan. *J. Geophys. Res.*, 112:B03S16. doi:10.1029/2006JB004345

De Batist, M., Imbo, Y., Vermeesch, P., Klerkx, J., Giralt, S., Delvaux, D., Lignier, V., Beck, C., Kalugin, I., and Abdrakhmatov, K.E., 2001. Bathymetry and sedimentary environments of Lake Issyk-Kul, Kyrgyz Republic (Central Asia): A large, high-altitude, tectonic lake. *In* Klerkx, J., and Imanackunov, B. (Eds.), *Lake Issyk-Kul: Its Natural Environment*: Dordrecht (NATO Science Series, Kluwer), 101–123.

Duchkov, A.D., Shvartsman, Yu.G., and Sokolova, L.S., 2001. Deep heat flow in the Tien Shan: Advances and drawbacks. *Geologiya i Geofizika (Russian Geology & Geophysics)*, 42:1436–1452.

Garcia-Castellanos, D., 2007. The role of climate during high plateau formation. Insights from numerical experiments. *Earth Planet. Sci. Lett.*, 257:372–390. doi:10.1016/j.epsl.2007.02.039

Gillespie, A., and Molnar, P., 1995. Asynchronous maximum advances of mountain and continental glaciers. *Rev. Geophys.*, 33:311–364. doi:10.1029/95RG00995

Giralt, S., Klerkx, J., Riera, S., Julia, R., Lignier, V., Beck, C., De Batist, M., and Kalugin, I., 2002. Recent paleoenvironmental evolution of Lake Issyk-Kul. *In* Klerkx, J., and Imanackunov, B. (Eds.), *Lake Issyk-Kul: Its Natural Environment*: Dordrecht (NATO Science Series, Kluwer), 125–145.

Ji, J., Luo, P., White, P., Jiang, H., Gao, L., and Ding, Z., 2008. Episodic uplift of the Tianshan Mountains since the late Oligocene constrained by magnetostratigraphy of the Jingou River section, in the southern margin of the Junggar Basin, China. *J. Geophys. Res.*, 113:B05102. doi:10.1029/2007JB005064

Kondorskaya, N.V., and Shebalin, N.V., 1977. *New Catalog of Strong Earthquakes in the Territory of the USSR*: Moscow (Nauka), in Russian.

Koppes, M., Gillespie, A.R., Burke, R.M., Thompson, S.C., and Stone, J., 2008. Late Quaternary glaciation in the Kyrgyz Tien Shan. *Quat. Sci. Rev.* 27:846–866.

Laverov, N.P., and Makarov, V.I., 2005. *Recent Geodynamics of Intracontinental Areas of Collision Mountain Building (Central Asia)*: Moscow (Sci. World).

Molnar, P., and England, P., 1990. Late Cenozoic uplift of mountain ranges and global climate change: Chicken or egg? Nature, 346:29–34. doi:10.1038/346029a0

Owen, L.A., Finkel, R.C., Barnard, P.L., Haizhou, M., Asahi, K., Caffee, M.W., and Derbyshire, E., 2005. Climatic and topographic controls on the style and timing of Late Quaternary glaciation throughout Tibet and the Himalaya defined by ^{10}Be cosmogenic radionuclide surface exposure dating. *Quat. Sci. Rev.*, 24:1391–1411. doi:10.1016/j.quascirev.2004.10.014

Pausata, F.S.R., Battisti, D.S., Nisancioglu, K.H., and Bitz, C.M., 2011. Chinese stalagmite δ^{18}O controlled by changes in the Indian monsoon during a simulated Heinrich event. *Nature* Geoscience, 4:474–480.

Reigber, Ch., Michel, G.W., Galas, R., Angermann, D., Klotz, J., Chen, J.Y., Papschev, A., Arslanov, R., Tzurkov, V.E., and Ishanov, M.C., 2001. New space geodetic constraints on the distribution of deformation in Central Asia. *Earth Planet. Sci. Lett.*, 191:157–165. doi:10.1016/S0012-821X(01)00414-9

Ricketts, R.D., Johnson, T.C., Brown, E.T., Rasmussen, K.A., and Romanovsky, V.V., 2001. The Holocene paleolimnology of Lake Issyk-Kul, Kyrgyzstan: Trace element and stable isotope composition of ostracodes. *Palaeogeogr. Palaeoclimatol. Palaeoecol.*, 176:207–227. doi:10.1016/S0031-0182(01)00339-X

Sun, J., and Zhang, Z., 2009. Syntectonic growth strata and implications for late Cenozoic tectonic uplift in the northern Tian Shan, China. *Tectonophysics*, 463:60–68. doi:10.1016/j.tecto.2008.09.008

Thompson, S.C., Weldon, R.J., Rubin, C.M., Abdrakhmatov, K., Molnar, P., and Berger, G.W., 2002. Late Quaternary slip rates across the central Tien Shan, Kyrgyzstan, central Asia. *J. Geophys. Res.*, 107(B9):2203. doi:10.1029/2001JB000596

Vermeesch, P., Poort, J., Duchkov, A.D., Klerkx, J. and De Batist, M., 2004. Lake Issyk-Kul (Tien Shan): Unusually low heat flow in an active intermontane basin. *Geologiya I Geofizika*, 45(5): 616–625.

Whipple, K.X., 2009. The influence of climate on the tectonic evolution of mountain belts. *Nature Geosci.*, 2:97–104. doi:10.1038/ngeo413

Willenbring, J.K., and von Blanckenburg, F., 2010. Long-term stability of global erosion rates and weathering during late-Cenozoic cooling. *Nature*, 465:211–214. doi:10.1038/nature09044

Xu, X., Kleidon, A., Miller, L., Wang, S., Wang, L., and Dong, G., 2010. Late Quaternary glaciation in the Tianshan and implications for palaeoclimatic change: A review. *Boreas*, 39:215–232. doi:10.1111/j.1502-3885.2009.00118.x

Zachos, J., Pagani, M., Sloan, L., Thomas, E., and Billups, K., 2001. Trends, thythms, and aberrations in global climate 65 Ma to present. *Science*; Apr 27, 2001; 292, 551. doi:10.1126/science.1059412

Zhang, P., Molnar, P., and Downs, W.R., 2001. Increased sedimentation rates and grain sizes 2–4 Myr ago due to the influence of climate change on erosion rates. *Nature*, 410:891–897. doi:10.1038/35073504

Zubovich, A.V., Wang, X., Scherba, Y.G., Schelochkov, G.G., Reilinger, R., Reigber, C., Mosienko, O.I., et al., 2010. GPS velocity field for the Tien Shan and surrounding regions. *Tectonics*, 29:TC6014. doi:10.1029/2010TC002772

Authors

Hedi Oberhänsli, Museum of Natural History Berlin, Invalidenstrasse 43, 10115 Berlin, Germany, e-mail: hedi.oberhaensli@mfn-berlin.de.

Peter Molnar, Department of Geological Sciences and Cooperative Institute for Research in Environmental Sciences (CIRES), University of Colorado at Boulder, Boulder, CO 80309-0216, U.S.A., e-mail: molnar@colorado.edu.

Workshop on Drilling of Lake Junin, Peru: Potential for Development of a Continuous Tropical Climate Record

by Donald T. Rodbell, Mark B. Abbott, and the 2011 ICDP Lake Junin Working Group

doi:10.2204/iodp.sd.13.10.2011

Lake Junin (11.0°S, 76.2°W; Fig. 1) is one of the few lakes in the tropical Andes that predates the last glacial maximum. Located at 4000 masl, it covers approximately 300 km^2 between the eastern and western cordillera of the central Peruvian Andes. Moraines from alpine glaciers that emanated from the eastern cordillera reach the eastern margin of the lake, but at no time in at least the last several hundred thousand years has the lake been overridden by ice.

Existing sediment cores (20–25 m long) from Lake Junin span ~50 ka and reveal intervals of high glacigenic siliclastic sediment input that alternate with interstadial intervals dominated by the rapid accumulation (~1 mm yr^{-1}) of authigenic marl (Fig. 2; Hansen et al., 1984; Seltzer et al., 2000). The last deglaciation is marked by a ~6‰ increase in the $\delta^{18}O$ of bulk marl that is nearly identical to the isotopic shift reported from the Huascaran ice core (Fig. 3), ~300 km to the north. Records of $\delta^{18}O$ from Junin and from other carbonate lakes and speleothems in the region are strongly affected by the hydrological balance of the central Andes, which, in turn, is controlled by the strength of the South American Summer Monsoon (SASM). Controls on the vigor of the SASM include long-term insolation receipts, the mean position of the intertropical convergence zone over the tropical Atlantic Ocean, and the mean state of El Niño Southern Oscillation (ENSO).

Figure 1. The Lake Junin basin with proposed coring localities 1–3 (Table 1). The eastern cordillera is extensively glaciated, and paleoglaciers reached the eastern edge of the lake on multiple occasions over the past several hundred thousand years. Relatively high rates of glacigenic sedimentation are expected during intervals of expanded ice cover at proposed core sites 1 and 2, whereas site 3 should contain the highest concentration of marl.

Lake Junin contains a sediment record that spans multiple glacial cycles—perhaps covering many hundreds of thousands of years—and the sediments contain high concentrations of authigenic calcite that can be used for both age control through U-Th measurements and production of a subdecadal record of hydrologic variability through stable isotope analyses. However, Lake Junin has never been cored to a depth greater than 25 m. The clear potential of Lake Junin to provide a well-dated high-resolution record of tropical climate evolution spanning several hundred millennia justifies the attention of the scientific community through the International Continental Scientific Drilling Program (ICDP) to ensure the successful acquisition of multiple cores at several locations in the Junin basin (Fig. 1; Table 1).

With this goal in mind, twenty-seven scientists from six countries participated in a workshop in Tarma, Peru on 15–17 June 2011 to discuss scientific priorities and logistical requirements of deep drilling of Lake Junin. Speakers presented overviews of the following topics:

1) the geologic setting of Lake Junin, and the four decades of Quaternary geologic and paleolimnologic research conducted there,
2) the global relevance of a long climate record from Lake Junin,
3) modern climatic controls on stable isotopes in the tropics, and recently-acquired high-resolution $\delta^{18}O$ records from carbonate lakes and speleothems in the Junin region,
4) recently acquired air gun seismic stratigraphy that reveals a total sediment thickness of at least 125 m, no evidence of faulting, and few if any unconformities,
5) the paleoecological potential of Lake Junin sediments,
6) promising new U/Th dates for Junin carbonates, and

Table 1. Proposed drill sites for Lake Junin.

Coring Site Number (Fig. 1)	Latitude (°S)	Longitude (°W)	Water Depth (m)	Distance to input streams of eastern siliclastic sediment*	Distance to input streams of northern siliclastic sediment*	Distance to input streams of western siliclastic sediment*
1	11.01	76.13	11	distal	intermediate	proximal
2	11.02	76.07	8	proximal	distal	distal
3	11.05	76.09	8	distal	distal	proximal

*Proximal indicates less than 5 km; intermediate indicates feature is between 5 km and 10 km, and distal indicates >10 km.

7) paleomagnetism as a potential dating tool for Junin sediments and as a means of fingerprinting glacigenic sediment in lakes.

One full day was spent circumnavigating Lake Junin by bus with stops to review the regional glacial chronology and to consider possible lake access points and base camps for future drilling and science teams.

Several discussion groups were organized to focus on the themes noted above and were charged with writing short reports to identify the major questions that could be addressed by studying Lake Junin sediments. These groups included 1) stratigraphy and geochronology, 2) organic geochemistry, 3) paleoecology, and 4) regional records of climate.

Lake Junin sits within a fault-bounded subsiding intermontane basin between the eastern and western cordillera of the central Peruvian Andes. Bedrock is dominated by late Paleozoic to Mesozoic carbonates, although glacial erosion of the eastern cordillera has exposed pre-Cambrian crystalline rocks. The lake basin, with a maximum water depth of ~15 m, is dammed at its northern and southern ends by coalescing alluvial fans that emanate from glacial valleys in both cordillera. These fans can be traced to moraines that are more than 250 ka, and thus the lake is at least this old. Detailed moraine mapping coupled with nearly 200 cosmogenic radionuclide (CRN; ^{10}Be, ^{26}Al) exposure ages from boulders on the crests of moraines clearly indicates that during the maximum extent of late Cenozoic glaciation on the Junin Plain, paleoglaciers reached the lake edge, but at no time in perhaps as much as one million years or more has Lake Junin been overridden by ice (Smith et al., 2005a, 2005b).

Figure 2. Marl exposed during the dry season along the western edge of Lake Junin; view is looking east across the lake to the eastern cordillera. The marl exposed in this photograph has precipitated on the leaves of rooted macrophytes and has accumulated to form a bioherm several meters thick. The glacier-clad summits in the distance fed valley glaciers that reached the eastern edge of Lake Junin on several occasions in the last million years (Smith et al., 2005a, 2005b).

Reconnaissance seismic-reflection surveys suggest that the Lake Junin basin contains a thick sedimentary sequence amenable to sampling by drill core. High-resolution chirp (4–24 kHz) data collected in 2008, combined with existing core data, reveal tens of meters of interbedded marl and lacustrine mud, the latter dominated by glacial flour. In shallow water (<6 m), these sediments are incised by chan-

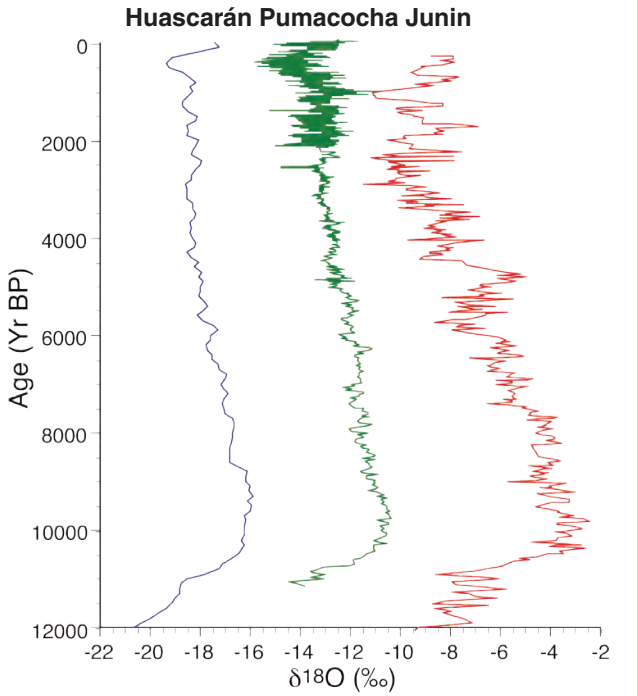

Figure 3. Oxygen isotope records from the central Peruvian Andes: Huascarán Ice Core (Thompson et al., 1995), Laguna Pumacocha (Bird et al., 2011), and Lake Junin (Seltzer et al., 2000 and unpublished data). The age model for the Junin record is based on a combination of radiocarbon and U/Th ages. The steeper Holocene isotope gradient of Junin reflects the hydrologically-closed nature of Junin, which makes Junin especially sensitive to changes in regional hydrologic balance.

nels related to a Holocene lowstand of the lake. An air gun seismic survey in 2011 successfully imaged as much as 150 m of nearly horizontal sediment with no evidence of deformation. Details of the stratigraphy were obscured by ringing in the shallow water column, but several prominent, continuous reflections were observed that could be traced across the lake basin. One of these, reaching a maximum depth of about 125 m below the lake floor, was especially prominent, but several additional deeper reflections were observed below it. The prominent deep reflection could be mapped throughout the survey area, and it is flatter than the modern lake floor. These relationships suggest broad-scale basin subsidence and a lack of local deformation. They also suggest that at the time that the deep reflector was formed, the lake was somewhat larger than at present. No evidence has been observed in the central part of the lake for large-scale lake-level fluctuations, such as wave-cut shorelines, fluvial channels, or low-stand deltas. No local tectonic deformation was observed, and no widespread gas, either volcanic or biogenic, was observed in the sedimentary sequence.

U/Th dating will be an essential element in developing age models for longer cores from Lake Junin. Preliminary analyses of radiocarbon-dated Holocene sediments from the lake indicate that these interglacial sediments are nearly ideal for U/Th measurements, with high carbonate percentages (~90%), very high $^{234}U/^{238}U$ ratios, and low contamination by detrital ^{230}Th. Though errors on dates are small compared to other lacustrine sediments, errors on Holocene dates are still on the order of 1000 yr and are dominated by uncertainty in the detrital $^{230}Th/^{232}Th$ ratio used to correct for detrital ^{230}Th. Uncertainty in this ratio is currently estimated at ±100%. Future work will seek to reduce these errors by 1) better characterizing $^{230}Th/^{232}Th$ ratios in the detrital material through analysis of zero-age samples and use of isochrones, and 2) careful selection of small (a few milligrams), extremely clean samples. In previous interglacials, relative errors will be substantially smaller due to decay of the initial detrital ^{230}Th; even assuming that uncertainty in the detrital $^{230}Th/^{232}Th$ is not reduced, errors in samples from 125 ka should be <1 kyr, assuming the sediments are similar in composition to Holocene sediments.

Lake Junin offers an excellent venue to test current hypotheses of paleoecological responses to climatic change. Abrupt and non-linear responses to change are among the most important issues to be investigated. The transitions of biota ranging from plants to ostracods into and out of previous interglacials, and responses to millennial-scale events will allow us to test a wide range of theories relating to community composition, ecosystem resilience, migratory response, and even extinction.

Workshop participants agreed that the regional-global scale rationale for a concerted effort through the ICDP to acquire multiple long cores from Lake Junin includes the following points. 1) Lake Junin is in a critical location with respect to long-term ENSO-Southern Hemisphere monsoon dynamics. 2) The potential of coupling a marl isotope record from Junin with the emerging nearby $\delta^{18}O$ record from speleothems to produce a paleohumidity record would be a unique contribution to the paleoclimatology and paleoecology of South America. 3) Lake Junin may provide a unique isotopic and paleoecological record of Dansgaard-Oeschger (D-O) and Heinrich events linked to conditions in the core of the SASM region of the Amazon Basin. 4) The glacigenic sediment record from Lake Junin will provide the first continuous record of glaciation and glacial erosion spanning several hundred millennia in tropical South America.

References

Bird, B, W., Abbott, M. B., Rodbell, D. T., and Vuille, M., 2011, Holocene tropical South American hydroclimate revealed from a decadally resolved lake sediment $\delta^{18}O$ record: *Earth and Planetary Science Letters* 310, 192–202.

Hansen, B.C.S., Wright, H.E., Jr., and Bradbury, J.P., 1984. Pollen studies in the Junín area, central Peruvian Andes. *GA Bull.*, 95:1454–1465, doi:10.1130/0016-7606(1984)95%3C1454:PSITJA%3E2.0.CO;2.

Seltzer, G., Rodbell, D., and Burns, S., 2000. Isotopic evidence for late Quaternary climatic change in tropical South America. *Geology*, 28:35–38, doi:10.1130/0091-7613(2000)28%3C35:IEFLQC%3E2.0.CO;2.

Smith, J.A., Finkel, R.C., Farber, D.L., Rodbell, D.T., and Seltzer, G.O., 2005a. Moraine preservation and boulder erosion in the tropical Andes: Interpreting old surface exposure ages in glaciated valleys. *J. Quat. Sci.*, 20:735–758, doi:10.1002/jqs.981.

Smith, J.A., Seltzer, G.O., Farber, D.L., Rodbell, D.T., and Finkel, R.C., 2005b. Early local last glacial maximum in the tropical Andes. Science, 308:678–677, doi:10.1126/science.1107075.

Thompson, L.G., Mosley-Thompson, E., Davis, M. E., Lin, P. -N, Henderson, K. A., Cole-Dai, J., Bolzan, J. F., and Liu, K. -b., 1995. Late glacial stage and Holocene tropical ice core records from Huascarán, Peru. Science 269, 46–50.

Authors

Donald T. Rodbell, Union College, Schenectady, NY 12308, U.S.A., e-mail: rodbelld@union.edu.
Mark B. Abbott, Department of Geology and Planetary Science, University of Pittsburgh, 4107 O'Hara Street, Room 200, SRCC Building, Pittsburgh, PA 15260-3332, U.S.A., e-mail: mabbott1@pitt.edu.
and the 2011 ICDP Lake Junin Working Group

Photo Credit

Fig. 2: Donald T. Rodbell, Union College

Continental Transform Boundaries: Tectonic Evolution and Geohazards

by Cecilia M.G. McHugh, Leonardo Seeber, M. Namik Çağatay, Pierre Henry, Christopher Sorlien, Michael Steckler, and Gülsen Uçarkuş

doi:10.2204/iodp.sd.13.11.2011

Introduction

Continental transform boundaries cross heavily populated regions, and they are associated with destructive earthquakes, for example, the North Anatolian Fault (NAF) across Turkey, the Enriquillo-Plantain Garden fault in Haiti, the San Andreas Fault in California, and the El Pilar fault in Venezuela. Transform basins are important because they are typically associated with 3-D fault geometries controlling segmentation—thus, the size and timing of damaging earthquakes—and because sediments record both deformation and earthquakes. Even though transform basins have been extensively studied, their evolution remains controversial because we don't understand the specifics about coupling of vertical and horizontal motions and about the basins' long-term kinematics. Seismic and tsunami hazard assessments require knowing architecture and kinematics of faults as well as how the faults are segmented.

A four-day workshop, 13–16 June 2011 at Istanbul Technical University, Istanbul, Turkey, focused on the seismo-tectonic evolution of the Marmara Sea, which is 150 km long and includes three ~1200-m-deep subsiding basins (Figs. 1, 2). The submerged Marmara segment of the NAF is considered a seismic gap presenting high risk to Istanbul and its surroundings. The workshop was sponsored by the Integrated Ocean Drilling Program (IODP) to lay the groundwork for a proposal in the Marmara Sea.

The NAF extends east-west for over 1600 km across Turkey (Fig. 1). The northern branch of the NAF crosses the Marmara Sea and now accommodates most of the 21–25 mm y^{-1} motion between the Anatolian block and the Eurasian plate (Reilinger et al., 2010). Since 1939, a sequence of seven M>7 earthquakes ruptured the NAF progressively westward across Turkey but to the east of Marmara Sea. The most recent two in 1999 were just east of the sea and particularly destructive (~17,000 deaths). West of the Marmara Sea an M_w7.4 earthquake ruptured the NAF's Ganos segment in 1912. The only unruptured segments of the NAF in the last century are within the Marmara Sea. They have been identified as a seismic gap with as much accumulated elastic strain as was released in the 1999 sequence (Parsons, 2004).

Details regarding the fault system beneath the Marmara Sea are challenging traditional models for transform tectonics. Some authors account for structural complexities and basins as relics and propose throughgoing transcurrent faults in the current regime (Le Pichon et al., 2001). Alternatively, basins may grow in a steady-state regime. Crustal thinning and subsidence may stem from pull-apart fault geometries and strain partitioning (Armijo et al., 2005) or from oblique slip on non-vertical throughgoing master faults (Okay et al., 2000; Seeber et al., 2006). Particulars of these models determine the segmenta-

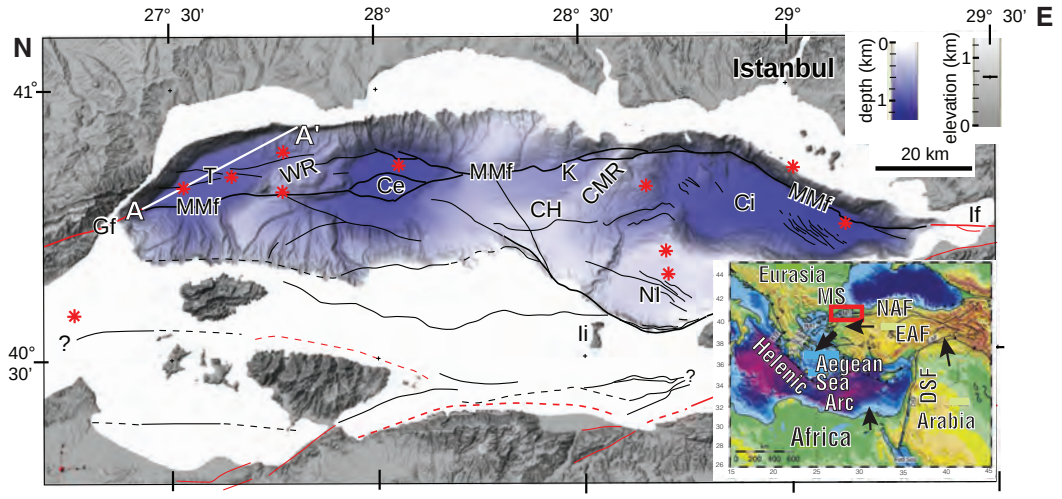

Figure 1. Bathymetry and topography of the Marmara Sea region (bathymetric data from Rangin et al., 2001) showing its basins from east to west: Cinarcik (Ci), North Imrali (NI), Kumburgaz (K), Central (Ce), Tekirdag (T). These basins are separated by the Central Marmara Ridge (CMR) and Western Ridge (WR). The main faults are shown as black lines (Sorlien et al., 2012); those in red are from several published sources as explained in Sorlien et al. (2012): Izmit fault (If), Main Marmara fault (MMf), and Ganos fault (Gf). The red stars mark the locations of the proposed drill sites. Inset shows the topography of the eastern Mediterranean with plate tectonic configuration and GPS-derived vectors (Reilinger et al., 2010). Red box locates Marmara Sea. Also shown are the North Anatolia Fault (NAF), East Anatolia Fault (EAF) and Dead Sea Fault (DSF).

tion of the gap and the size and number of future earthquakes and the hazard facing Istanbul.

Other large metropolitan regions are threatened by continental transforms. This workshop was held to discuss the research opportunities presented by drilling in the Marmara Sea.

Scientific Presentations

Forty scientists and fifteen graduate and undergraduate students from Europe, Turkey, and the USA attended the IODP Marmara-Trans workshop. The presentations covered the evolution of the plate boundary from subduction to strike slip. Thermal models of the Marmara Sea basins focused on whether the growth was steady, or whether the basins grew initially and passively rode along the transform later. Structural evidence suggests asymmetric fault-bend basins subsiding steadily into the present (Seeber et al., 2004). Unconformities were identified, tentatively dated, and correlated in all the Marmara Sea basins from seismic profiles (Sorlien et al., 2012). Constraining the age model would be critical for evaluating the basins' structural evolution. Large earthquakes and tsunamis have been known for 2000 years from the historical record, and into the upper Holocene from the geological record. Historical and geological data overlap and correlate. Earthquake-triggered deep-water sedimentation in Haiti and Marmara Sea are remarkably similar. They suggest "turbidite-homogenite" units with characteristic structures and chemistry (McHugh et al., 2006; Beck et al., 2007) that could be recognized in the stratigraphy and provide an earthquake record through the growth of the basin. Better understanding of how seismogenesis relates to other geologic observables would improve earthquake forecasting and hazard assessment along the North Anatolian Fault and other continental transforms.

Reconnections between the Black, Marmara, and Aegean Seas in response to eustasy and climate have been much debated in recent years. These freshwater and saltwater exchanges were accompanied by dramatic transitions in flora, fauna, and geochemistry that have been recorded in the sediments of Marmara Sea. But, available piston and gravity cores extend back for only ~130 ka (Çağatay et al., 2009). A longer sedimentary record would recover repeated eustatic and climate cycles and thus distinguish the role of tectonics from sea-level fluctuations.

Seafloor gas emissions and fluid expulsions, observed with ROV and manned submersibles, appear to be focused along active faults in the Marmara Sea (Zitter et al., 2008; Géli et al., 2008). Surveys based on multichannel seismic reflection profiles, chirp, and multibeam data found a widespread distribution of gas in the sediment and the strongest gas discharge in the water column above the topographic highs between basins (Shillington et al., in press). Conduits along the main transform on the Western High expel thermogenic gas and associated brines. 3-D high-resolution seismic data in the same area document the interplay of sediment deformation and formation of fluid conduits (Bourry et al., 2009; Tryon et al., 2010). Authigenic carbonates and associated biogeochemical communities were recently discovered in Marmara Sea. These findings reveal that hydrological and biogeochemical activities along continental transforms are as intense as in other plate boundaries.

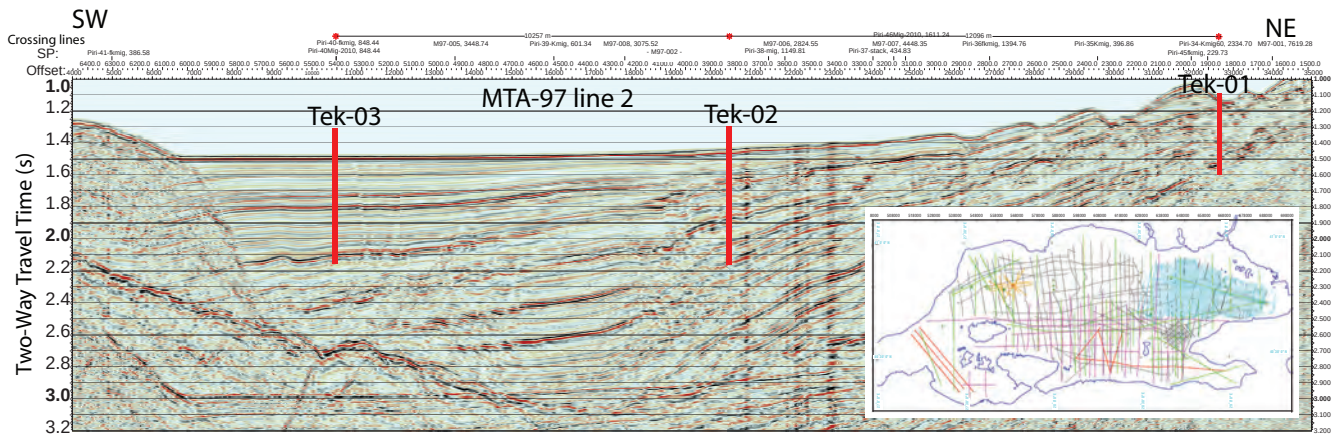

Figure 2. Multichannel seismic reflection (MCS) line MTA97 line 2 across Tekirdag Basin (white A–A' line on Fig. 1; data from Parke et al., 2003). The red rectangles show the locations of potential drilling sites. Tek-03: this SW location was targeted to reach Pleistocene to Holocene strata deposited at high sedimentation rates at the deepest part of the basin (1200 m of water depth). Tek-02 (projected 2.7 km from the SE): targeted to reach Pliocene to Pleistocene strata. Tek-01 (projected 2.6 km from the SE): targeted at the condensed margin of the basin to reach Miocene to Holocene strata.
Inset showing available high-resolution MCS data. Gray lines: TAMAM-2008 and PirMarmara Leg a4 (Sorlien et al., 2012). Orange lines are PirMarmara 2010 Leg a2 (P. Henry, G. Çifçi, and others, unpublished). Red lines are PirMarmara 2010 Legs a1, a3 (G. Çifçi and others, unpublished). The dense cyan grids are from Carton et al., 2007. Magneta are Marathon industry lines (C&K Petroleum, 1974). Green lines are from MTA97 (Parke et al., 2003).

Links to Other Programs

Several seafloor observatories, which monitor seismic hazards long-term, and continental drilling programs are being carried out in Marmara Sea and surroundings by Turkey and international groups. Observatories have been deployed in Marmara Sea for understanding the long-term relationship between fluids and seismicity as part of the Marmara Demonstration Mission project funded by the European Seafloor Observatory Network and the European Multidisciplinary Seafloor Observatory. The International Continental Scientific Drilling Program (ICDP) project GONAF (a deep Geophysical Observatory at the North Anatolian Fault) plans to drill two boreholes in the Princes Islands, Turkey. Representatives of this program presented their preliminary results on seismotectonics. Future programs include the development and implementation of submarine geodetics as part of seismic risk assessment in collaboration with Istanbul Technical University and the Turkish Navy. Deployment of seafloor drilling rig MeBo is also being considered to investigate the interactions between sediment deformation and fluids.

Outcome of the Workshop

The working group participants selected locations for drilling sites based on existing data. These were recorded from geophysical investigations (multichannel seismic reflection profiles, multibeam bathymetry, high-resolution sub-bottom profiles, side scan sonar), sediment sampling (piston cores up to 30 m long and many gravity cores), and explorations by manned and unmanned submersibles. The data were acquired during the following cruises and research vessels: Seismarmara, Marmarascarps, Marnaut, Marmesonet, R/V *Marion Dufresene*, R/V *Urania* (2002, 2009), and R/V *Piri Reis* (project TAMAM: 2008, 2010) (Rangin et al., 2001; Le Pichon et al., 2001; Polonia et al., 2004; Armijo et al., 2005; Cormier et al., 2006; Steckler et al., 2008; Géli et al., 2008; Görür and Çağatay, 2010).

These proposed drilling sites target the main Marmara Sea basins with the following goals.

1. Their deepest parts are intended to recover an expanded Holocene to Pleistocene strata with high sedimentation rates.

2. The condensed margins of the basins could reach older, possibly Miocene, strata.

3. They are located at and near fluid emission sites within the main fault zone to characterize the nature of the conduits and the timing of past activity, and to install borehole monitoring systems for fluid pressure and chemistry.

4. Additional plans for borehole instrumentation include monitoring of strain rates and seismic activity. These objectives would address major issues, such as the partitioning between fluid from deep sources possibly relevant to earthquakes and fluid from the compaction and dewatering of sediments.

These scientific and drilling objectives target the new International Ocean Discovery Program focusing on the "Earth's driving tectonics which reveal its inner workings and cause major geological hazards".

Acknowledgments

We thank IODP-MI, the Eastern Mediterranean Centre for Oceanography and Limnology, and Queens College, City University of New York for their support.

References

Armijo, R., Pondard, N., Meyer, B., Uçarkus, G., Mercier de Lepinay, B., Malavieille, J., Dominguez, S., et al., 2005. Submarine fault scarps in the Sea of Marmara pull-apart (North Anatolian Fault): Implications for seismic hazard in Istanbul. *Geochem. Geophys. Geosys.*, 6:Q06009. doi:10.1029/2004GC000896

Beck, C., de Lepinay, M., Schneider, J.-L., Cremer, M., Çağatay, N., Wendenbaum, E., Boutareaud, S., Mynot, G., Schmidt, S., and Weber, O., 2007. Late Quaternary co-seismic sedimentation in the Sea of Marmara's deep basins. *Sed. Geol.*, 199:65–89. doi:10.1016/j.sedgeo.2005.12.031

Bourry, C., Chazallon, B., Charlou, J.-L., Donval, J.P., Ruffine, L., Henry, P., Géli, L., Çağatay, M.N., Sedat, İ., and Moreau, M., 2009. Free gas and gas hydrates from the Sea of Marmara, Turkey: Chemical and structural characterization. *Chem. Geol.*, 264:197–206. doi:10.1016/j.chemgeo.2009.03.007

C&K Petroleum, 1974. Report covering geophysics–geology Marmara offshore, Turkey, 71 pp.

Çağatay, M.N., Eriş, K., Ryan, W.B.F., Sancar, Ü., Polonia, A., Akçer, S., Biltekin, D., et al., 2009. Late Pleistocene-Holocene evolution of the northern shelf of the Sea of Marmara. *Mar. Geol.*, 265:87–100. doi:10.1016/j.margeo.2009.06.011

Carton, H., Singh, S.C., Hirn, A., Bazin, S., de Voogd, B., Vigner, A., Ricolleau, A., Cetin, S., Ocakoglu, N., Karakoc, F., and Sevilgen, V., 2007. "Seismic imaging of the three-dimensional architecture of the Cinarcik Basin along the North Anatolian Fault. *J. Geophys. Res.*, 112:B06101, doi:10.1029/2006JB004548.

Cormier, M.-H., Seeber, L., McHugh, C.M.G., Polonia, A., Çağatay, M.N., Emre, Ö., Gasperini, L., et al., 2006. North Anatolian fault in the Gulf of Izmit (Turkey): Rapid vertical motion in response to minor bends of a nonvertical continental transform. *J. Geophys. Res.*, 111:B04102. doi:1029/2005JB003633

Géli, L., Henry, P., Andre, C., Zitter, T., Çağatay, M.N., Mercier de Lepinay, B., Le Pichon, X., et al., 2008. Gas emissions and active tectonics within the submerged section of the North Anatolia Fault zone in the Sea of Marmara. *Earth Planet.*

Sci. Lett., 274(1-2):34–39.

Görür, N., and Çağatay, M.N., 2010. Geohazards rooted from the northern margin of the Sea of Marmara since the late Pleistocene: A review of recent results. *Nat. Hazards*, 54(2):583–603. doi:10.1007/s11069-009-9469-x

Le Pichon, X., Sengör, A.M.C., Demirbag, E., Rangin, C., Imren, C., Armijo, R., Görür, N., et al., 2001. The active main Marmara fault. *Earth Planet. Sci. Lett.*, 192:595–616.

McHugh, C.M.G., Seeber, L., Cormier, M.-H., Dutton, J., Çağatay, M.N., Polonia, A., Ryan, W.B.F., and Görür, N., 2006. Submarine earthquake geology along the North Anatolian Fault in the Marmara Sea, Turkey: A model for transform basin sedimentation. *Earth Planet. Sci. Lett.*, 248:661–684. doi:10.1016/j.epsl.2006.05.038

Okay, A.I., Kaslilar-Ozcan, A., Imren, C., Boztepe-Guney, A., Demirbag, E., and Kuscu, I., 2000. Active faults and evolving strike-slip fault basins in the Marmara Sea, northwest Turkey: A multichannel reflection study. *Tectonophysics*, 321:189–218. doi:10.1016/S0040-1951(00)00046-9

Parke, J.R., White, R.S., McKenzie, D., Minshull, T.A., Bull, J., Kuscu, I., Görür, N., and Sengör, A.M.C., 2003. The Sea of Marmara: A two-dimensional seismic reflection data archive. *Geochem. Geophys. Geosys.*, 4:1084. doi:10.1029/2002GC000493

Parsons, T., 2004. Recalculated probability of M>7 earthquakes beneath the Sea of Marmara, Turkey. *J. Geophys. Res.*, 109:B05304. doi:10.1029/2003JB002667

Polonia, A., Gasperini, L., Amorosi, A., Bonatti, E., Bortoluzzi, G., Çağatay, M.N., Capotondi, L., et al., 2004. Holocene slip rate of the North Anatolian Fault beneath the Sea of Marmara. *Earth Planet. Sci. Lett.*, 227:411–426.

Rangin, C., Demirbag, E., Imren, C., Crusson, A., Normand, A., Le Drezen, E., and Le Bot, A., 2001. *Marine Atlas of the Sea of Marmara (Turkey)*, Ifremer.

Reilinger, R., McClusky, S., Paradissis, D., Ergintav, S., and Vernant, P., 2010. Geodetic constraints on the tectonic evolution of the Aegean region and strain accumulation along the Hellenic subduction zone. *Tectonophysics*, 488:22–30. doi:10.1016/j.tecto.2009.05.027

Seeber, L., Cormier, M.-H., McHugh, C.M.G., Emre, Ö., Polonia, A., and Sorlien, C.C., 2006. Subsidence and sedimentation at a transform bend: The Çinarcik Basin and the North Anatolian Fault in the Marmara Sea, Turkey. *Geology*, 34(11):933–936.

Seeber, L., Emre, Ö., Cormier, M.-H., Sorlien, C.C., McHugh, C.M.G., Polonia, A., and Scientific Team of Marmara, 2004. Uplift and subsidence from oblique slip: The Ganos-Marmara Bend of the North Anatolian Transform, Western Turkey. *Tectonophysics*, 391:239–258. doi:10.1016/j.tecto.2004.07.015

Shillington, D.J., Seeber, L., Sorlien, C.C., Steckler, M.S., Kurt, H., Dondurur, D., Çifç, G., et al., in press. Slow-motion collapse on the flanks of the Sea of Marmara transform basins. *Geology*.

Sorlien, C.C., Akhun, S.D., Seeber, L., Steckler, M., Shillington, D., Kurt, H., Çifçi, G., et al., 2012. Uniform basin growth over the last 500 ka, North Anatolian Fault, Marmara Sea, Turkey. *Tectonophysics*, 518–521:1–16. doi: 10.1016/j.tecto.2011.10.006

Steckler, M.S., Cifci, G., Demirbag, E., Akhun, S.D., Buyukasik, E., Cevatoglu, M., Coskun, S., et al., 2008. High resolution multichannel imaging of basin growth along a continental transform: The Marmara Sea along the North Anatolian Fault in NW Turkey. *Eos Trans. AGU*, 89(53):T21A-1921.

Tryon, M.D., Henry, P., Çağatay, M.N., Zitter, T.A.C., Géli, L., Gasperini, L., Burnard, P., Bourlange, S., and Grall, C., 2010. Pore fluid chemistry of the North Anatolian Fault Zone in the Sea of Marmara: A diversity of sources and processes. *Geochem. Geophys. Geosys.*, 11:Q0AD03. doi:10.1029/2010GC003177

Zitter, T.A.C., Henry, P., Aloisi, G., Delaygue, G., Çağatay, M.N., Mercier de Lepinay, B., Al-Samir, M., et al., 2008. Cold seeps along the main Marmara fault in the Sea of Marmara (Turkey). *Deep Sea Research Part I*, 55:552–570.

Authors

Cecilia M.G. McHugh, School of Earth and Environmental Sciences, Queens College, City University of New York, 65-30 Kissena Boulevard, Flushing, NY 11367, U.S.A., e-mail: cmchugh@qc.cuny.edu.

Leonardo Seeber, Lamont-Doherty Earth Observatory of Columbia University, Route 9W, Palisades, NY 10964, U.S.A., e-mail: nano@ldeo.columbia.edu.

M. Namik Çağatay, Geology Department, Istanbul Technical University, Ayazaga 80626, Istanbul, Turkey, e-mail: cagatay@itu.edu.tr.

Pierre Henry, Centre National de la Recherche Scientifique (CNRS), College de France, Bat Trocadero, Europole de l'Arbois, BP80, 13545 Aix en Provence Cedex 04, France, e-mail: henry@cerege.fr.

Christopher Sorlien, Earth Research Institute, 6832 Ellison Hall, University of California, Santa Barbara, CA 93106-3060, U.S.A., e-mail: sorlien@eri.ucsb.edu.

Michael Steckler, Lamont-Doherty Earth Observatory of Columbia University, Route 9W, Palisades, NY 10964, U.S.A., e-mail: steckler@ldeo.columbia.edu.

Gülsen Uçarkuş, Geology Department, Istanbul Technical University, Ayazaga 80626, Istanbul, Turkey, e-mail: gulsen.ucarkus@gmail.com.

Related Web Links

http://www.emcol.itu.edu.tr/Icerik.aspx?sid=9300
http://www.ldeo.columbia.edu/TAMAM/
http://cdf.u-3mrs.fr/~henry/marmara

ECORD Summer School on "Submarine Landslides, Earthquakes and Tsunamis"

3–14 September 2012, Bremen, Germany

The 6th ECORD Summer School to be held at the Center for Marine Environmental Sciences (MARUM) at the University of Bremen, Germany, aims to bring Ph.D. students and young postdocs in touch with IODP at an early stage of their careers, inform them about research within this international scientific program, and prepare them for future participation on IODP expeditions. Such training will be achieved by taking the summer school participants on a "virtual ship" by exploiting the unique facilities linked to the IODP Bremen Core Repository (photo below). They will be introduced to a wide spectrum of state-of-the-art analytical technologies and core description methods, including core logging/scanning according to IODP expedition standards. In addition, the topic "Submarine Landslides, Earthquakes and Tsunamis" will be covered by lectures and discussions with leading geoscientists in the field. The latter will include specialists in sedimentology, seismics, tectonics, and sediment transport modeling. This comprehensive approach—combining scientific lectures with practicals on IODP-style "shipboard" measurements—is the blueprint for the Bremen ECORD summer school series, which now rounds off its second three-year cycle of ECORD summer schools covering the three major topics of the IODP Initial Science Plan. For detailed information about the summer school, the application procedure and the scholarship options, visit http://www.marum.de/en/ECORD_Summer_Schools.html.

2012 IODP-Canada Activities

2012 is shaping up to be a busy year for IODP-Canada! In January, we awarded IODP research grants to three Ph.D. students: John Evangelatos (Dalhousie University)–The origin and evolution of the Canada Basin, Arctic Ocean; Olivia Gibb (Université du Québec à Montréal)–The paleoceanographic conditions of Baffin Bay during the interglacials of MIS 5e and 11; and Matthew Izawa (University of Western Ontario)–Integrated mineral, chemical and isotopic study of microbial ichnofossil preservation in basaltic glass. Student travel grants and summer school scholarships will also be offered this year.

In February, the workshop "Coordinated Scientific Drilling in the Beaufort Sea: Addressing Past, Present and Future Changes in Arctic Terrestrial and Marine Systems" took place in Kananaskis, Alberta. Participants defined and integrated the scientific questions and drilling strategies required to assess environmental change and geohazards in the Beaufort Sea. The workshop was funded by IODP-MI, IODP-Canada, ICDP-Canada and Natural Resources Canada.

IODP-Canada will again share an exhibition booth with ICDP-Canada at the joint annual meeting of the Geological Association of Canada and the Mineralogical Association of Canada in St. John's, Newfoundland and Labrador on 27–29 May 2012. IODP-Canada will also participate in the IODP-ECORD booth at the Goldschmidt conference in Montréal, Quebec on 24–29 June, 2012. In conjunction with Goldschmidt, we plan to host a "town hall" reception to stimulate discussion about Canada's continued participation in IODP post-2013. Planning is also underway to help organize activities for the public and scientific community during the port call of the *JOIDES Resolution* in St. John's in August.

ECORD/ICDP/IODP-Canada 2012 Summer School

5–21 July 2012
Registration deadline: 1 June 2012

An ECORD/ICDP/IODP-Canada summer school "Impacts of the cryosphere dynamics from land to ocean" will be held in Québec on 5–21 July 2012 in partnership with ECORD, IODP-Canada and ICDP. The main goal of the summer school is to train graduate students and postdoctoral fellows in the fields of paleoceanography, paleoclimatology, marine geology and their associated methodological approaches and techniques. The program will be centered on four days of fieldwork on the north shore of the St. Lawrence River, which will be complemented with classes given by international invited lecturers, workshops involving the students, and four days of hands-on exercises in Montréal. A special attention will be given to polar and subpolar environments and to ice-ocean-atmosphere interactions and their role in climate dynamics. The school is open to graduate students and postdoctoral fellows from all over the world.

Find more information, visit at IODP-Canada website (http://www.iodpcanada.ca) or contact Diane Hanano (coordinator@mail.iodpcanada.ca).

Poland Joins ECORD and IODP

Poland became the 18th member of ECORD (European Consortium for Ocean Research Drilling) and the 25th member of IODP on 14 December 2011, when the Director of the Polish Geological Institute – National Research Institute (PGI – NRI) signed the ECORD MoU during a visit to Warsaw by Catherine Mével, ECORD Managing Agency Director.

The PGI – NRI has a long tradition of working in the Baltic Sea, and the prospect of the implementation of the Baltic Sea proposal by the ECORD Science Operator in 2013 has certainly contributed in this excellent decision.

However, there is a move in Poland to expand the scope of marine sciences and a plan to build a Polish research vessel. We therefore expect the Polish science community to be strongly involved in all ocean drilling activities.

As a member of ICDP and now of IODP through ECORD, Poland will definitively play an important role in scientific drilling (More information available at http://www.ecord.org/p/new_members.html)

International Symposium on Submarine Mass Movements and Their Consequences

In October 2011, 137 researchers from sixteen countires gathered in Kyoto for the IODP-MI co-sponsored 5th International Symposium on Submarine Mass Movements and Their Consequences. The meeting represents the continuation of a series of conferences initiated by UNESCO-IGCP Project 511 and its successor and ongoing project IGCP Project 585 (Earth's continental margins: Assessing the geohazard from sub-marine landslides–www.igcp585.org). The main objective of the conference was to bring a worldwide per-

Southwest Pacific Ocean IODP Workshop

Sydney, Australia, 9–12 October 2012

For more information, write: Neville.Exon@anu.edu.au

This workshop, to be held at Sydney University, will address global geoscience problems in the southwest Pacific Ocean by building on existing and new geophysical and geological information including earlier scientific drilling. Its aim is to commence building coherent and well-integrated IODP proposals. The convenors are Neville Exon, Maria Seton and Stephen Gallagher (Australia), Minoru Ikehara (Japan) and Walter Roest (France), with many others in key roles. At this stage IODP-MI and ANZIC funding is assured. More information will be sent to likely participants soon.

This region has had a complex tectonic history, with plate boundary interactions resulting in an assemblage of deep oceanic basins, volcanic arcs, back-arc and fore-arc basins, continental ribbons, and emerged and submerged carbonate platforms. The workshop will identify the global scientific hypotheses and questions in this region that require ocean drilling to resolve them. The region's extensive plateaus and basins can provide crucial sedimentary records to help understand the developing interactions between the tropics and Antarctica, and between the Pacific and Indian Oceans. Furthermore, Australia has been one of the two major land masses (the other being India) undergoing major northward migration during the Cretaceous and Cenozoic with resulting fundamental changes in the tectonic and climate development of Earth and its biota. The workshop themes are:

1) Climate and Ocean Change: Reading the Past, Informing the Future

This will cover questions related to climate and paleoceanographic change in this complex region, on all timescales.

2) Biosphere Frontiers: Deep Life, Biodiversity, and Environmental Forcing of Ecosystems

Almost nothing is known about the deep biosphere in the region, so pioneering studies of both sediments and basalts should lead to exciting results.

3) Earth Connections: Deep Processes and Their Impact on Earth's Surface Environment

The links between surface lithosphere and deep earth processes are of great interest in this tectonically complex region.

4) Earth in Motion: Processes and Hazards on Human Timescales

This region has its share of earthquakes, tsunamis and submarine slides that have impacted on populations and will continue to do so. Targeted scientific drilling will help address some of these hazards.

5) Marine Resources: Opportunities and Responsibilities: Opportunities and Responsibilities

What contribution can IODP make to the exploration, characterization and responsible exploitation of marine resources in the southwest Pacific region and under what arrangements? These resources may include offshore oil and gas, gas hydrates and offshore minerals.

spective of submarine mass movements and their consequences by assembling state-of-the-art contributions from international researchers of academic institutions and the offshore industry. The symposium provided full coverage of the scientific and engineering aspects of this type of marine and coastal geo-hazards. It also highlighted the role of scientific ocean drilling to be well positioned to elucidate submarine slope failure and mass movement processes through direct sampling and *in situ* measurements within active systems, as well as sampling and dating of event deposits to determine timing and size of past geohazards.

The elevated awareness of the need for better understanding of submarine landslides is coupled with great advances in submarine mapping, sampling and monitoring technologies. Laboratory analogue and numerical modeling capabilities have also developed significantly of late. Multibeam sonar, 3-D seismic reflection, and remote and autonomous underwater vehicle technologies provide hitherto unparalleled imagery of the geology beneath the oceans, permitting investigation of submarine landslide deposits in great detail. Increased and new access to drilling, coring, *in situ* measurements and monitoring devices allows for ground truth of geophysical data and provides access to samples for geotechnical laboratory experiments and information on *in situ* strength and effective stress conditions of underwater slopes susceptible to failure. Great advances in numerical simulation techniques of submarine landslide kinematics and tsunami propagation have also led to increased understanding and predictability of submarine landslide consequences.

The symposium provided a refreshing view on these state of the art in submarine landslide research. A total of 103 contributions presented the latest scientific research results by international experts in geological, geophysical, engineering and environmental aspects of submarine mass failures, focused on understanding the full spectrum of challenges presented by submarine mass movements and their consequences. Seven presentations were directly related to recent IODP expeditions, and many more provided links to data and studies resulting from scientific offshore drilling efforts.

As a result of the conference the fourth edition of the 'Submarine Mass Movements and Their Consequences' book containing peer-reviewed manuscripts by symposium presenters was published (Yamada, Y., Kawamura, K., Ikehara, K., Ogawa, Y., Urgeles, R., Mosher, D., Chaytor, J., and Strasser M., (Eds.) 2012. *Submarine Mass Movement and Their Consequences 5th International Symposium*. Advances in

International Geothermal Center in Bochum (Germany) Announces Start of Drilling Services with "BO-Rex"

icdp

Since October 2011 the International Geothermal Center (GZB) in Bochum, Germany started to operate its brand new track-mounted, mobile drill rig for depths up to 2000 m using rod diameters of up to 350 mm. The "BO-Rex" (HRB 207 GT) rig has been designed together by GZB and the manufacturer. It is capable of running any drilling process like mud rotary, DTH hammer drilling with water, mud or air, GeoJetting, geotechnical work, coring and sampling, augering, etc. It is equipped with a double head drilling setup to run and turn two rod strings independently of each other. For all kinds of hydraulic high-pressure drilling applications an external powerful triplex plunger pump is available for "BO-Rex" covering pressure regimes of 100 bar (max. 1000 L min^{-1}), 200 bar (max. 600 L min^{-1}) and 1500 bar (max. 80 L min^{-1}).

Technical Data:

Total gross weight: 32 t
Rotary heads torque: 50.000 and 20.000 Nm
Diesel engine: 250 kW engine
Pull force: 33 t + 20 t in the clamp
Feed force: 17 t
Max. drill rod length: 4.5 m
Mast length overall: 10 m
Winch system for rod handling: 2 t
Pumps: 20 bar robust mud pump, small Triplex water pump
Remote control: Track unit for full hydraulic operation
Manufacturer: Hütte GmbH, subsidiary of Casagrande Group, Italy

Both drill rig and pump are available to be used in scientific drilling, exploration, coring or other kind of project. Terms and conditions will be discussed per case. For more information please contact: Volker Wittig (e-mail:volker.wittig@hs-bochum.de) at the GZB website (www.geothermie-zentrum.de).

Natural and Technological Hazards Research, 31: Dordrecht, The Netherlands (Springer). doi:10.1007/978-94-007-2162-3

Contact details: Yasuhiro Yamada, yamada@earth.kumst.kyoto-u.ac.jp.

Small, Portable Drilling Rig Available for Research

DOSECC has acquired a small man-portable drilling rig suitable for drilling small coreholes and collecting core samples (1.06-inch/27 mm diameter) in remote areas or in places inaccessible by conventional drilling rigs. The rig weighs just 185 lbs (84 kg) and can be hand-carried to the drilling location. It can be used to collect rock cores to about 200 ft (60 m) deep. The system comes complete with all tools and materials included in a parts trailer. Perfect for small budget projects, it is rented for a low daily fee. Purchased with funding from the U.S. National Science Foundation, it is available to the scientific community for sampling projects and field lab experiments, including field camps. More information and photos can be found at http://www.dosecc.org/index.php/equipment/winkie-drill-system

New U.S. Continental Scientific Drilling Initiative Report Available

Follow-up Workshop: 21–22 May 2012, Arlington, Virginia, U.S.A.

As societies around the world seek an economic balance between environmental and energy needs while planning effectively for a wide range of natural hazards, the need for subsurface information about our planet has never been greater. DOSECC annual workshops in 2009 and 2010 produced the background narrative justifying a new interdisciplinary consortium of research scientists who could lever-age funds more effectively across national and international interests in the geosciences. The DOSECC workshop held on 23–24 May 2011 in Arlington, Virginia focused on the next phase: producing a vision of how the United States, under the auspices of the U.S. National Science Foundation and other federal agencies, would promote scientific drilling as a critical tool in the earth sciences to grapple with major societal issues. To that end, the workshop laid out the initial architecture for a U.S. Continental Scientific Drilling (USCSD) Initiative, to be guided by a revitalized Interagency Coordinating Group linking federal and academic stakeholders.

The workshop produced themes and workshop needs for planning future U.S. continental drilling ranging from pre-site surveys to facilities and data management, emphasizing the synergies to be developed and coordinated with a larger, stronger US CSD program. While large challenges exist in coordinating across mission-based agencies and NSF-program goals, it is clear that the transformative scientific payoffs are far greater and cost effective than the current structure for leveraging both science and mission. The full workshop report will be available at http://www.dosecc.org/index.php/publications/reports-and-brochures.

The follow-up workshop will be held on 21–22 May 2012 in Arlington, Virginia. This workshop will further define the USCSD initiative. More information on this workshop can be found at www.dosecc.org.

New Drilling and Coring Tools

The Engineering Geology Department of Lund University, Sweden, was recently awarded a Science Council grant for buying, implementing and operating a drilling infrastructure. Currently the implementation and testing phase of a high-capacity, modern diamond wireline coring rig is starting. The rig is lightweight and has a small footprint and a high capacity. It is highly atomized and fully diesel-hydraulic operated under strict safety regulations and complying to the latest environmental noise and exhaust rules. The depth coring capacities are as follows:

P-size (hole size 123 mm, core size 85 mm): 1050 m
H-size (hole size 96 mm, core size 63 mm): 1600 m
N-size (hole size 76 mm, core size 48 mm): 2500 m

The core rig has a main hoist with 178 kN, an hydraulic feed cylinder with 200 kN and 3.5-m feed stroke. It is equipped with drilling equipment for all coring sizes, at the moment including 11-km long drill rods and casing, fifty diamond core bits, and core barrels as double and single tubes in doublets. Additional drilling equipment such as wellhead, preventer, mud and cementing systems, deviation and fishing tools, logging and MWD-recording capability make the system versatile for all kinds of scientific drilling projects in various environments.

It will be utilized in the Swedish Deep Drilling Program but is also available for the international scientific community.

History of Controlled-Source Seismology Onshore and Offshore

In March 2012 the Geological Society of America has published its new Memoir 208 entitled "Exploring the Earth's Crust. History and Results of Controlled-Source Seismology", written by Claus Prodehl (University of Karlsruhe, Germany) and Walter D. Mooney (U.S. Geological Survey, Menlo Park, California, U.S.A.). This volume presents a comprehensive, worldwide history of seismological studies of the Earth's crust using controlled sources from 1850 to 2005. Essentially, all major seismic projects on land and the most important oceanic projects are presented. The time period of 1850 to 1939 is presented as a general synthesis, and from 1940 onward the history and results are subdivided into a separate chapter for each decade, with the material ordered by geographical region. Each chapter highlights the major advances achieved during that decade in terms of data acquisition, processing technology, and interpretation methods. For all major seismic projects, we provide specific details regarding the field observations, interpreted crustal cross-section, and key references. The Memoir concludes with global- and continental-scale maps of all field measurements and interpreted Moho contours. An accompanying DVD contains important out-of-print publications and an extensive collection of controlled-source data, location maps, and crustal cross- sections.

Contact: Claus Prodehl, Geophysical Institute, University of Karlsruhe, Karlsruhe Institute of Technology, Hertzstr. 16, 76187 Karlsruhe, Germany, e-mail: claus.prodehl@gmx.net

Rob McKay Wins the Prime Minister's MacDiarmid Emerging Scientist Prize

Dr. Rob McKay, a postdoctoral researcher at Victoria University's Antarctic Research Centre in Wellington, New Zealand, has been awarded the New Zealand Prime Minister's MacDiarmid Emerging Scientist Prize (worth NZ$200,000) for his work on Antarctic ice sheet response to past climate fluctuations. His research uses glacial deposits and marine sedimentary records to investigate changes in ice volume and thermal regime of the Antarctic ice sheets since their inception approximately 34 million years ago and the resulting influence on eustatic sea level. This has particular relevance today as climate scientists struggle with how the

The Rodderberg Quaternary Climate Archive

A suite of three shallow boreholes (164 m, 74 m, and 102 m) have explored the filling of the main crater of the Late Quaternary Rodderberg volcanic system near Bonn, Germany. The age of the volcano is dated to 300 ka (Paulick et al., 2008). The drilling activities finished in February, 2012. Two parallel cores were recovered from closely neighboring holes, each of them more than 70 m long, representing the sedimentary and volcano-clastic crater fill. The core material offers the unique opportunity to study a long complete climate archive representative for the Eifel region. Mainly lacustrine and aeolian (loess-like) sediments accumulated in the bowl-shaped crater since its last eruption (Zöller et al., 2010). Intercalated tephra layers of other dated volcanoes of the Eifel give a dense stratigraphic framework. A high-resolution reconstruction of past climate conditions during the last three glacial cycles may be derived from the core samples and the open hole borehole logging data. This is the central objective of the DUST TRAP project. It will study the geometry, volcanic evolution, and tectonic setting of the Rodderberg crater as well as the sedimentology, geophysics, and geochronology of its loess and loess-derived sediments. DUST TRAP is coordinated by the Steinmann Institute of Bonn University, the Leibniz Institute for Applied Geophysics, Hanover, and the Geological Survey NRW, Krefeld, and comprises groups from the Universities of Bayreuth, Braunschweig, Bremen, and Cologne.

References

Paulick, H., Ewen, C., Blanchard, H., and Zöller, L., 2008. The Middle Pleistocene Rodderberg (~300 ka) maar-scoria cone volcanic complex (Bonn, Germany): Eruptive history, geochemistry, and thermoluminescence dating. – *Int. J. Earth Sci. (Geol. Rundsch.),* 98:1879–1899. doi:10.1007/s 00531-008-0341-0

Zöller, L., Hambach, U., Blanchard, H., Fischer, S., Köhne, S., and Stritzke, R., 2010. Der Rodderberg-Krater bei Bonn. *E&G – Quat. Sci. J.*, 59:1–2

Authors

Franz Binot, Leibniz Institute for Applied Geophysics, Stilleweg 2, D-30655 Hannover, Germany, e-mail: franz.binot@liag-hannover.de

Nikolaus Froitzheim, Steinmann Institute of Bonn University, Poppelsdorfer Schloss, D-53115 Bonn, Germany, e-mail: niko.froitzheim@uni-bonn.de

and the DUST TRAP science team

Related Web Link

www.rodderberg.org

Antarctic ice sheets will respond to future climate change.

Much of his recent work has been a result of his participation on two scientific drilling expeditions to Antarctica. The first was the ANDRILL McMurdo Ice Shelf Project (2006–2007), which collected a 1280-m-long core representing the last 13 million years to study ice shelf response to past climate forcing. Rob's research focuses on investigating the glacial-interglacial cycles preserved in this record and the concomitant change in thermal regime of the Antarctic ice sheet. He is also working to improve the chronology of West Antarctic Ice Sheet changes in the Ross embayment over the last 18,000 years to better assess Antarctica's role in global sea-level change.

Rob returned to Antarctica in 2010 when he sailed as a sedimentologist on Integrated Ocean Drilling Program (IODP) Expedition 318 to the Wilkes Land margin of Antarctica. The primary goal of the expedition is to collect long-term sedimentary records in a nearshore to offshore transect off of the Wilkes Land margin to examine the influence of Cenozoic Antarctic glaciation on global climate. As part of the Wilkes Land science team, he is currently developing a cyclostratigraphy and geochemical record of the past ice sheet, sea ice and oceanographic variability at the East Antarctic margin of the Southern Ocean for the past 5 million years.

Another avenue of Rob's research utilizes Ocean Drilling Program (ODP) Leg 181 legacy cores, collected from the New Zealand region, to examine how changes in ice sheet and sea ice extent in Antarctica and the Southern Ocean over the last five million years are manifested in the ocean/climate system farther afield. This record will document how changes in Antarctica affected the New Zealand region, and should be important for predicting future changes as the climate warms.

Rob will receive $50,000 of the prize money, with the remainder used to support his ongoing research. He intends to use some of the award to

fund a Ph.D. student. In addition, the money will help to support lab work with international collaborators, concentrating on the IODP Exp. 318 Wilkes Land cores and the archive ODP Leg 181 cores from the New Zealand region.

IODP-MI Announces Upgraded IT Systems

IODP-MI is pleased to announce the development of several IT systems to support mission critical tasks in IODP science. More information can be found at the newly re-designed IODP.org website.

As of 1 April 2012 drilling proposal submission deadline, proponents will be able to submit electronic proposals to the new Proposal Database version 2.0 (PDB 2.0). The PDB 2.0 (proposals.iodp.org) is a user-friendly, webforms system for compiling the many documents required for a drilling proposal. The PDB 2.0 offers significant benefits to proponents and in managing the proposal process from submission through SAS and to operations and scheduling.

Planned developments of Scientific Earth Data Information System (SEDIS: sedis.iodp.org) are completed for the user interface. An exciting functionality now available is parameter queries of the data across IOs and Expeditions. Using the SEDIS search interface to retrieve a subset from the SEDIS catalogue, the user can then click the Data Warehouse link where they can then select specific parameters (and methods) and construct aggregated data sets by retrieving rows matching the specific criteria from all of the data sets preselected by the initial search. The SEDIS catalogue currently comprises approximately 100,000 data sets and 30,000 publications from IODP/ODP/DSDP.

The Sample Materials Request Management (SDRM v.2) system has also been updated by IODP-USIO. The new SDRM v.2 will be launched soon.

The Site Survey Data Bank (SSDB) has been upgraded to use the INT Enterprise Seismic Viewer for web-based visualization of SEGY data.

IODP-MI appreciates feedback on these new systems.

Joint IODP/ICDP Activities at the 34th IGC in Brisbane, Australia

Several ICDP and IODP activities are scheduled for the forthcoming 34th International Geological Congress in Brisbane, Australia (6–10 August 2012). IODP and ICDP will run a joint booth to provide information about current drilling activities and latest scientific results. An introduction to the International Continental Scientific Drilling Program (Workshop #20) will be offered to inform delegates who are not familiar with the ICDP about the ways of support and funding for continental scientific drilling through ICDP. Symposium #25.1 will report on important results of deep ocean drilling of the Integrated Ocean Drilling Program. Times, dates and locations will be announced in the near future on the congress website (http://www.34igc.org/)

Peering into the Cradle of Life: Scientific Drilling in the Barberton Greenstone Belt

by N.T. Arndt, A. Wilson, A. Hofmann, P. Mason, D. Lowe, M. Tice, G. Byerly, and G. Chunnett

The Barberton greenstone belt in South Africa is one of the best-preserved successions of mid-Archean (3.5–3.2 Ga) supracrustal rocks in the world, and, as such, a remarkable natural laboratory where conditions and processes at the surface of the Archean Earth can be studied in detail. A scientific drilling program supported by the International Continental Drilling Program (ICDP) started in August 2011 under the direction of the international team listed on two web sites: http://www.icdp-online.org/front_content.php?idart=2709 and http://www.peeringintobarberton.com/. Updates on drilling progress are also found on these sites.

Planning of this project—the choice of targets, drilling strategies and scientific goals—started in October 2006 at University of the Witwatersrand in Johannesburg, and continued during meetings at San Francisco, Berlin and Vienna, and a one-week field conference in the Barberton belt. A research networking program of the European Science Foundation, "Archean Environment: the Habitat of Early Life", supported this part of the project. ICDP approved the drilling proposal in August 2009, but problems related to the procurement of drilling permission from the South African Department of Mineral Resources held up the start of drilling for more than a year.

Two main drilling targets were identified:

(1) Sedimentary sequences will provide information about erosion and sedimentation on the early Earth, the composition and temperature of Archean seawater, and one possible site where life may have emerged and evolved;

(2) Successions of ultramafic to mafic volcanic rocks will provide new insights into volcanic processes, dynamics of the crust and mantle, interaction between oceanic volcanic crust and the hydrosphere and biosphere.

At the time of writing in mid-January 2012, two holes had been drilled at the Tjakastad komatiite site in the southern part of the belt. The first—BARB1, 425 m in length—intersected an unusual tumulus structure composed of highly magnesian, vesicular komatiite basalts and 300 m of overlying spinifex-textured and massive komatiitic and basaltic flows. The hole BARB2 intersects an adjacent sequence of komatiic flows. Petrological and geochemical study of the core will address questions such as the nature of komatiitic volcanism, the origin of komatiite magmas, alteration of volcanic rocks following their eruption, and the composition and evolution of the Archean mantle.

The second site is in the Buck Reef, a thick sequence of cherts and shales. Hole BARB3 is currently at a depth of 709 m, about 100 m from its target of 800 m. This hole has sampled over 500 m of banded cherts with remarkable sedimentary and diagenetic structures such as those illustrated in Fig. 1a. Study of these samples and interlayered ferruginous and black shale will focus on the other origin of the sedimentary rocks, the evidence of early life that they contain, and the composition and temperature of Archean seawater.

The fourth hole, BARB4 in the middle Fig Tree Group in the eastern part of the belt, is currently at 352 m, 200 m short of its target. It has sampled turbiditic graywackes, mudstones, sideritic banded ferruginous chert and banded iron formations (Fig. 1b). Drilling at the last two sites, one in barite-rich sediments of the Barite Valley and another in silicified komatiites on the Mendon Formation, should be completed before April.

The distribution of samples and post-drilling research will be coordinated by a steering committee comprising representatives from all major participating countries. Compositions of the drilling teams and steering committee are given on the web sites. Once the core has been described and archived, a call will be made for proposals to work on the core. This call will be open to all scientists but priority will be given to those involved in the drilling or working in South African institutions.

Figure 1. [A] Core from hole BARB3 in the Buck Reef. Alternating chert and ferruginous shale with soft-sediment deformation and replacement structures. [B] Core from hole BARB4 in the middle Fig Tree Group. Jasperlites and cherts intruded by veins of carbonate and fine-grained quartz.

Schedules

IODP – Expedition Schedule http://www.iodp.org/expeditions/

	ESO Operations	Platform	Dates	Port of Origin
1	347- Baltic Sea Paleoenvironment	MSP	Spring/Summer 2013	TBD
	USIO Operations *	**Platform**	**Dates**	**Port of Origin**
2	340 - Lesser Antilles Volcanism and Landslides	*JOIDES Resolution*	3 Mar.–17 Apr. 2012	San Juan, Puerto Rico
3	342 - Paleogene Newfoundland Sediment Drifts	*JOIDES Resolution*	2 Jun.–1 Aug. 2012	St. George, Bermuda
4	344 - Costa Rica Seismogenesis Project 2 (CRISP)	*JOIDES Resolution*	23 Oct.–11 Dec. 2012	Balboa, Panama
5	345 - Hess Deep Plutonic Crust	*JOIDES Resolution*	11 Dec.2012–10 Feb. 2013	Puntarenas, Costa Rica
6	341 - Southern Alaska Margin Tetonics, Climate & Sedimentation	*JOIDES Resolution*	29 May–29 Jul. 2013	Victoria, Canada
	346T - Transit	*JOIDES Resolution*	29 Jul.–21 Aug. 2013	
7	346 - Asian Monsoon	*JOIDES Resolution*	21 Aug.–28 Sep. 2013	Hakodate, Japan
	CDEX Operations **	**Platform**	**Dates**	**Port of Origin**
8	343 - Japan Trench Fast Drilling Project	*Chikyu*	1 Apr.–21 May 2012	Shimizu, Japan
9	337 - Deep Coalbed Biosphere off Shimokita	*Chikyu*	6 Jul.–15 Sep. 2012	Shimizu, Japan
10	338 - NanTroSEIZE Plate Boundary Deep Riser - 2	*Chikyu*	19 Sep.2012–31 Jan. 2013	Shingu, Japan

MSP=Mission-Specific Platforms TBD=to be determined

* Sailing dates may change slightly. Staffing updates for all expeditions to be issued soon.

** CDEX schedule subject to OTF and SAS approval.

ICDP – Project Schedule http://www.icdp-online.org/projects/

	ICDP Projects	Drilling Dates	Location
1	Campi Flegrei	Apr. 2012–Jun. 2012	Naples, Italy
2	GONAF	Jun. 2012–Jul. 2013	Istanbul, Turkey
3	Songliao Basin	Jun. 2012–Jun. 2013	Daqing, China
4	Colorado Plateau	Sep. 2012	Arizona, U.S.A.
5	COREF	Jul. 2012–Sep. 2012	Ryukyu Islands, Japan
6	Lake Ohrid	Sep. 2012–Oct. 2012	Macedonia, Albania
7	Human Origins	Jul. 2013–Jan. 2014	Kenya and Ethiopia, Africa